



Flood protection using the 'Holwerd West' salt marsh

UNIVERSITY OF TWENTE.

Witteveen + Bos

Flood protection using the ‘Holwerd West’ salt marsh

Master thesis in Civil Engineering and Management

Faculty of Water Engineering and Management

University of Twente

Author: Robin de Boer (s1462121)
E-mail: r.m.deboer@student.utwente.nl
Location: Enschede

Graduation committee:

dr.ir. D.C.M. Augustijn (Denie)

University of Twente

Supervisor

E-mail: d.c.m.augustijn@utwente.nl

dr.ir. B.W. Borsje (Bas)

University of Twente

Daily supervisor

E-mail: b.w.borsje@utwente.nl

ir. J. Lansink (Joost)

Witteveen+Bos

Supervisor

E-mail: joost.lansink@witteveenbos.com

ir. C. Steetzel (Coen)

Witteveen+Bos

Daily supervisor

E-mail: coen.steetzel@witteveenbos.com

Preface

Over the last several months I have been investigating the potential of the Holwerd West salt marsh in terms of coastal flood protection. I have focused on its development, since its existence, in order to explain how a salt marsh system works and deals with waves. This, in order to recommend alternatives in order to improve wave reduction, which is needed now and will be in the future.

During my master thesis period at Witteveen+Bos, I enjoyed working in an open atmosphere in which colleges were willing to assist me. I would like to thank Coen for our weekly meetings in which we talked about the process and anything that was doubtful, and inviting me to do bathymetry measurements at the Marker Wadden. Besides, I want to thank Denie for his precise feedback and Bas for his to-the-point feedback and for inviting me to the Young Wadden Academy. Thereby, I am glad that Joost gave me the opportunity to work in his group ('Waterkeringen') and his way of probing questions.

Next to this, I am thankful for modelling advice that Wim Ridderinkhof and Pim Willemsen have given me. Moreover, I am glad that I met TU Delft student Ineke van der Reijden with whom I discussed modeling techniques. In addition, Vincent Vuik gave me expert advice when this was needed.

I want to thank Jaap de Vlas for the beautiful front-page picture of Holwerd West made in 1995 and for other aerial pictures used in this report. Finally, I want to thank my fellow graduate students and friends for their interest and support.

Robin de Boer

Enschede, October 2019

Summary

Coastal risks are likely to increase the coming decades because of increasing storm intensity and sea-level rise as a result of climate change. This has resulted in the rejection of many dike trajectories along the Wadden Sea dike, such as at Holwerd West. The use of salt marshes in combination with a dike, is an ecologically sound alternative for further raising dikes. These vegetated forelands are namely capable of reducing waves so that the hydraulic load on the adjacent dike is lowered.

Since 1950, the growth of the salt marsh of Holwerd West has been stimulated by human interventions as the salt marsh works, composed by brushwood dams and ditches. Wave action subsequently assured that sand, sludge and organic matter were supplied to the platform, especially during high water events. As a consequence, vegetation could develop; creating an intertidal landscape of high biodiversity, which is maintained by the grazing of different animals. Since 1979, higher elevated salt marsh zones have solely been subject to storms rather than tides, which caused that the platform has reached a maximum height of 2 m+NAP. Meanwhile, the lower salt marsh zone is extending with 20 m/year due to tidal influences.

Wave reduction over a salt marsh is achieved as a consequence of three bio-physical processes: (1) depth-induced wave breaking, (2) wave energy dissipation by bottom friction and (3) wave attenuation by vegetation. The significant wave height reduction of Holwerd West was determined by a SWAN wave model and appears 0.61-0.77 m (45-53%) during a T=100-year storm event while accounting for spatial variety. Wave damping due to vegetation obstruction contributes most to this. In case of a rarer T=1000-year event, this effect is 0.31-0.63 m (18-36%), mainly due to depth-induced wave breaking. During a T=10,000-year event the reduction is 0.31-0.73 m (15-35%) and during a T=37,500-year event 0.28-0.71 m (13-31%). In case of the latter return period, representing the norm for an overtopping failure mechanism (GEKB), the normative dike height is 23-41 cm lower than the original.

In order to increase the wave reducing effect of Holwerd West, it is recommended to stimulate salt marsh growth so that a high (elevation) varying bottom profile is created. This can be achieved by preserving the high vegetation diversity so that sediment particles are captured in a scattered way. In addition, a sludge nourishment could account for a sufficient (clay-containing) sediment supply, which will decrease the erodibility of the bed.

Samenvatting

Door klimaatverandering worden stormen steeds extremer en stijgt de zeespiegel de aankomende decennia. Als gevolg hiervan worden overstromingsrisico's groter en dus zijn veel dijkvakken langs de Waddenzeekust afgekeurd, zoals Holwerd West. Een alternatief voor het verder verhogen van dijken, is gebruik maken van een kwelder voor de dijk. Deze begroeide voorlanden zijn namelijk in staat om golven te reduceren en daarbij de hydraulische belasting op de aanliggende dijk te verlagen.

Sinds 1950 is de groei van de Holwerd West kwelder gestimuleerd door menselijke ingrepen, zoals kwelderwerken ('landaanwinningswerken') bestaande uit rijshoutdammen en greppels. Golfwerking heeft vervolgens tijdens hoogwater periodes gezorgd voor de aanvoer van zand, slib en organische materialen. Als gevolg hiervan kon vegetatie ontstaan wat gezorgd heeft voor een getijdenlandschap met veel biodiversiteit, dat is onderhouden door het grazen van verschillende diersoorten. Vanaf 1979 waren de hoger gelegen kwelder zones niet meer beïnvloedbaar door getij; enkel nog door stormen, wat gezorgd heeft dat het plateau een maximumhoogte van 2 m+NAP heeft bereikt. Ondertussen breidt de lage kwelderzone zich nog ieder jaar uit met 20 m onder invloed van getij.

Golfreductie boven een kwelder is te danken aan drie biofysische factoren: (1) diepte-geïnduceerde golfbreking, (2) golfenergie verlies door bodemwrijving en (3) golf demping door vegetatie. De significante golfhoogte reductie over Holwerd West was bepaald met een SWAN-golfmodel en bleek 0.61-0.77 m (45-53%) tijdens een T=100-jaar gebeurtenis, rekening houdende met ruimtelijke onzekerheid. Golf demping als gevolg van vegetatie obstructie droeg hier het meest aan bij. Tijdens zeldzamere T=1000-jaar, T=10,000-jaar en T=37,500-jaar stormen, was dit effect 0.31-0.63 m (18-36%), 0.31-0.73 (15-35%) en 0.28-0.71 m (13-31%); voornamelijk dankzij diepte-geïnduceerde golfbreking. Dit biofysisch proces heeft een hogere relatieve contributie aan de golfhoogte reductie naarmate de stormen extremer worden en vegetatie zal afbreken. De storm met een herhalingstijd van 1/37,500 jaar representeert de norm waarop golfoverslag berekend wordt binnen het faalmechanisme 'Grasbekleding erosie kruin en binnentalud' (GEKB). De benodigde kruinhoogte (HBN) kan 23 tot 41 cm lager zijn wanneer de kwelder hierin wordt meegenomen.

Om het golf reducerende effect van Holwerd West te vergroten, wordt er aanbevolen om kweldergroei te stimuleren, waardoor een bodemprofiel met lokale hoogteverschillen ontstaat. Hiervoor zal de grote diversiteit aan plantensoorten moeten worden behouden, zodat sediment deeltjes verspreid over het platform worden opgevangen. Als aanvulling hierop kan een slib suppletie zorgen voor voldoende (kleihoudend) sediment, waardoor de erosiebestendigheid van de kwelder zal toenemen.

Table of Contents

| | |
|--|-----|
| Preface..... | i |
| Summary..... | ii |
| Samenvatting | iii |
| 1. Introduction | 1 |
| 1.1. Background..... | 1 |
| 1.1.1. Flood protection in the Wadden Sea | 1 |
| 1.1.2. Flood protection using salt marshes | 2 |
| 1.2. Problem definition | 4 |
| 1.3. Research aim and questions | 5 |
| 1.4. Study area..... | 5 |
| 1.5. Report outline..... | 7 |
| 2. Salt marsh system..... | 8 |
| 2.1. External factors | 8 |
| 2.1.1. Wave action | 8 |
| 2.1.2. Human interventions | 10 |
| 2.1.3. Sediment availability..... | 11 |
| 2.2. Internal factors | 12 |
| 2.2.1. Geometry | 12 |
| 2.2.2. Bed characteristics..... | 14 |
| 2.2.3. Vegetation..... | 15 |
| 2.3. Overview of salt marsh dynamics | 19 |
| 2.4. Internal (salt marsh) development | 21 |
| 3. Quantification of the wave reducing effect | 23 |
| 3.1. Methodology..... | 23 |
| 3.1.1. Model description | 23 |
| 3.1.2. Modeling approach..... | 23 |
| 3.1.3. Wave height reduction and relative contribution | 26 |
| 3.1.4. Translation to normative dike height..... | 27 |
| 3.1.5. Reliability of model outcomes..... | 27 |
| 3.2. Results | 29 |
| 3.2.1. Wave height reduction and relative contribution | 29 |
| 3.2.2. Sensitivity analysis | 30 |
| 3.2.3. Normative dike height..... | 31 |
| 4. Salt marsh adaptations..... | 32 |

| | |
|---|----|
| 5. Discussion..... | 34 |
| 6. Conclusions and recommendations..... | 35 |
| 6.1. Conclusions..... | 35 |
| Salt marsh development..... | 35 |
| Quantification of the wave reducing effect | 35 |
| Salt marsh adaptations..... | 35 |
| 6.2. Recommendations | 36 |
| References..... | 37 |
| Appendixes | 41 |
| Appendix A - Terminology and dictionary | 41 |
| Appendix B - List with abbreviations | 44 |
| Appendix C - Wadden Sea dike assessment Koehool-Lauwersmeer..... | 45 |
| Appendix D - Considered locations of the POV-W | 47 |
| Appendix E - Sublocations of NFB | 48 |
| Appendix F - Geometry of Holwerd West..... | 49 |
| Appendix G - Transformation of the soil map of 2014 | 50 |
| Appendix H - Physical processes in SWAN (version 41.20) | 51 |
| Appendix I - Choice from transects of Holwerd West | 56 |
| Appendix J - SWAN model parameters..... | 57 |
| Appendix K - Wave energy change along both transects | 60 |
| Appendix L - Method for HBN calculations..... | 67 |
| Appendix M - Latest flood protection projects along Koehool-Lauwersmeer | 68 |

1. Introduction

In this chapter, background information about coastal flood protection in the Wadden Sea is provided with the focus on salt marshes. Thereafter, the problem is defined by means of scientific reports that leave a research gap. Then, the research objective and questions are set up, after which the study area is clarified. At last, the report outline is explained.

1.1. Background

1.1.1. Flood protection in the Wadden Sea

The Wadden Sea arose about 8000 years ago when the postglacial sea level rise began to stagnate (Common Wadden Sea Secretariat, 2018). It is the largest (1.143.403 ha) interconnected tidal inlet system in the world formed by barrier islands and sand flats on the seaside, and mudflats and salt marshes on the land side. Since the degree of sea level rise and the amount of sediment supply varied over time, a continuous dynamic in the coastal morphology was born. At times when the sediment supply was unable to keep up with the sea level rise, the Wadden Sea coast shrank locally.

In early years, inhabitants had not tried to fight against high water; they started building their houses on higher artificial grounds, called 'dwelling mounds' ('terpen'). The first coastal flood protection measure along the Wadden Sea coast took place between 1000-1250 A.D. with the construction of the Wadden Sea dike (Essink *et al.*, 2014). From the 1500s, impoldering took place to reclaim land and during the 1700s, farmers started constructing salt marsh works. These accelerated the process of accretion so that (semi-artificial) salt marshes were formed on which livestock farming and agriculture could take place.

Nowadays, the Wadden Sea Region covers the coastal flood defense system of the Northern part of the Netherlands. Its barrier islands and mudflats form a natural buffer against the force of the (high) waves. Over time, dike construction techniques have improved (Zijlstra *et al.*, 2017). Additionally, sand and mud nourishments take place to prevent coastal erosion. The man-made coastal flood defenses (e.g. dikes, dams and revetments) together with the natural dunes on the barrier islands form the flood protection along the Wadden Sea coast as it is now.

A map showing current flood protection techniques is presented on the next page in Figure 1. The Wadden Sea dike creates the boundary between towns and the salty water of the Wadden Sea. In 2009, the Wadden Sea region became part of the European Natura 2000 network and is appointed UNESCO World Heritage, so that its protection is ensured.

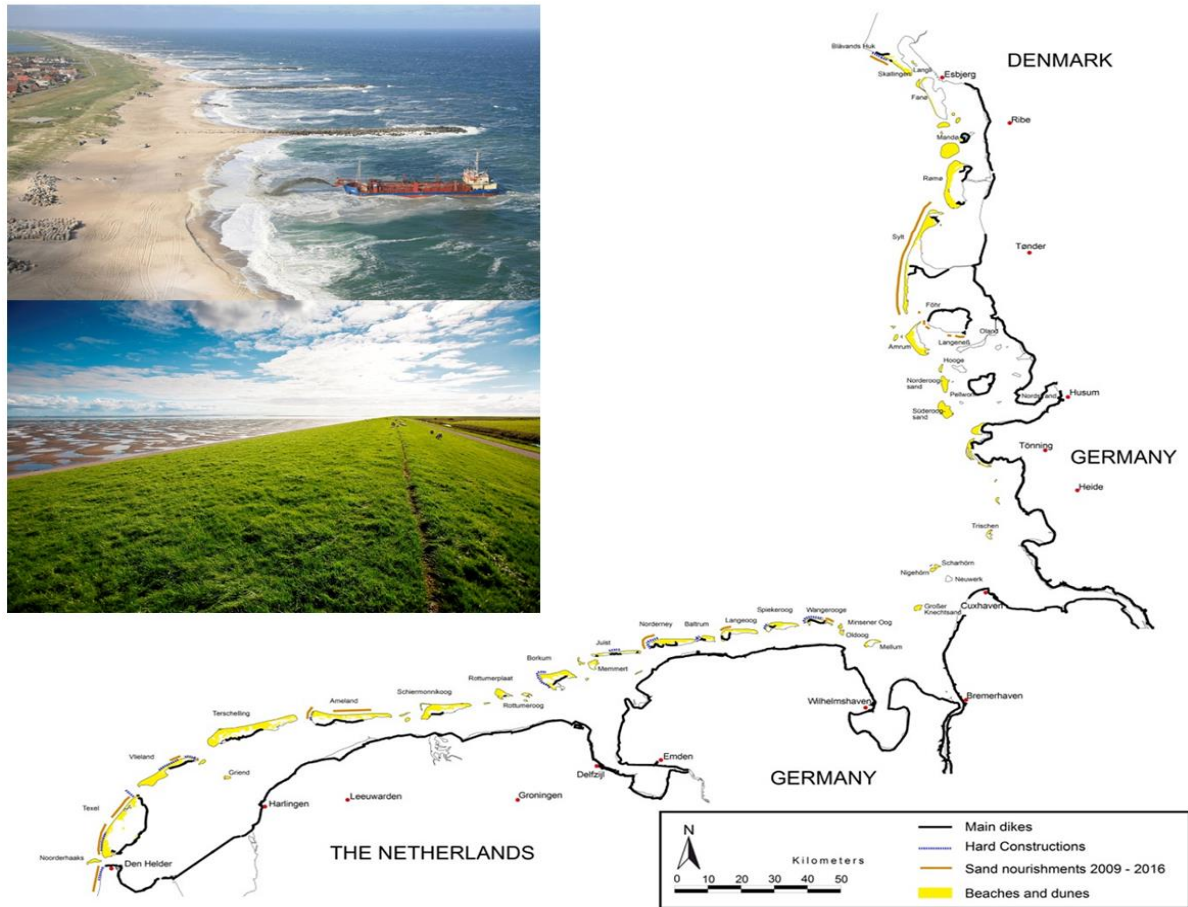


Figure 1 - Coastal flood defenses along the Wadden Sea coast. Photos: Upper left: Groynes and sand nourishments in Denmark. Lower left: Typical green Wadden Sea dike (Zijlstra et al., 2017).

1.1.2. Flood protection using salt marshes

Salt marshes are surfaces outside the dike consisting of sediment deposits with salt-tolerant plants that partly flood during tides and entirely during storms. Naturally, these overgrown forelands are formed in front of dikes by waves that supplied the coast with sediment. They are mainly situated in areas that have a low coastal gradient, experience a relatively low wave energy, and have a relatively large tidal range; which is the case for the Wadden Sea coast (Alterra, 2012a; van Duin and Dijkema, 2012).

Semi-artificially, salt marshes can develop using 'salt marsh works', as portrayed on the next page in Figure 2. This method was first applied by farmers and well along taken over by the state following the principles of an adapted version of the German 'Sleeswijk-Holstein' method (Dijkema et al., 2001). This land reclamation method has offered a fertile landscape for farming. Nonetheless, in the period of 1969-1980 additional goals were set up for salt marsh works (Dijkema et al., 2001). The first was coastal protection (1969), the second protection and recovery of natural values (1980) and the third to meet the requirements of shore owners. The coastal protection principle entailed that a certain foreland area had to be maintained. For Groningen and Friesland this meant that the total area of salt marshes had to be at least 1250 ha, which is currently fulfilled with a surface of 1820 ha (van Duin et al., 2013).



Figure 2 - Semi-artificial salt marshes have developed in front of the Wadden Sea dike, supported by salt marsh works (Aerial pictures by Jaap de Vlas) (van Duin et al., 2013); (Steezel et al., 2019).

The salt marsh works aim at favorable conditions for sedimentation and establishment of salt-tolerant vegetation, using sedimentation fields as basis, as can be seen below in Figure 3. Its boundaries are formed by dams (or 'groynes') constructed of wooden poles filled with brushwood or willow branches, held together by a metal wire. The top of the dams is on average 30 cm above average high water level (GHW) so that they reduce wave action and longshore flows. The elastic construction offers resistance to the water where its permeability prevents that great pressure differences arise on both sides of the dam. Sediment is left behind between the dams or else accumulated around vegetation stems. Moreover, the system of parallel ditches ensures that forelands are drained after flooding. This prevents vegetation from perishing and that water ponds can emerge.

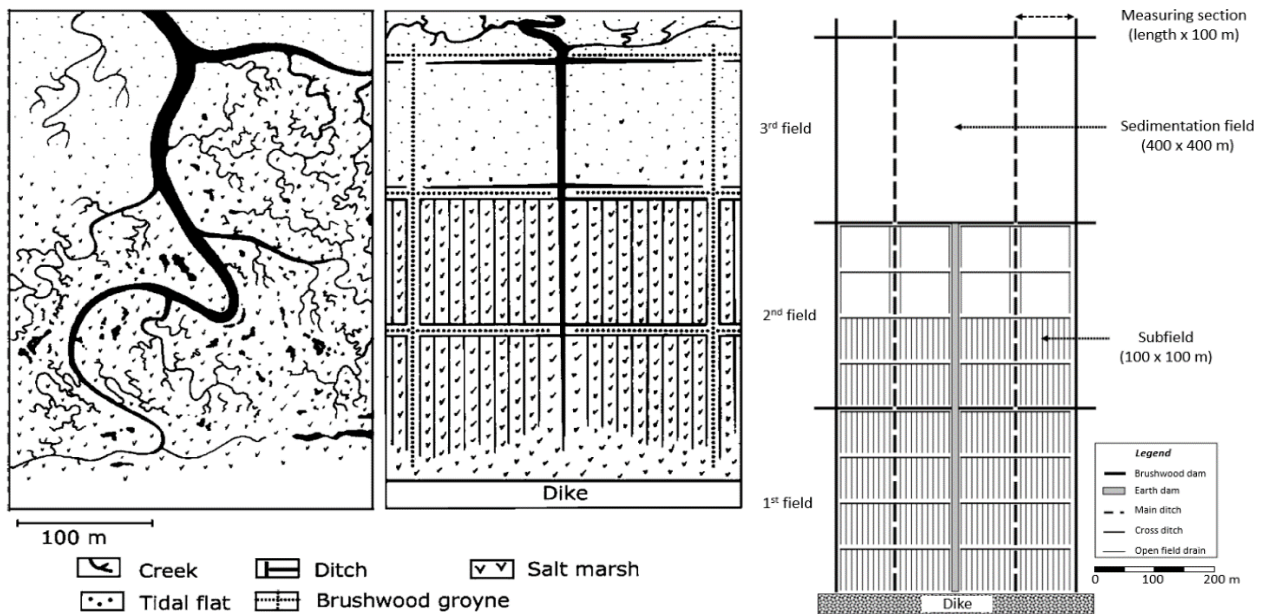


Figure 3 - Left: Overview of a natural salt marsh versus a semi-artificial one (Reise, 2005). Right: Schematic layout of one set of sedimentation fields of the Frisian salt marsh works (Dijkema et al., 2001).

1.2. Problem definition

Coastal risks are likely to increase the coming decades because of increasing storm intensity, sea-level rise and land subsidence (Ministry of Transport Public Works and Water Management, 2000; Temmerman *et al.*, 2013). This has resulted in the rejection of many trajectories along the Wadden Sea dike. Next to traditional coastal protection (e.g. further raising the dikes), there is a growing need for sustainable, ecologically sound and cost-effective alternatives (Borsje *et al.*, 2011; Poppema, 2017). An alternative is the use of salt marshes in combination with a dike, which builds on the 'Building with Nature' concept. These vegetated forelands are namely capable of reducing waves so that the (hydraulic) load on the adjacent dike is lowered (Alterra, 2012a; Vuik *et al.*, 2016; Poppema, 2017; Vuik *et al.*, 2018; Vuik *et al.*, 2018; Steetzel *et al.*, 2019). Moreover, forelands are capable of moving upward with the rising sea level as its vegetation captures sediment particles (Alterra, 2012a; Vuik *et al.*, 2016; Poppema, 2017; Vuik *et al.*, 2018; Willemsen *et al.*, 2018; Steetzel *et al.*, 2019).

The revaluation of salt marshes appears in many projects worldwide in which these are being restored or created (Poppema, 2017). For example, along the Frisian Wadden Sea coast, projects have been executed in which summer dikes were breached so that salt marshes were restored (Esselink *et al.*, 2015). Besides, similar projects take place with mangroves in tropical environments such as the coastal restoration project in Java, Indonesia (Witteveen+Bos, 2019).

The contribution of salt marshes in flood protection can be quantified by determining their wave reducing effect. It is known that there are three main (bio-physical) processes causing wave reduction over a salt marsh: (1) depth-induced wave breaking, (2) wave energy dissipation by bottom friction and (3) wave attenuation by vegetation (Möller *et al.*, 1999).

Many studies have quantified the wave reducing effect of salt marshes. One current project of the POV-Waddenzeedijken (POV-W) concluded that the presence of a salt marsh along the Wadden Sea coast leads to an average wave height reduction of 50 to 70 cm during a storm event with a return period of 1/10,000 years (Steetzel *et al.*, 2019). Depth-induced wave breaking contributed most to this (50 cm) followed by bottom friction (0 to 20 cm). The influence of vegetation was investigated separately but appeared to be negligible during (normative) storm conditions rarer than 1/1000 years due to stem breakage. This was confirmed by more studies that stated that salt marsh vegetation only reduces wave energy when water levels are not too high (Alterra, 2012a; Vuik *et al.*, 2018). However, field experiments performed in Norfolk (United Kingdom) revealed that the wave height reduction as a result of salt marshes was 46% higher than on unvegetated forelands (61% versus 15%) during tidal flooding events, implying that vegetation caused wave reduction for a high degree (Möller *et al.*, 1999). Besides, for a salt marsh in 'Brouage' (France) it was found that bottom friction was dominant for wave energy reduction (Le Hir *et al.*, 2000). Consequently, the wave reducing effect differs per location and flood event.

Furthermore, the translation of the wave reducing effect towards flood protection is lacking. Currently, the POV-W are investigating the effect of salt marshes on the normative load of the adjacent flood defense (e.g. dike) and are striving to implement this into national dike assessment norms (Steetzel *et al.*, 2019). However, the bathymetry of these forelands along the Wadden Sea are schematized. Besides, this investigation will last until the end of 2019 and it is unsure whether this inclusion will succeed. Assuming that this succeeds, and it appears that dike trajectories do fulfil the current requirements, it is still unsure whether this will be the case for future scenarios.

1.3. Research aim and questions

This research aims to solve the identified research gaps using the salt marsh of 'Holwerd West' as study area. The following main research question is therefore formulated:

What is the wave reducing effect of the 'Holwerd West' salt marsh during storm events and which salt marsh adaptations can be implemented to increase this effect?

To answer the main research question, the following research questions are defined:

1. How did the 'Holwerd West' salt marsh develop?

The goal of this question is to investigate the dynamics of the Holwerd West salt marsh. In this way, insight is obtained into salt marsh characteristics that determine its wave reducing effect.

2. What is the wave reducing effect of the 'Holwerd West' salt marsh during storm events?

The goal of this question is to determine the (realistic) wave reducing effect and corresponding relative contribution of each of the three bio-physical processes. Accordingly, the change in normative dike height can be determined, which indicates the height at which dikes can withstand wave overflow and overtopping.

3. Which salt marsh adaptations can be implemented to increase its wave reducing effect?

The goal of this question is to use the results of the previous questions to set up recommendations, for salt marsh adaptations striving for higher wave reduction so that salt marshes will contribute more to coastal flood protection.

1.4. Study area

Engineering consultancy Witteveen+Bos has performed a dike safety assessment along the Wadden Sea dike between 'Koehool' and 'Lauwersmeer' of which the result is shown on the next page in Figure 4 and further explained in Appendix C. In addition, it is described which failure mechanisms can be reduced by salt marshes. Dike trajectories that did not fulfill the requirements have become part of the Flood Protection Program (Hoogwaterbeschermingsprogramma). As a follow up step, Witteveen+Bos supports waterboard Wetterskip Fryslân during the exploration phase for this area. Reinforcement measures should namely be analyzed and realized so that the dike between this trajectory will fulfil the current dike norm.

From west to east there are four salt marshes ('kwelders') located along this dike trajectory as can be seen in Figure 4:

- (A) 'Noard-Fryslân Bûtendyks' or 'Noord-Friesland Buitendijks' (NFB) (dp 20-43)
- (B) 't Skoar' or 'Schoorsterpollen', on the north of 'Ternaard' (dp 46-47)
- (C) 'Kromme Horne', on the east of 'Wierum' (dp 50-51)
- (D) 'Peazemerlannen' (dp 53-58)



Figure 4 - Salt marshes (in dark green) along the Wadden Sea dike between Koehool and Lauwersmeer. Dike poles are used as location marker (Alterra, 2012b; Witteveen+Bos, 2017a)

For this research, the study area is 'Holwerd West' (dp 38-41) which is part of the salt marsh 'Noord-Friesland Buitendijks' (NFB), located against the Wadden Sea dike in the northeast of the province of Friesland. This subarea was selected because it is rejected and has not yet explicitly been investigated by the POV-W. A map of the considered locations in the POV-W is presented in Appendix D and a map of the subareas of NFB is depicted in Appendix E.

The salt marsh 'Holwerd West' is situated on the northwest of the town Holwerd. The area is enclosed by the Wadden Sea in the north, a breakwater (used for the ferry service to Ameland) in the east, the Wadden Sea dike (elevated 8.5-9.0 m+NAP) in the south, and a 'tidal creek' (main ditch) in the west, as depicted in Figure 5. The area is used for livestock grazing for which paths and drinking wells ('dobben') have been created. Its width (cross-shore direction) varies between 0.8 km and 1.3 km, and its length (longshore direction) between 2.7 and 2.8 km, in the same year (2017). The salt marsh consists of a former summer polder and a salt marsh platform, having an area of 50 ha and 180 ha respectively.



Figure 5 - Study area: the salt marsh of 'Holwerd West' (Google Earth, 2017). The breakwater ('Grândyk) and the ferry route ('Holwerd-Ameland) are indicated.

1.5. Report outline

At first, in chapter 2, the salt marsh development is investigated. This information is largely the data source for the quantification of the wave reducing effect which is elaborated in chapter 3. Chapter 4 subsequently presents the recommendations for salt marsh adaptations. Hereafter, the results are discussed in chapter 5 and conclusions and recommendations, for further research and towards salt marsh management parties, are stated in chapter 6.

2. Salt marsh system

Salt marsh systems are dynamic, which can be explained by many time and space dependent factors. External factors are wave action (e.g. due to tides and storm surges), human interventions (e.g. presence of salt marsh works) and sediment availability (e.g. sediment amount). For the sake of the research, the internal development (RQ1) is analyzed using factors that are related to the three bio-physical processes causing wave reduction, respectively salt marsh geometry (e.g. height and width), bed characteristics (e.g. soil composition) and vegetation (i.e. types and development). These factors are interconnected by which salt marshes change over time.

In this chapter, these external and internal factors are described first. Then, an overview of salt marsh dynamics is provided. At last, the development of Holwerd West since its establishment is explained. For this, most data was derived from measurements during the monitoring period of the Frisian salt marshes between 1960 and 2014 (van Duin *et al.*, 2013).

2.1. External factors

2.1.1. Wave action

Wave action is the key process in the development of salt marshes (Best *et al.*, 2018). It namely suspends sediment and subsequently transports it towards the coast, especially during high water events. This results in the heightening of these platforms and the formation of mudflat-salt marsh transitions, as can be seen in Figure 6 below. It is acknowledged that relatively high wave heights produce more elevated, but narrower salt marshes. Conversely, relatively low wave heights yield less elevated, but wider salt marsh platforms (Best *et al.*, 2018).

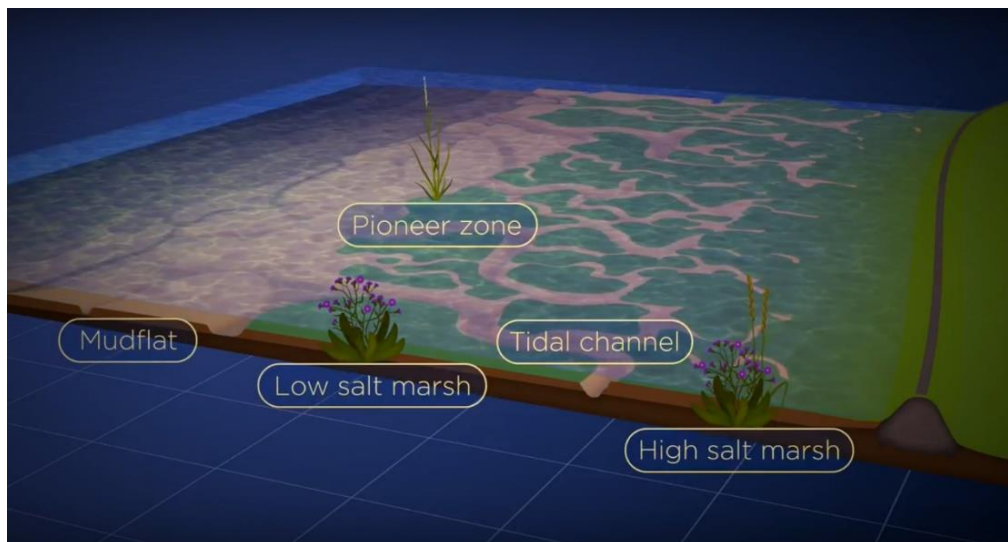


Figure 6 - An example of a (natural) mudflat-salt marsh system including salt marsh zones (BE SAFE, 2017)

Wave action exists because of tides and wind waves which provide energy for erosion and sediment transport (Alterra, 2012a). Whether a wave in the Wadden Sea reaches a salt marsh depends on the source of the wave action and obstacles that influence wave propagation (e.g. barrier islands, bottom structure and composition, and vegetation). From Figure 7 can be seen that the tidal channels (dark blue) on the north of Friesland are approximately situated parallel to the coast. Consequently, deep water waves from the North Sea cannot propagate far towards the Frisian coast and turn into shallow waves with relatively low wave energy. Being subjected to low wave energy is a precondition for salt marsh formation (van Duin and Dijkema, 2012).

Tides

Tides are the result of gravitational influences of the Moon and the Sun on the Earth's water surface. The average tide (one period of ebb and flood) in the Wadden Sea lasts 12.4 hours (Dijkema *et al.*, 2001), with a tidal amplitude (difference between high tide and low tide level) at Holwerd of 2.3 m (Esselink *et al.*, 2015). This relatively large water level fluctuation causes a natural in- and outflow within tidal channels on salt marshes.



Figure 7 - Map of the bottom elevation (bathymetry) in the Wadden Sea in 2017 in which tidal channels are visible (Alterra, 2012b)

Storm surges

Storm surges are extreme (wind speed) events that increase sediment transportation as well (Alterra, 2012a). Depending on the location of the salt marsh, this can lead to erosion or sedimentation on the platform. It is possible that thick layers of sludge are deposited up to several decimeters thick. This is most likely to happen in November or December, called 'the mud months' ('de moddermaanden'). In a year with a lot of storm events, net sedimentation (accretion) is likely to take place. However, it is likely that in the succeeding years erosion will occur, because of vegetation stem breakage and loss of above-ground biomass (Vuik *et al.*, 2018). Due to climate change, the storm intensity will increase the upcoming decades (Suzuki *et al.*, 2012; Temmerman *et al.*, 2013; Willemsen *et al.*, 2018).

Sea level rise and subsidence

A moderate relative sea level rise (absolute sea level rise minus subsidence) and a salt marsh situated around the annual average high water level (GHW) are preconditions for salt marsh formation (Alterra, 2012a). A salt marsh platform will namely not grow higher than the highest springtide level as depicted in Figure 13.

Land subsidence on salt marshes along the Wadden Sea is either caused by isostasy (due to increased mass by sedimentation) or gas extraction. By the process of isostasy, this is 0.3 mm/year (van Duin *et al.*, 2013; Esselink *et al.*, 2015). Gas extraction is performed in Groningen and is therefore assumed not to affect salt marsh platforms altitudes in Friesland (Dijkema *et al.*, 2001).

Since the end of the 19th century, a significant sea level rise has been measured along the Wadden Sea coast by Rijkswaterstaat (Ministry of Transport Public Works and Water Management, 2000; van Duin *et al.*, 2013; Esselink *et al.*, 2015). At several measurement stations (e.g. Harlingen, Nes and Schiermonnikoog) both the mean sea level and annual average high water levels have been estimated to have increased by 2 mm/year within the period of 1960-2014 (van Duin *et al.*, 2013). As a result, the mean sea level (MSL) is approximately 0 m+NAP and the annual average high water level (GHW) is 1 m+NAP in 2014.

2.1.2. Human interventions

Between 1000-1250 A.D., the first Wadden Sea dikes have been constructed (Zijlstra *et al.*, 2017). In 1580, sea dikes ('Zeedijk') seawards from these were constructed creating the 'Holwerd Westpolder' (Vroom, 2013), depicted on the left in Figure 8 below. After the completion of the breakwater (used for the ferry service to Ameland) in 1910, salt marshes started to form against the sea dike (Esselink *et al.*, 2015). In the beginning, farmers accelerated this process of accretion by constructing salt marsh works (Dijkema *et al.*, 2001). This was realized by digging ditches (creek system) and creating dams of packs of straw (Dijkema *et al.*, 2001; Vroom, 2013). Around the land that had washed up as a result, a summer dike was created in 1932. The resulting *summer polder* at Holwerd is shown on the right in Figure 8 ('Omkade zomerpolders').

Later in 1950, the construction of salt marsh works was taken over by Rijkswaterstaat (Figure 3). These measures are shown on the right in Figure 8 as well. In the same map can be observed that there were plans to create a future polder dike seaward of the salt marsh works to reclaim (even) more land; nevertheless this plan has never been executed. Besides, the breakwater extension by 1 kilometer is depicted. This measure was executed in 1953, so that ferries would still be able to moor at all times.

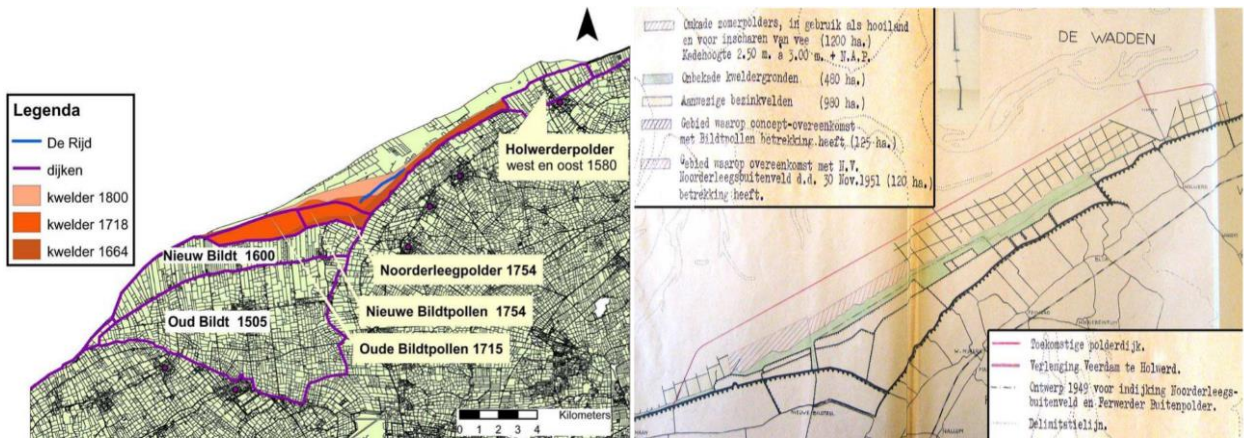


Figure 8 - Left: Impoldering between 1500-1800 along the Frisian Wadden coast at NFB. In light green is observable how the salt marsh was situated in 1990. Right: Sketch of first salt marsh works (drawn as black rectangles) at NFB in 1950 (Vroom, 2013)

The Delta Act (Delta wet) required the reinforcement of dikes since 1958. Afterwards, a discussion was born about the priority of salt marshes. On the one hand, they provide land for livestock farming and agriculture. On the other hand, they provide habitats for vegetation and wild animals (e.g. birds and hares). The application of salt marsh works and (later) impoldering improved agriculture and coastal protection, while dike raising would not harm natural areas. In 1969, coastal protection became an official goal for salt marshes.

However, in 1979, this was overruled as the parliament stated that natural values were of highest importance. Nowadays, the nature conservation organization is called 'It Fryske Gea'.

This decision was followed up by the consideration that NFB is an international wetland area (1984), in which birds (1991) and habitats (2004) should be protected. In 2006, the parliament specified that the area of natural salt marshes should be enlarged and that cultural values (e.g. summer polders, salt marsh works and traces of agricultural use) should be preserved. In 2009, the Wadden Sea region became part of the European Natura 2000 network and is appointed UNESCO World Heritage, so that its (natural and culture historical) protection is ensured.

From 2010 onwards, the Trilateral Wadden Sea Cooperation (i.e. Denmark, Germany and the Netherlands) is striving for a natural and sustainable ecosystem (Common Wadden Sea Secretariat, 2019). Accordingly, salt marsh management has gradually been adjusted to more sustainable and less artificial, so that natural processes proceed in an (almost) undisturbed way.

An overview of the interventions and management perspectives is given in Figure 9 below. From this figure can be seen that the salt marsh formation started in 1910 and has (officially) been stimulated from 1950 onwards by the construction of Rijkswaterstaat's salt marsh works. In 1979, the priority of salt marshes changed from land reclamation (for livestock grazing and agriculture) to natural area. As a result, ditches were no longer dredged. From the perspective of nature, depoldering of the summer polder of Holwerd was the best option for salt marsh enlargement (Esselink *et al.*, 2015). From 1989 onwards, sea water could flow again on the polder land. Since the priority of salt marshes changed, its management (e.g. maintenance of brushwood dams, drainage and grazing) has become variable.

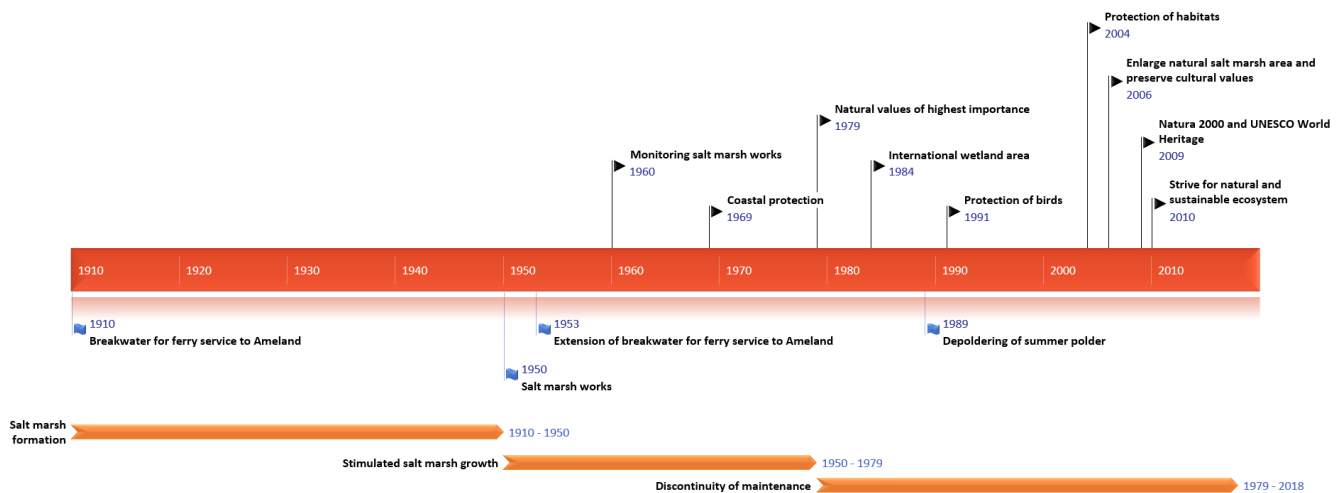


Figure 9 - Historical timeline of the salt marsh 'Holwerd West'. Milestones in the upper part (black flags) refer to management perspectives, while the milestones below the diagram (blue flags) indicate measures. The chevrons below (orange arrows) refer to stage (Boer, 2019).

2.1.3. Sediment availability

The amount of sediment forms a precondition for salt marsh development (Alterra, 2012a). Sediment is supplied by the sea in terms of wave action and (longshore) currents or can originate from erosion events. The main provider of sediment is the flow through tidal channels towards mudflats and subsequently to a salt marsh (Alterra, 2012a). In the case of Holwerd West, the major tidal channel offshore is the navigation channel 'Vaargeul Holwerd-Ameland', which is on the southwest side connected to the 'Dantziggat'; both indicated on the next page in Figure 10.

Asymmetry in tides causes a net transport of sediment (sand/silt/clay) in a certain direction. In the Wadden Sea, ebb lasts longer than flood, implying that flow velocities during flood are higher so that more and bigger sediment particles are being transported towards the coast. This has caused a net import of sediments towards the coast when comparing the situation in the Wadden Sea in 1927 to the situation in 2005 (Alterra, 2012b; Best *et al.*, 2018). This is indicated with the yellow/red colors in Figure 10 below.

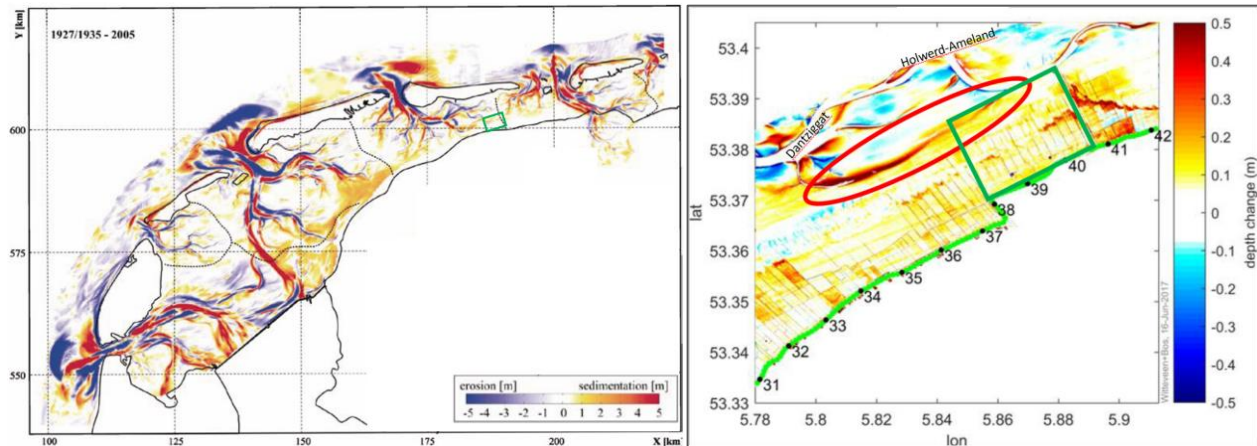


Figure 10 - Left: Sedimentation and erosion (depth change) in the Wadden Sea between 1927/1935 and 2005 (Alterra, 2012b). Right: Depth change along the study area determined from 2004 to 2008 (Witteveen+Bos, 2017c). Holwerd West is indicated with a green rectangle.

Accordingly, accreted fields can be perceived just offshore of Holwerd West (location indicated with a green rectangle in Figure 10) on the south of the navigation channel of Holwerd to Ameland. Evidence for this is strengthened from a map of the sea bed depth change from 2004 to 2008 (Witteveen+Bos, 2017c). Thereby, from the bathymetry figures (Appendix F) from the Vaklodingen and Kusthoogte data sets, further explained in the next paragraph, can be seen that the 0 m+NAP surface areas, offshore of the salt marsh bounded on the north by the navigational channel, have not changed much in shape from 1989 until 2011. This implies that the available amount of sediment has been stable within this period. All in all, the sediment availability for Holwerd West is assumed to have been sufficient for morphological development (i.e. salt marsh raising and widening) between 1960 and 2014.

2.2. Internal factors

2.2.1. Geometry

The geometry (bathymetry) of a salt marsh through time represents its morphological development, which depends on wave action in combination with sediment availability, and human interventions. The salt marsh geometry can be derived from elevation maps generated by Rijkswaterstaat: 'Vaklodingen', 'Kusthoogte' and 'Actueel Hoogtebestand Nederland' (AHN). The Vaklodingen data set has been composed since 1926 using 'single beam echo sounders' (SBES) on boats on the Wadden Sea (Deltares, 2015). This set was measured within rectangles of 12.5 km by 10 km. Both the Kusthoogte data set and the AHN are derived using laser altimetry (LIDAR) on dry surfaces. The Kusthoogte set addresses coastal regions since 1996 and is measured in rectangles of 625 m by 500 m (Deltares, 2013), while AHN is focused on the entire surface area of the Netherlands since 1997 (AHN, 2019).

The data of the Vaklodingen and Kusthoogte was combined to obtain the salt marsh elevation maps for the years 1949, 1958, 1989, 2004, 2007, 2008 and 2011, provided in Appendix F. Hereby was assumed that the partial complete geometric data for Holwerd West represents the entire salt marsh. Since the Vaklodingen and Kusthoogte data sets were not available in raster form, AHN is additionally used to withdraw elevation profiles of transects of Holwerd West, explained in Appendix I.

The salt marsh height was estimated by measuring the different colored surfaces and subsequently their corresponding height at the color bar (Appendix F). Thereafter, the average was calculated, resulting in a rounded average salt marsh height per year. Its width was estimated by averaging several transect lengths from the dike until the +1.0 m depth contour while measuring in the lateral ditch direction. The +1.0 m depth contour is in accordance with the mean GHW in the Wadden Sea between 1960 and 2014 (see Figure 5), and this is the lower boundary of the 'low salt marsh' (see Figure 13). The lateral ditch direction is mostly perpendicular to the dike and nearly equal to the dominant wind direction of 330 degrees North.

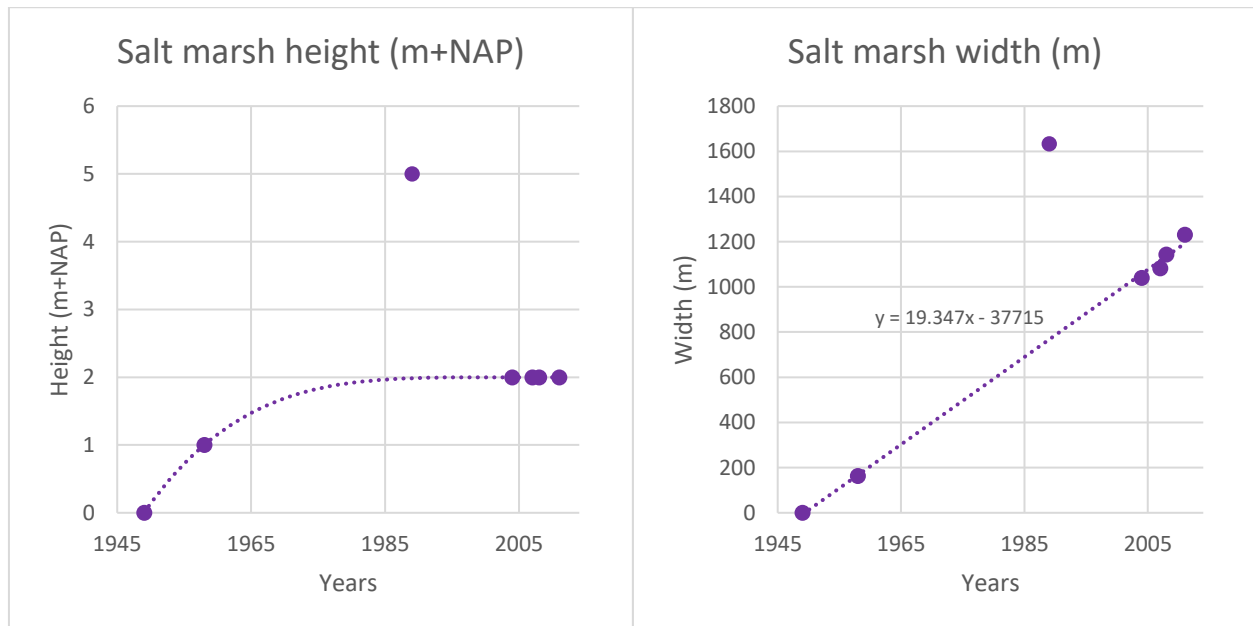


Figure 11 - Geometry of Holwerd West. Left: Average salt marsh height (1949-2011). Right: Average salt marsh width including a linear trendline (1949-2011).

From Figure 11 can be concluded that the salt marsh height and width have increased since 1949, when the height was 0 m+NAP and the width 0 m. This implies that there was no salt marsh present in 1949. This is in accordance with the fact that Rijkswaterstaat started constructing salt marsh works in 1950 (2.1.2 Human interventions), after which the mudflat turned into a salt marsh.

While drawing a trend through both the salt marsh height and width diagram for the period of 1949-2011 (approximately 1960-2014), it seems that both the salt marsh height and width of 1989 is an outlier. Assuming this, the salt marsh height of Holwerd West seems to stagnate at a height of 2 m+NAP while its width still shows a (linear) growth of almost 20 m per year.

2.2.2. Bed characteristics

The bed characteristics of a salt marsh depend on the available sediment composition in combination with wave action and whether human interventions have taken place. Hence, the bed is characterized by bottom shapes (e.g. ripples) consisting of different types of sediment.

The Wadden Sea is by nature a system with sand, sludge (composed of silt and clay) and organic matter (e.g. seaweed) and shells (Alterra, 2012a). Relatively large particles mostly settle in tidal channels while smaller particles contribute to salt marsh raising.

The variation (heterogeneity) in suspended sediment composition is large on the spatial and time scale. Especially at high tide, water gets turbid due to a high sediment concentration so that it settles more easily. This process is supported by salt marsh works or established estuaries in which salt and fresh water can mix. The latter measure is beneficial for nature development and fish migration as well¹.

There are many ways in which the (top) soil composition can be classified. One way is classification according to the 'lutite ratio' (lutumgehalte) of a soil sample. This is a parameter to address the clay content in the soil; the higher, the more clay. It was principally used in the Netherlands to address whether the soil was sufficient for agricultural purposes. This procedure was followed for the determination of the soil map of NFB of 1960. Nowadays, soil maps are more complex and soil types are distinguished in many different classes. Therefore, a transformation of the soil map of 2014 was performed so that comparison was possible. This procedure is described in Appendix G. The soil map of 1960 and the adapted one of 2014 are depicted in Figure 12 below.



Figure 12 - Left: Soil map of NFB of 1960 (Hoekstra et al., 1998). Right: Soil map of NFB of 2014 (Figure adapted from Nationaal Georegister, 2019).

The characteristics of these soil types are presented on the next page in Table 1 in which they are classified according to their lutite ratio, grain diameter and wet density value. The latter two are important parameters for the calculation of the bottom friction in SWAN, because sediment grains counteract the water flow (De Waal, 1999; The SWAN Team, 2019b). This is further explained in paragraph 3.1.2.

¹ This process was used in Project Vijfhuizen 'fan swiet nei sâlt' (2017-2018) (Wetterskip Fryslan, 2018)

While comparing both soil maps for Holwerd West, and considering Table 1, the following conclusions can be made: the amount of very fine sand ('sterk lutumhoudend zand') and coarse/medium silt ('lichte zavel') has increased, at the cost of (very) fine silt ('zware zavel') and clay ('klei'). This implies that, in 2014, bigger sediment particles were present that contained a lower percentage of clay. Next to this, the overall wet density has increased.

Moreover, cohesive sediment is primarily composed of clay and silt, which in general reduces the erodibility of the bed (Grabowski, Droppo and Wharton, 2011). Since the clay content of the salt marsh is lower in 2014, the probability of erosion is higher.

Table 1 - Classification of soil types according to the lutite ratio and grain diameter (Hoekstra *et al.*, 1998; TU Delft, 1999; Ribberink, 2011; Arcadis, 2018) The soil class names in italic format, between brackets, refer to soil type names according to their lutite ratio. N/A = not applicable.

| Soil class (English) | Soil class (Dutch) | Lutite ratio(%) | Grain diameter (µm) | Wet density (kg/m ³) |
|----------------------|--|-----------------|---------------------|----------------------------------|
| Boulders | Rotsblokken | N/A | >256000 | >2500 |
| Cobbles | Stenen/Keien | N/A | 256000 - 64000 | 2400-2500 |
| Gravel | Grind | N/A | 64000 - 2000 | 2000-2400 |
| Sand | | | | 1900-2000 |
| Very coarse sand | Zeer grof zand } (<i>Grof zand</i>) } Klei-arm zand Matig grof zand } (<i>Fijn zand</i>) } Zeer fijn zand (<i>Sterk lutumhoudend zand</i>) | 0 - 1.5 | 2000 - 1000 | |
| Coarse sand | | 1.5 - 3 | 1000 - 500 | |
| Medium sand | | 3 - 5 | 500 - 250 | |
| Fine sand | | 1.5 - 5 | 250 - 125 | |
| Very fine sand | | 5 - 8 | 125 - 62 | |
| Silt | | | | 1100-1400 |
| Coarse silt | Grof silt (<i>Lichte zavel</i>) | 8 - 12 | 62 - 31 | |
| Medium silt | Matig grof silt (<i>Lichte zavel</i>) | 12 - 17 | 31 - 16 | |
| Fine silt | Fijn silt (<i>Zware zavel</i>) | 17 - 25 | 16 - 8 | |
| Very fine silt | Zeer fijn silt (<i>Zware zavel</i>) | 17 - 25 | 8 - 4 | |
| Clay | | | | 1400-2000 |
| Coarse clay | Grof klei (<i>Lichte Klei</i>) | 25 - 35 | 4 - 2 | |
| Medium clay | Matig groffe klei (<i>Matig zware Klei</i>) | 35 - 50 | 2 - 1 | |
| Fine clay | Fijne klei (<i>Zware Klei</i>) | 50 - 100 | 1 - 0.5 | |
| Very fine clay | Zeer fijne klei (<i>Zware Klei</i>) | 50 - 100 | < 0.5 | |

2.2.3. Vegetation

The speed of salt marsh raising (accretion) and dewatering via a tidal creek system (ditches) are found decisive for vegetation growth and determine the speed of vegetation succession (Temmerman *et al.*, 2007; Alterra, 2012a). These factors namely determine the inundation time of the vegetation and the level of salinity. In general, plants start developing at the seaside on the mudflat ('Wad zone'), with the presence of algae (e.g. Diatoms) and bacteria that promote sedimentation. Afterwards, vegetation evolves when the salt marsh is elevated and reaches a high zone where vegetation can eventually reach a climax stage, which is depicted on the next page in Figure 13.

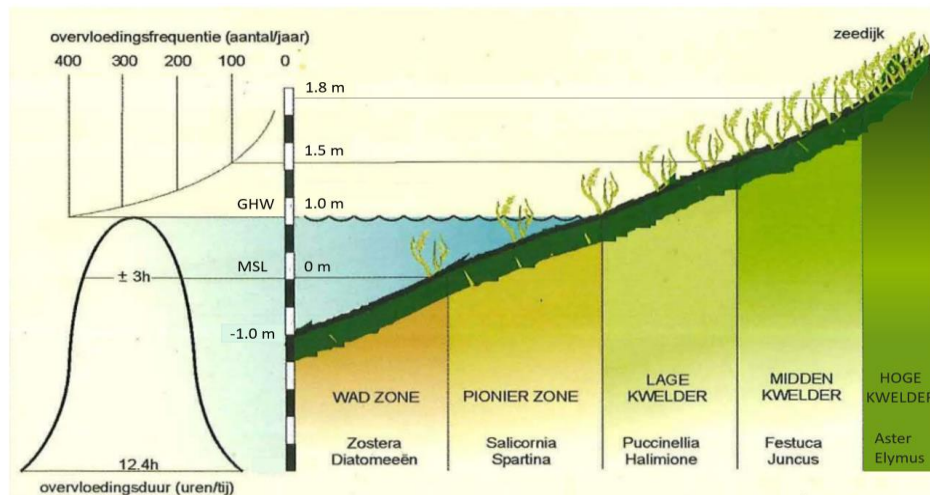


Figure 13 - Salt marsh height (in m+NAP) corresponding to Holwerd West, zonation of salt marsh vegetation and inundation frequency (Figure adapted from Dijkema *et al.*, 2001).

The different salt marsh vegetation types can thus be categorized using the salt marsh zonation which was applied to obtain Table 2 below. The high salt marsh vegetation consists of sea aster and sea couch grass. This final stage is in principle dominated by sea couch grass, which is climax vegetation, providing little room for other vegetation types.

Table 2 - Salt marsh vegetation types categorized per zone (C = climax stage) (Ministry of Transport Public Works and Water Management, 2000; Alterra, 2012a; van Duin *et al.*, 2013; Steetzel *et al.*, 2019).

| Vegetation group/Succession stage (Zoning) | Vegetation type (English) | Vegetation type (Dutch) | Vegetation type (Scientific) | Sort |
|--|---------------------------|-------------------------|---|-------------|
| <i>Pioneer zone</i> | Cordgrass | Engels slijkgras | <i>Spartina anglica</i> | Tall grass |
| | Samphire | Zeekraal | <i>Salicornia europaea</i> | Flower |
| <i>Low salt marsh</i> | Common saltmarsh-grass | Gewoon kweldergras | <i>Puccinellia maritima</i> | Short grass |
| | Herbaceous seepweed | Schorrenkruid | <i>Suaeda maritima</i> | Flower |
| | Sea purslane | Zoutmelde | <i>Halimione portulacoides</i> | Flower |
| <i>Middle salt marsh</i> | Creeping bentgrass | Fioringras | <i>Agrostis stolonifera</i> | Short grass |
| | Red fescue | Rood zwenkgras | <i>Festuca rubra</i> | Short grass |
| | Saltmarsh rush | Zilte rus | <i>Juncus gerardii</i> | Short grass |
| | Sea milkwort | Zeemelkkruid | <i>Glaux maritima</i> | Short grass |
| | Sea thrift | Engels gras | <i>Armeria maritima</i> | Flower |
| | Sea wormwood | Zeealsem | <i>Artemisia maritima</i> | Flower |
| <i>High salt marsh</i> | Sea aster | Zeeaster/Zulte | <i>Aster tripolium</i> | Flower |
| | Sea couch grass (C) | Zeekweek/Strandkweek | <i>Elytrigia atherica/ Elymus athericus</i> | Tall grass |

Vegetation maps

The biodiversity of vegetation has been determined using aerial photo interpretation according to the VEGWAD program of Rijkswaterstaat (van Duin *et al.*, 2013). Vegetation maps of the study area are available for the years 2008 and 2014. These maps are constructed between July and September; by the end of the summer, when vegetation is full-grown (Vuik *et al.*, 2018).

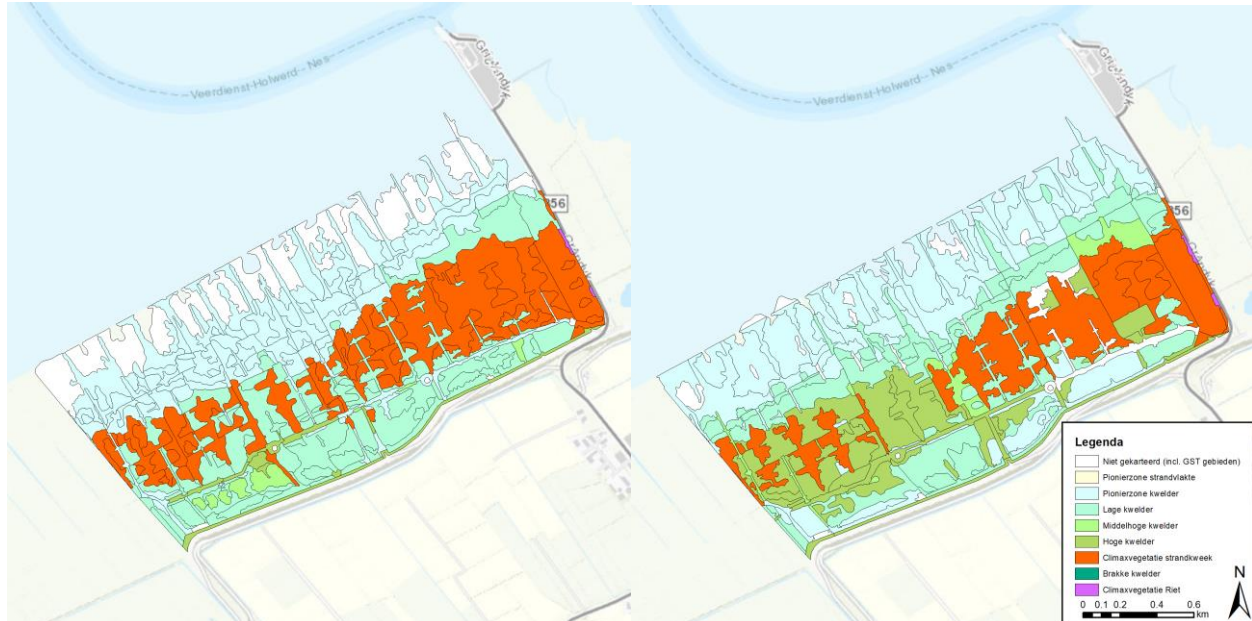


Figure 14 - Biodiversity of vegetation in 2008 (left) and 2014 (right) (Rijkswaterstaat, 2019).

From the vegetation maps of 2008 and 2014 (see Figure 14 above) the following conclusions can be formulated. Parts of the pioneer zone have developed into a low salt marsh, while parts of the low and middle salt marsh have transformed to the high salt marsh zone. Besides, climax vegetation has lost area to high salt marsh vegetation (sea aster), especially in the western part of the study area. In the former summer polder (between the summer and the sea dike), middle salt marsh vegetation has disappeared and against the sea dike a strip of pioneer vegetation has established.

Monitored vegetation

The speed of vegetation succession is decreased by grazing of animals (e.g. cattle, sheep and horses). Within measurement section 167, which is located in the study area at dike pole 38.8 (see Figure 20), extensive grazing has been applied during the period 1960-2014. This grazing method generally results in patterns of both low and high vegetation (van Duin *et al.*, 2013). The change in biodiversity of vegetation was determined in this measurement section. For this, covering percentages of salt-tolerant plants, classified per succession stage, were estimated in the subfields (100 x 100 m) C until G (from summer dike towards Wadden Sea). The resulting diagram is shown in Figure 15 for the period 1960-2014.

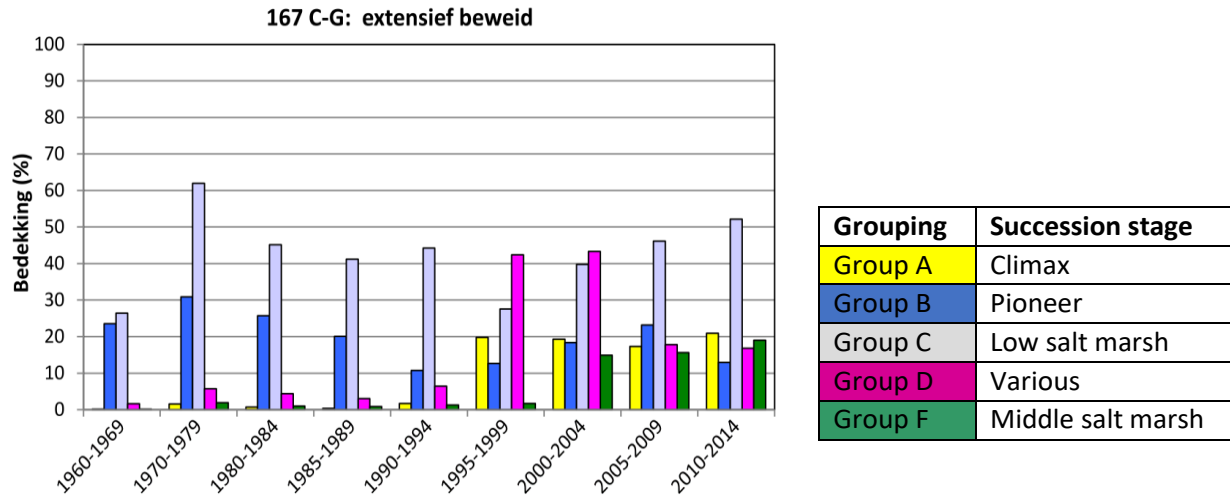


Figure 15 - Change in biodiversity of vegetation in measurement section 167 C-G during the period of 1960-2014 (van Duin *et al.*, 2013).

From Figure 15 above can be concluded that there is a pattern of succession visible in the period 1960-2014: at first there is mainly vegetation in the pioneer and low salt marsh zone, while later vegetation in the middle salt marsh and climax stage was observed. Consequently, the different vegetation zones from low to high follow each other in time until the succession reaches the climax stage. However, in comparison to intensive grazing, this process is slowed down in extensive grazing areas, so that different vegetation zones continue to co-exist, maintaining a relatively high biodiversity.

Vegetation properties

Salt marsh vegetation is capable of capturing and retaining sediment particles (Alterra, 2012a; Vuik *et al.*, 2016; Poppema, 2017; Vuik *et al.*, 2018; Willemsen *et al.*, 2018; Steetzel *et al.*, 2019). The higher the vegetation density of the patches, the more the flow is obstructed. Depending on sea dynamics and vegetation properties (e.g. type, stem height, diameter and flexibility), plants can withstand flows and grow and subsequently trap sediment or cannot withstand flows and break so that vegetation is constantly rejuvenated along the salt marsh platform. In general, it is assumed that the threshold for vegetation stem breakage is a T=1000-year event (Vuik *et al.*, 2018).

Vegetation stems exert (drag) force on the incoming water, so it functions as fluid resistance. The stability of the thin and highly flexible sea couch grass is highest in comparison to other common high growing (>50 cm) vegetation types (Steetzel *et al.*, 2019). Sea aster is thicker, high vegetation, but not as flexible. The vegetation properties of these types are presented in Table 3 below.

Table 3 - Vegetation properties expressed as model parameters (Vuik, 2019).

| Vegetation type (English) | Uniform height (m) | Uniform diameter (m) | Density (stems/m ²) | Drag coefficient (-) |
|---------------------------|--------------------|----------------------|---------------------------------|----------------------|
| Sea couch grass | 0.5 | 0.0013 | 1000 | 0.3 |
| Sea aster | 0.6 | 0.008 | 120 | 0.8 |

2.3. Overview of salt marsh dynamics

In order to understand the salt marsh system, an overview figure covering its dynamics is presented on the next page in Figure 17. It is known that salt marshes reduce waves in three ways: (1) depth-induced wave breaking, (2) wave energy dissipation by bottom friction and (3) wave attenuation by vegetation. The goal of this research is to quantify the wave reducing effect over the Holwerd West salt marsh considering the relative contribution of each of these three *bio-physical processes*. However, salt marshes are dynamic systems thus the wave reducing effect varies over time and differs per location. Its dynamics can be explained according to several time and space dependent *factors* that have been subdivided into *elements*. The factors are interconnected (see Figure 16 below) by which salt marshes develop (Internal development). For the quantification of the wave reducing effect, corresponding *model parameters* are mentioned, which are further described in chapter 3.

As mentioned before, there exist many interrelationships between the former discussed internal and external factors causing salt marsh dynamics and thus salt marsh development. An overview of these is depicted below in Figure 16. To be noted is that the internal factor 'Sediment availability' does not cause salt marsh growing in itself, but in combination with 'Wave action'. Besides, 'Wave action' can damage the salt marsh platform directly resulting in erosion and stem breakage.

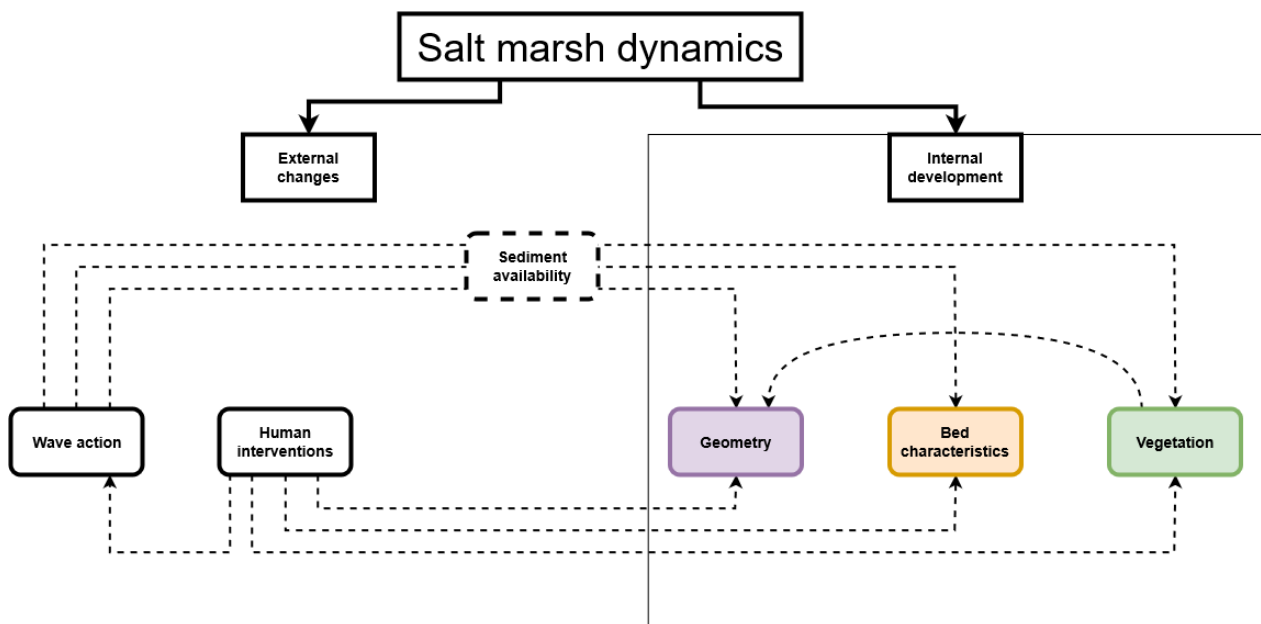
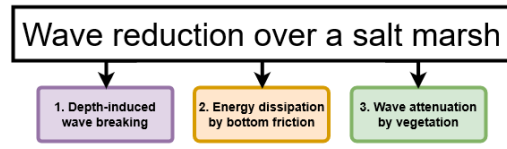
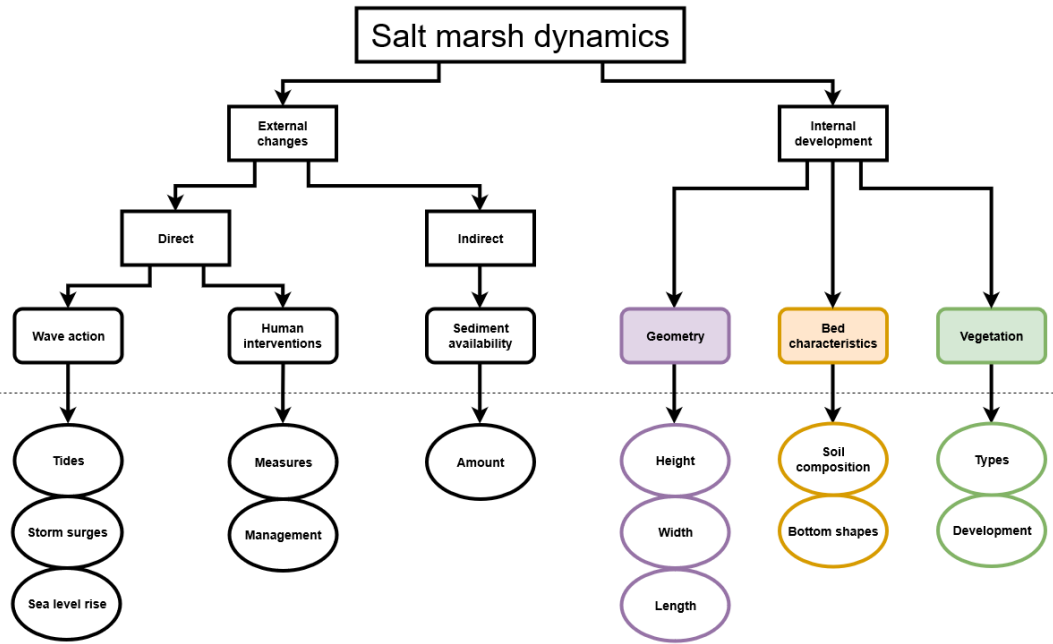


Figure 16 - Interconnectivities between factors responsible for salt marsh dynamics (Boer, 2019).

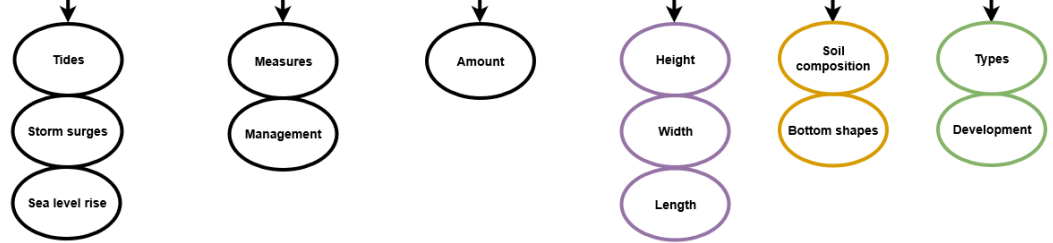
Bio-physical processes



Factors



Elements



Model parameters

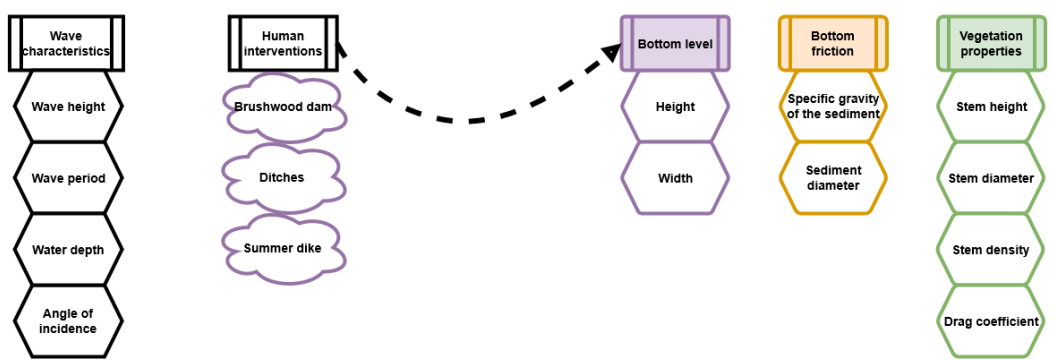


Figure 17 - Overview of salt marsh dynamics, which explains the wave reducing effectiveness over a salt marsh. Based on the three bio-physical processes, the most important factors that explain salt marsh dynamics were chosen. These were subdivided into elements and subsequently to (one-dimensional) model parameters (Boer, 2019).

2.4. Internal (salt marsh) development

The change of several factors was (mainly) investigated within the period of 1960 to 2014. In this subchapter, these findings together with knowledge about salt marsh dynamics are combined to explain the development of Holwerd West.

Salt marsh growing can be explained by wave action in combination with sediment availability (sediment supply) and vegetation, and human interventions. The sediment availability has been assumed sufficient for morphological development between 1960 and 2014.

Human interventions have stimulated the development of salt marshes in Friesland and Groningen since the Wadden Sea dike was constructed in the year 1250. In front of this coastal flood defense, mudflats could establish which have grown into salt marshes. This transition started in 1910, when the breakwater for the ferry service to Ameland was built. Since the dominant wave direction is northwest, this construction, together with the Wadden Sea dike, formed the boundaries of the Holwerd West coast against which salt marshes initiated to form.

Since 1950, Rijkswaterstaat has accelerated this accretion process by constructing salt marsh works and extending the breakwater. Within 8 years, the mudflat had turned into a salt marsh with a height of 1 m+NAP and a width of 160 m (Figure 11), due to the influence of tides and storms. On the platform, pioneer and low salt marsh vegetation could establish (Figure 18), which most likely have stimulated sedimentation by capturing and retaining grains. In the years afterwards the salt marsh height began to stagnate. This could be due to the fact that its platform increased faster (125 mm/year) than the sea level rise of 2 mm/y and therefore the GHW remained (approximately) 1 m+NAP. As a result, tides had less effect on salt marsh heightening and the relative effect of storms (high wave height events) increased. Since tides cause relatively low wave heights, these are the main driver of the salt marsh widening at a rate of 20 m/year.

From 1979 onwards, Holwerd West seems to have reached an equilibrium height of 2 m+NAP. Besides from the above-mentioned reason, this can be explained by the perspective change of salt marshes from land reclamation to natural areas. This namely induced that ditches were not maintained any longer. In 1989, the summer dikes were breached so that the salt marsh 'extended' and the (lower-elevated) summer polder was exposed to tides again. From this year onwards, salt-tolerant vegetation could establish between the summer and Wadden Sea dike. On higher grounds of the platform, vegetation development, in combination with the constant extensive grazing, has caused a high biodiversity of vegetation types. In most regions, the climax stage in this succession was reached with sea couch grass. Moreover, the top soil layer in 1960 consisted mostly of (very) fine silt and clay, while it is currently composed of very fine sand and coarse or medium silt. This implies that bigger and denser (thus heavier) grains (Table 1) had been transported to the foreland by means of wave action. On the one hand, this could mean that there had been a lack of relatively small particles (e.g. clay) for salt marsh raising. On the other hand, this could imply that more extreme storms had been taking place during which bigger particles were supplied. Meanwhile, the current (low-cohesive) soil composition is more likely to erode during storm events, which may be the reason that the salt marsh does not grow higher.

Nowadays, Holwerd West is 2.8 km in length (longshore direction), 1.2 km wide (cross-shore direction), and elevated at almost 2 m+NAP. An average elevation profile of Holwerd is displayed in Figure 18 below in which changes in salt marsh geometry between 1950 until 2014 are incorporated. In this figure, the annual average high water level (GHW) and the locations of the summer dike and sea dike are specified as well.

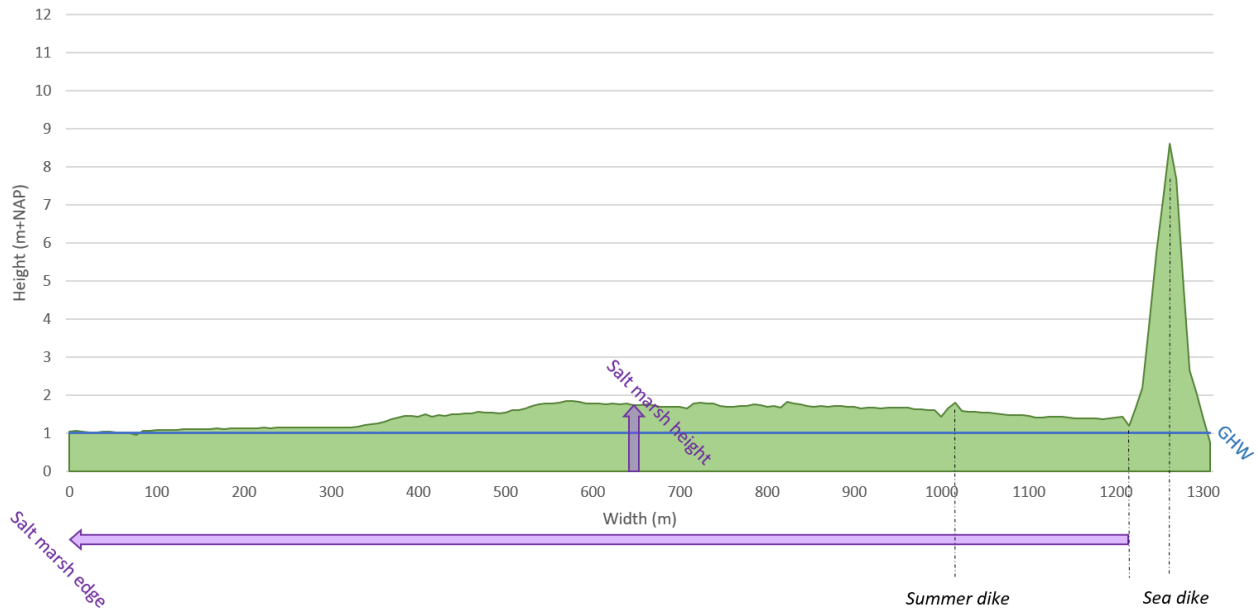


Figure 18 - An average elevation profile of Holwerd West in 2014 showing the morphological development of Holwerd West between 1950 and 2014 (AHN, 2019). The resolution is 5 m. The increase (m/y) in the salt marsh height and salt marsh edge is indicated with (purple) arrows. The locations of the summer and (Wadden) Sea dike, and the ditch in front of this, are indicated with black dotted lines.

Currently, brushwood dams can still be perceived in the pioneer zone (see Figure 9 below). On the low, middle and high salt marsh, these have disappeared underneath the surface, but the demarcation by ditches assures that sedimentation fields can be distinguished. People are not allowed to enter the landscape for recreation, so that cattle can graze next to breeding birds.



Figure 19 - Photos of the Holwerd West salt marsh taken in July 2019. Left: Brushwood dam in the pioneer zone. Right: The salt marsh seen from the Wadden Sea dike (Boer, 2019).

3. Quantification of the wave reducing effect

In this chapter is described what the wave reducing effect over the salt marsh of Holwerd West is in 2014, during storm events (RQ2). Firstly, the SWAN wave model is explained by which the wave height reduction and change in normative dike height was quantified. Thereafter, these results are provided considering the sensitivity of model input parameters.

3.1. Methodology

3.1.1. Model description

Simulating Waves Nearshore (SWAN) is a third-generation discrete spectral wave model to compute random, short-crested waves (Booij *et al.*, 1999a, 1999b). It does so by assembling all relevant processes of wave generation, dissipation, and nonlinear wave-wave interactions in a numerical code to simulate waves towards a shallow coast (e.g. a salt marsh).

The model is based on the (spectral) action balance equation according to Hasselmann *et al.* (1973) written as the properties of a flow field as described as functions of space coordinates and time. Due to the situation of salt marsh works and depth-contours at Holwerd West, waves are mainly refracted perpendicular to the coast (dike), thus a one-dimensional (1D) model without (longshore) currents is appropriate [$\partial(\dots)/\partial y = 0$]. Besides, since the salt marsh system is based on data of one year (2014) and changes in the geometry, bed characteristics and vegetation are not considered while using a storm event (for wave action), stationary modelling was applied [$\partial(\dots)/\partial t = 0$]. All in all, the energy balance equation for this situation reads (Holthuijsen, 2007):

$$\frac{\partial c_{g,x}E}{\partial x} + \frac{\partial c_{\theta}E}{\partial \theta} = S_{in} + S_{nl3} + S_{nl4} + S_{ds,w} + S_{ds,di} + S_{ds,bf} + S_{ds,veg} \quad (1)$$

Herein is E the energy density spectrum (m^2/s) and $c_{g,x}$ the group wave celerity perpendicular to the coast (m/s), and c_{θ} the wave celerity in the direction of wave propagation (m/s). On the right-hand side, physical processes are present that are either sink/source (m^2/s) terms or redistribute wave energy. In this, S_{in} is the wave growth by the wind (source), S_{nl3} and S_{nl4} represent non-linear transfer of wave energy through wave-wave interactions (redistribution), $S_{ds,w}$ denotes wave decay due to whitecapping (sink), and $S_{ds,di}$, $S_{ds,bf}$ and $S_{ds,veg}$ indicate wave reduction because of the bio-physical processes (sink): depth-induced wave breaking, bottom friction and vegetation. These (bio-)physical processes are described in more detail in Appendix H and the consideration of the bio-physical processes is explained in the next paragraph. The relationship between the (significant) wave height and the wave energy E is as follows:

$$E = \frac{1}{8} \rho_w g H_{rms}^2 \quad (2)$$

Where ρ_w is the density of water (kg/m^3), g gravitational acceleration (m/s^2) and H_{rms} root mean square wave height (m). The significant wave height H_s can be obtained by dividing the latter parameter by 0.71 (Holthuijsen, 2007).

3.1.2. Modeling approach

As mentioned before, the wave reducing effect of a salt marsh differs per location and moment in time (e.g. storm conditions). The salt marsh system was schematized using factors (see Figure 17) that explain its wave reducing effect.

In this way, the system of 2014 was implemented, which is the year for which most up-to-date data is available and on which the dike assessment had been carried out in 2017. Consequently, the salt marsh characteristics of 2014 were used to approximate the current wave reducing effect of Holwerd West.

The corresponding model parameters (i.e. wave characteristics, bottom level, bottom friction and vegetation properties) are described in the upcoming paragraphs. The factor human interventions was hereby incorporated in the bottom level, while sediment availability was left out because of stationary modelling.

Model area

Wave characteristics were taken from the Hydraulic Boundary Conditions of the dike assessment database of Hydra-NL (Rijkswaterstaat WVL, 2018b). These values for wave height, wave period, angle of incidence and water level, are based on 2D SWAN calculations of the Wadden Sea (Klein and Kroon, 2011; Deltares, 2017a, 2017b). An overview of these values is presented in Appendix J.

The resulting set of wave characteristics are available at hydraulic boundary locations ('HR locaties'): WTI 2011 and WBI 2017 locations (see Figure 20 below). The most recent set of wave characteristics that could be used for salt marsh calculations (e.g. stability, wave reduction) is from 2011 and was therefore used to implement wave events in 2014. These WTI2011 locations were situated at the edge of the salt marsh in 2005, approximately at the NAP+1.0 m depth-contour, 800-900 m from the outer (Wadden Sea) dike toe. The WBI2017 locations are situated 50 m from the outer dike toe and are usually used to base calculations for dike assessment (i.e. failure mechanisms) on. All in all, the transects were taken from a WTI 2011 location to a WBI 2017 location in the lateral ditch direction, which is approximately perpendicular to the dike and corresponds to the dominant wind direction range of 300-330 degrees North (see Appendix J).



Figure 20 - The transects that were modeled from a WTI2011 location to a WBI2017 location (Rijkswaterstaat WVL, 2018b). The left one had high wave reducing potential and the right one low wave reducing potential. The elevation map represents the geometry of Holwerd West in 2005, in which the WTI2011 locations are approximately located at the NAP+1.0 m depth contour, at GHW level (Figure created from Klein and Kroon, 2011).

Two representative transects were chosen: one with high wave reducing potential and one with low wave reducing potential, so that spatial extremes are covered. These were picked assuming that wave reduction due to depth-induced wave breaking has the largest relative contribution. This is in accordance with findings of the POV-W along the Wadden Sea coast of Friesland (Steetzel *et al.*, 2019). Consequently, the widest (cross-shore) and most (elevation) varying bottom profile of 2014 represented the high wave reducing potential and vice versa.

The chosen transects are shown on the previous page in Figure 20 in which their location and names of the hydraulic boundary locations are specified. The method used to choose these transects, from a set of 12, is described in Appendix I. Their elevation profiles are provided in Appendix K.

Input parameters and initial and boundary conditions

The different transects of Holwerd West were modelled according to model parameter values that approximate the salt marsh system in 2014 best. These are described in the paragraphs below of which an overview is presented in Appendix J. The input consisted of a wave spectrum, a bottom level profile, and the wind speed and water level during a storm event.

The wave spectrum corresponded to waves that are distributed over the transects. Since SWAN is based on wind-generated waves and the Wadden Sea contains waves with periods between 0.5 s and 33 s, its frequency range was 0.03 – 2 Hz (Steetzel *et al.*, 2019).

The bottom level profiles of both the high and low wave reducing potential transect were implemented with a resolution of 0.5 m (AHN, 2019). In these profiles, both the salt marsh geometry and human measures were considered, such as ditches and summer dikes. However, brushwood dams were not considered because these are only emergent in the pioneer zone below the (low) salt marsh (elevated lower than 1 m+NAP).

The water level and wind speed corresponded to a storm event with a certain return period. Interesting storm events were $T=100$, $T=1000$, $T=10,000$ and $T=37,500$ years. The first event represented a storm without vegetation stem breakage (Vuik *et al.*, 2018). The second included stem breakage and represented the maximum allowable probability of flooding, which indicates the minimum level of protection that the flood defense should provide. Inclusion of the more extreme third allowed for determining a trend through the results. The final storm represented the failure mechanism 'grass erosion on the inner crest and slope' (GEKB), which incorporates wave overtopping (Ministerie van Infrastructuur en Milieu, 2017). Using this event, the translation from wave reduction towards normative dike height could be performed.

For each $T=x$ event, the water levels were more or less similar at the WT12011 and WBI2017 locations (Rijkswaterstaat WVL, 2018b). Consequently, the water level above the transects was kept constant. Wave-induced water level changes are thus neglected. In this way the change of the significant wave height along the transect was better modeled. For a $T=x$ event, the average wind speed and dominant direction were applied, and both the initial and hydraulic boundary conditions were represented by the (significant) wave height, (peak) wave period and angle of incidence. The latter corresponded to the dominant wind direction during an extreme event.

Physical parameters

The three bio-physical processes were modeled considering their model parameters, which is described in the paragraphs below. The values for these model parameters were derived from findings in Chapter 2.

Depth-induced wave breaking, collapsing waves due to a change in water depth as a result of a varying bottom level, was modelled according to Salmon *et al.* (2015). This method is namely applicable for platforms for which the slope is smaller than 1:700, which is the case for Holwerd West (on average 1:4000) (AHN, 2019). This approach was set up after the conclusion that significant wave heights over approximately horizontal bathymetries were typically underpredicted in locally generated wave conditions (Salmon *et al.*, 2015).

Wave energy dissipation by bottom friction was generated following principles of Smith *et al.* (2011). This process was schematized by bedforms that counteract flow, which are solid in case of cohesive sediments (e.g. silt and clay) (Smith *et al.*, 2011). Ripples were schematized using the grain diameter and specific gravity of the sediment and translated to a (Nikuradse) roughness length. In case of no ripples, the formulation incorporated that friction was solely based on the grain size. The main soil types on the top layer are very fine sand and coarse or medium silt. Both very fine sand and coarse silt have grain sizes of 62 μm , which correspond to a wet density of 1400 kg/m^3 (see Table 1). This value is in accordance with the wet density of sludge (TU Delft, 1999). The density of (salt) sea water is 1025 kg/m^3 . Consequently, the specific gravity of sludge is 1.37.

Wave attenuation by vegetation was realized using the vegetation module of Dalrymple *et al.* (1984). This method was especially implemented in SWAN to model salt marsh vegetation fields (Dalrymple *et al.*, 1984; The SWAN Team, 2019b). Herein vegetation stems are schematized as cylinders, of a certain height, diameter, density and a drag coefficient, that obstruct flow. This was appropriate to model sea couch grass with (Vuik *et al.*, 2018; Steetzel *et al.*, 2019), which is mostly present along the transects. Its corresponding parameter values are presented in Table 3. As mentioned before, vegetation stems were assumed to break for $T=1000$ years or rarer events. In these cases, the stem height was assumed 20% of the original (Vuik *et al.*, 2019).

Other physical processes that were considered are wave growth by wind, wind drag, whitecapping, wave-wave interactions (i.e. quadruplets and triads) since these increase the reliability of the outcomes (Ministry of Transport Public Works and Water Management, 2000; Klein and Kroon, 2011). The first two serve as wind (wave) input, whitecapping causes wave energy dissipation (as do the bio-physical processes), and quadruplets and triads (i.e. wave-wave interactions) redistribute waves. Their values were taken according to the default values of SWAN (The SWAN Team, 2019b). These are namely based on literature studies (i.e. calibration, validation and verification studies) (Gautier, 2010). More explanation about these processes is provided in Appendix H.

3.1.3. Wave height reduction and relative contribution

Wave height reduction

In order to estimate the influence of a salt marsh on waves, the salt marsh system of 2014 was implemented in SWAN. The SWAN model transformed offshore wave conditions to nearshore conditions per spatial step (0.5 m) so that the wave height was calculated at 50 m from the Wadden Sea dike toe (at the WBI2017 location). Subsequently, the wave height reduction was determined by subtracting this outcome to the initial wave height (at the WTI2011 location), which formed a hydraulic boundary condition.

Relative contribution

The relative contribution was determined by stating that a certain bio-physical process contributed x% to the total wave energy dissipation resulting in the final wave height reduction. Wave energy dissipation is induced by the bio-physical processes and whitecapping. This latter steepness-induced wave breaking process was neglected for the calculation of the relative contribution because it could not directly be assigned to a salt marsh characteristic.

In formula form:

$$rc_{di} = \frac{\sum_{i=1}^N S_{ds,di}}{E_{ds}} = \frac{\sum_{i=1}^N S_{ds,di}}{\sum_{i=1}^N S_{ds,di} + \sum_{i=1}^N S_{ds,bf} + \sum_{i=1}^N S_{ds,veg}} \quad (3)$$

In which rc_{di} denotes the relative contribution of depth-induced wave breaking, N the number of grid points, $S_{ds,di}$, $S_{ds,bf}$ and $S_{ds,veg}$ indicate wave dissipation due to the three respective bio-physical processes, and E_{ds} the sum of these latter three. This equation was adapted to obtain rc_{bf} and rc_{veg} , in a similar way.

3.1.4. Translation to normative dike height

The normative dike height ('Hydraulisch Belastingniveau') is the required crest height at which water levels and waves can be attacked safely (Deltares, 2017a). In case of the Wadden Sea dike, the critical overtopping rate is 0.1 L/s/m for the failure mechanism GEKB at a dike cross section (Witteveen+Bos, 2017b). The input for the HBN calculations consists of the wave characteristic values and bottom level profiles for the corresponding T=37,500-year event.

Wave characteristic values (i.e. water level, wave height, wave period and angle of incidence) were calculated by the SWAN model at 50 m from the outer dike toe. Based on the sensitivity analysis for the final wave height outcome, best and worst scenarios were chosen to indicate a change in HBN.

Bottom level profiles were implemented from a WBI2017 location perpendicular to the dike crest. These profiles were used for the dike assessment of Koehool-Lauwersmeer (which includes Holwerd West) in 2017, as well (see Appendix C). The HBN calculations were performed using Hydra-NL (Rijkswaterstaat WVL, 2018b). A more detailed description of the method for determining the HBN at both locations, is provided in Appendix L.

3.1.5. Reliability of model outcomes

Wave measurements have not been performed on the Holwerd West salt marsh; thus validation was not possible in this research. Nonetheless, SWAN default parameter values are based on studies (i.e. calibration, validation and verification studies) (Gautier, 2010). It has been proven that these values compare well with analytical solutions, laboratory observations, and (generalized) field observation (Booij *et al.*, 1999a). This implies that the values have been tested and were able to represent a random shore situation, such as a salt marsh, sufficient.

For verification, the wave height calculated at a WBI2017 location has been compared to the original hydraulic boundary condition value at this location, on which dike safety assessments are currently based (see Table 6). These original values are based on a 2D SWAN model of the Wadden Sea. The corresponding SWAN settings, except for the consideration of bio-physical processes, form the 'basis script' for the SWAN calculations for this thesis (see Appendix J).

Moreover, by simulating two transects with minimum and maximum wave reducing potential while considering different considerations for the bio-physical processes, spatial variety was taken into account.

Sensitivity analysis

Sensitivity analysis was used to obtain insight into the relative importance of model input on the outcome (relative importance should not be confused with the relative contribution of a bio-physical process to wave reduction). This was performed by varying input values for bio-physical processes and subsequently calculating the final wave height at a WBI2017 location. In this way, the sensitivity of depth-induced wave breaking, bottom friction and vegetation was investigated in terms of spatial uncertainty.

Since each of the input parameters for a bio-physical process is proportional to the wave energy dissipation, one parameter per bio-physical process was sufficient to determine its relative importance (The SWAN Team, 2019a). During storm events, vegetation is subject to stem breakage. If this occurs, the stem height was 20% of the original (Vuik *et al.*, 2019), thus a reduction of 80%. Since the influence of vegetation is debatable among researches, stem breakage was explicitly investigated. Accordingly, in case of vegetation stem height, 80% reduction (stem breakage) was used for a T=100 years event, while an 80% increase (no stem breakage) was used for rarer events. Representative parameters for the other bio-physical processes were reduced accordingly. The breaking parameter was thus set to 0.2 implying a lower breaking percentage (Salmon *et al.*, 2015). In case of no bottom ripples, the bottom friction only depends on the grain diameter (Smith *et al.*, 2011). Therefore, the grain size was reduced by 80%, resulting in a value of 12 μm which represents fine silt (Table 1). An overview of the range of input values used for the sensitivity analysis is presented below in Table 4.

Table 4 - Input values of bio-physical processes for sensitivity analysis.

| Bio-physical process | Parameter | Range |
|--|--------------------|-----------------------|
| (1) Depth-induced wave breaking | Breaking parameter | 0.2 - 1.0 (-) |
| (2) Wave energy dissipation by bottom friction | Grain size | 12 - 62 μm |
| (3) Wave attenuation by vegetation | Stem height | 10 - 50 cm |

3.2. Results

3.2.1. Wave height reduction and relative contribution

Wave energy changes along the transect, from the start (WTI2011 location) to the end (WBI2017 location). This is depicted in figures in Appendix K. At this end, the significant wave height was calculated (H_s_{calc}) and compared to the initial WTI2011 value (H_s_{WTI}), resulting in a significant wave height reduction (ΔH_s) over the salt marsh. Besides, the relative contribution (rc) of each of the bio-physical processes (i.e. di, bf, veg) resulting in this outcome was determined using Equation (3). The results are presented in Table 5 below.

Table 5 - Significant wave height reduction (ΔH_s) and corresponding relative contribution (rc) of each of the three bio-physical processes. 'Low' and 'High' refer to the low and high wave reducing (potential) transect, and 'T=x' represents the return period of a storm event.

| Transect | T=x (years) | rc_di (%) | rc_bf (%) | rc_veg (%) | Hs_calc (m) | Hs_WTI (m) | ΔH_s (m) | ΔH_s (%) |
|----------|-------------|-----------|-----------|------------|-------------|------------|------------------|------------------|
| Low | 100 | 30% | 24% | 45% | 0.75 | 1.36 | -0.61 | -45% |
| | 1000 | 28% | 52% | 20% | 1.37 | 1.68 | -0.31 | -18% |
| | 10000 | 32% | 48% | 20% | 1.69 | 2.00 | -0.31 | -15% |
| | 37500 | 30% | 48% | 21% | 1.90 | 2.18 | -0.28 | -13% |
| High | 100 | 41% | 20% | 38% | 0.68 | 1.45 | -0.77 | -53% |
| | 1000 | 46% | 38% | 15% | 1.14 | 1.77 | -0.63 | -36% |
| | 10000 | 51% | 35% | 15% | 1.37 | 2.10 | -0.73 | -35% |
| | 37500 | 52% | 34% | 15% | 1.57 | 2.28 | -0.71 | -31% |

From the table can be derived that, over the low wave reducing transect in case of a T=100-year event, the wave height is reduced by 0.61 m (45%). This is mainly due to wave attenuation by vegetation (45%), followed by depth-induced wave breaking (30%) and energy dissipation by bottom friction (24%). In case of more extreme events for the same Hs transect, energy dissipation by bottom friction is dominant. This can be explained by the relative high occurrence of this bio-physical process above gentle bottom level slopes (Le Hir *et al.*, 2000).

In general, during the T=100-year event, wave heights are most reduced, which is mainly due to the contribution of vegetation. On the contrary, during more extreme events, the relative contribution of vegetation is lowest because of stem breakage. When comparing the outcomes for both transects, it appears that waves are more reduced along the high potential profile for each T=x event. This confirms the hypothesis that waves are more reduced above a wide (cross-shore) and highly (elevation) varying bottom profile during storm events. Along this profile, depth-induced wave breaking is dominant for all storm events, and its relative contribution increases when storms get more extreme.

In addition, the relative contribution was visualized along both transects for the storm events, which depicted in Appendix K. From these observations, some general conclusions can be drawn. At first, most wave energy gets dissipated along the first part of the salt marsh; within 100-450 m. This is mainly because of depth-induced wave breaking which occurs when waves are relatively high compared to the water depth (i.e. relatively high H/d-ratio), which is the case in the first 50-70 m (near the WTI2011 boundary). Further onshore, vegetation has the largest relative contribution in case of a T=100-year event and bottom friction in case of more extreme storm events.

Furthermore, the significant wave height decreases most in the first 25-100 m, which is thus mostly due to depth-induced wave breaking. In case of the high profile, the wave height reduces above the summer dike as well. On average, this summer dike locally reduces waves by 30 cm (24%) during storm events (see Appendix K).

Besides, during all storms, the wave height increases over the last part of the transect. Wave growth by wind is here namely higher than the total energy dissipation caused by whitecapping and the three bio-physical processes. In other words: $S_{in} > S_{ds,w} + S_{ds,di} + S_{ds,bf} + S_{ds,veg}$ (see Equation 1).

3.2.2. Sensitivity analysis

By alternately changing input values of the bio-physical processes by 80% according to Table 4, their sensitivity on the wave height reduction at the WBI2017 location (ΔH_s) was determined. The sensitivity of each of the bio-physical processes per transect and T=x event is depicted in Figure 21.

From the figure below can be concluded that the input value for wave attenuation by vegetation (veg) is most sensitive, because it differs most from the reference value for the wave height reduction during different storm events (see Table 5). This implies that the occurrence of stem breakage makes a significant difference in the outcome for wave height reduction (ΔH_s). This is especially the case for the low wave reducing profile (Low). For example, in case of a T=100-year event over the low wave reducing transect, the final wave height would be reduced by 28% rather than 45% when all vegetation stems had broken down. In case of extremer storms if stems would not break, the wave height would on average decrease by another 18%. In case of the high wave reducing profile, the sensitivity of the input for depth-induced wave breaking and wave attenuation by vegetation is comparable but relatively low (< 8%), and that of bottom friction is lowest (2%). This implies that spatial changes do not affect the wave height reduction much. In other words, the wave reducing capacity is relatively stable compared to the low wave reducing profile.

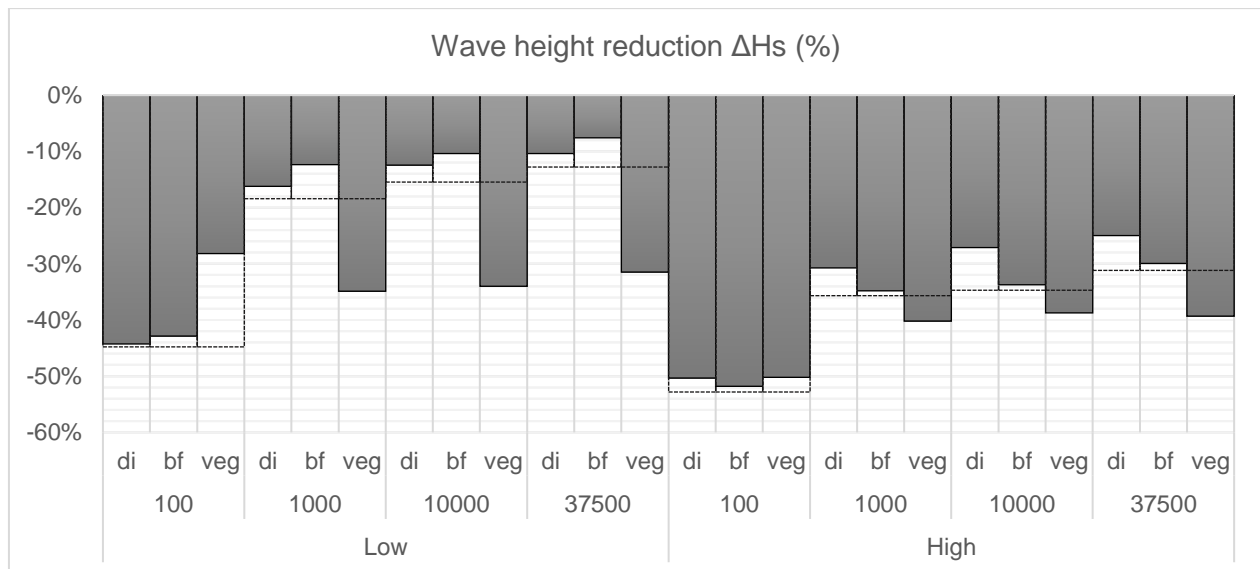


Figure 21 - Sensitivity of the input for the bio-physical processes (i.e. di, bf and veg) expressed in the resulting wave height reduction ΔH_s (in grey). 'Low' and 'High' refer to the low and high wave reducing (potential) transect, and the numbers 100, 1000, 10000 and 35000 represent return periods of storm events. Stem breakage (veg) occurs in case of T=100-events while stems withstand flows in case of extremer storm events. The horizontal dotted lines (in black) depict the reference values of the latter according to the current situation, presented in Table 5.

3.2.3. Normative dike height

Because of salt marsh characteristics, the wave height (H_{s_calc}) and spectral wave period ($T_{m-1,0_calc}$) calculated at the WBI2017 location are different than the original WBI2017 values (H_{s_WBI} and $T_{m-1,0_WBI}$) at this location. Together with the water level and angle of incidence during a storm event, these wave characteristics are used to determine the normative dike height of the adjacent dike for a $T=37,500$ -year event. The spread in the final wave height (H_{s_calc}) is based on the current situation (best case scenario) and the least wave reducing scenario (worst case scenario). Although scenarios without stem breakage allow for the most wave reduction, it is unlikely that this occurs during such an extreme storm event. Therefore, the outcomes for the current situation, presented in Table 5, were used to represent the best-case scenario. In Table 6 below, the HBN outcomes are presented.

Table 6 - Calculation of the normative dike height (HBN). The location of the dike poles adjacent to both transects is indicated. The values are sorted according to the final wave height values (H_{s_calc}).

| Transect | T=x (years) | h (m+NAP) | H_{s_calc} (m) | H_{s_WBI} (m) | $T_{m-1,0_calc}$ (s) | $T_{m-1,0_WBI}$ (s) | dir (°N) | HBN_calc (m+NAP) | HBN_WBI (m+NAP) | Δ HBN (m) |
|----------------|-------------|-----------|-------------------|------------------|-----------------------|----------------------|----------|------------------|-----------------|------------------|
| Low (dp 40.5) | 37500 | 5.31 | 1.90 | 1.89 | 4.29 | 4.27 | 330 | 8.70 | 8.68 | 0.02 |
| | | | 2.02 | | 4.35 | | | 8.84 | | 0.16 |
| High (dp 38.8) | 37500 | 5.23 | 1.57 | 1.91 | 4.57 | 4.27 | 330 | 8.42 | 8.83 | -0.41 |
| | | | 1.71 | | 4.57 | | | 8.56 | | -0.27 |

From the table can be derived that the normative dike height is lowest when the calculation is performed with parameter values that correspond to the lowest significant wave height (best case scenario in which waves are most reduced). Moreover, the normative dike height at dike pole 38.8 can be reduced in case of the $T=37,500$ -year event by 27 cm (3%) and 41 cm (5%), respectively in the worst- and best-case scenario. However, for the low transect, the HBN is higher because of the relatively low original (WBI) wave condition values.

The Wadden Sea dike is elevated at 9.0 m+NAP at both locations. Since the calculated normative dike heights are lower than this, the dike section would be accepted. This is in line with the approval of the dike trajectory along Holwerd West on the failure mechanism GEKB (see Appendix C). Nonetheless, this may not be the case along other dike trajectories along the Dutch coast. Furthermore, the salt marsh characteristics reduce wave heights and thus the hydraulic load on the adjacent dike. Consequently, salt marshes can have a positive effect on failure mechanisms that are affected by this, such as the group 'wave impact on revetments' (e.g. AGK and GEBU). More information about this is provided in Appendix C.

To be noted is that the calculated spectral wave period is higher than the original values. This finding is strengthened by measurements performed above a salt marsh in the province of Groningen (Steetzel *et al.*, 2019). Here was namely perceived that the wave period increases from the salt marsh boundary towards the dike.

4. Salt marsh adaptations

Salt marshes are dynamic systems as a result of an interplay between external and internal factors. In this chapter, the focus is on the external factor 'human interventions'. There are many alternatives for salt marsh adaptations that improve flood protection for the hinterland. In this chapter, recommendations for Holwerd West (RQ3) are provided. The previous chapters provided insight into the factors and elements of a salt marsh system. This knowledge combined with the findings about the relative contribution and relative importance (sensitivity) during extreme conditions forms the basis for these recommendations for salt marsh adaptations. Adaptations towards higher wave reduction due to the characteristics of salt marshes namely assure a higher level of protection for the hinterland, now and in the future.

Recommendations for salt marsh adaptations are thus made in favor of flood protection while assuming that each of the three bio-physical processes can (regulatory) be adjusted by humans. It should be mentioned that natural values (e.g. conservation of wetland area and habitats) have the highest importance since 1979 and that the Wadden Sea region has become part of the European Natura 2000 network and is appointed UNESCO World Heritage since 2009. Salt marsh management has therefore adjusted to a more sustainable way in which natural processes can proceed in an (almost) undisturbed way. However, since a few years, the perspective of coastal protection is gaining more attention. This has resulted in many flood protection projects along the Wadden Sea coast. Examples of these are a 'mud motor', depoldering of a summer polder into a salt marsh, creating a fresh-salt water environment, and dike improvements. An overview of the latest projects along the Wadden Sea coast between Koehool and Lauwersmeer is presented in Appendix M.

Based on the results, a distinction can be made between the low and high wave reducing transect. The wave reducing effect above a narrow, low (elevation) varying salt marsh profile is mostly contributed to bottom friction as a result of bed characteristics (i.e. large average sediment grain size). In favor of wave attenuation by vegetation and subsequently depth-induced wave breaking, a landscape with high vegetation diversity can be created. This diversity causes a difference in salt marsh elevations as a result of the different extents in capturing of sediment particles. In this way, a high (elevation) varying bottom profile can develop which reduces waves most (see Table 5). This process can be stimulated by planting (stable and flexible) vegetation such as common saltmarsh-grass in low zones and sea aster in high salt marsh zones (see Table 2 and Table 3). Meanwhile, the extensive grazing regime should be sustained (by cattle, horses and sheep) because this results in a high plant diversity rather than solely sea couch grass (see Figure 14 and Figure 15). Even though this climax vegetation causes highest fluid resistance (Steetzel *et al.*, 2019), if it breaks, it only contributes 20% to the wave height reduction (see Table 5).

In case of the high wave reducing profile, the wave reducing effect is relatively stable, even when the spatial variability is large (see Figure 21), and mainly contributed to depth-induced wave breaking (see Table 5). Simultaneously, wave attenuation by vegetation and possible stem breakage has less effect on the wave height reduction. Summer dikes play a big role in causing wave reduction and should thus be maintained by Rijkswaterstaat.

In general, the wave reducing effect can thus be increased by stimulating salt marsh growth. This can be achieved by maintaining the salt marsh works, both the brushwood dams and ditches. However, if chosen for a sludge nourishment, the maintenance of the ditches should be postponed after all the sediment has been supplied.

In this way, relatively small sediment grains can settle on the platform so that it raises more easily during high water events (even tides). For this, dredged sediment from the waterway Holwerd-Ameland could be used. The expectation is that this measure accounts for an extra accretion of 1 cm/year, according to results of a 'mud motor' experiment at Koehool (Arcadis, 2018). Next to this, the salt marsh will widen more than 20 m/year until the navigation channel (see Figure 5 and Figure 10) has been reached. In addition, the erodibility of the bed will decrease because of the relatively high clay content. The urge for sludge nourishment is strengthened by statements of Best et al. (2018) indicating that salt marshes will partially or completely drown under sea level rise scenarios. When the ditches are being maintained again, vegetation will rejuvenate so that low salt marsh vegetation can flourish again (de Groot *et al.*, 2013).

5. Discussion

Whether a salt marsh can contribute to flood protection, depends on its wave reducing effect during a storm event. However, as salt marshes are dynamic systems, this effect differs per location and changes over time and corresponding flood event. Nevertheless, the results for the wave reducing effect of Holwerd West are comparable to the ones obtained by the POV-W at another location within the salt marsh of NFB. This transect is located 3 km southwest of Holwerd West, 1000 m wide (cross-shore) and called 'Waddenzee_locatie0501' (see Appendix D). Here, a wave height reduction of 0.68 m was calculated in case of a storm event with a return period of 1/10,000 years (Steetzel *et al.*, 2019). Depth-induced wave breaking contributed most to this (71%), followed by bottom friction and vegetation (together 29%). These findings are more or less similar to the results for the high wave reducing transect (827 m wide) for Holwerd West for both a T=10,000-year and a T=37,500-year event for which an average wave height reduction of 0.72 m was determined. However, depth-induced wave breaking only caused 52% of this. The reasons for this are explained in the next paragraphs.

Firstly, this can be explained by the different consideration of bottom level profiles. The POV-W uses a schematized transect, while realistic bottom profiles were used in this research. The salt marsh is approximated as a horizontal platform with a height of 1.5 m+NAP and descends with a slope of 1:100 towards a height of 0.5 m+NAP. In this study, the high wave reducing profile had an average height of 1.5 m+NAP, included a summer dike, but did not descend with a slope towards the WT12011 location. This is because the WT12011 locations are currently located at a (middle salt marsh) height of 1.5 m+NAP. The low salt marsh was thus not considered in this study and no slope was implemented as a consequence. If this would have been considered, the wave reducing effect would be higher. Since the influence of depth-induced wave breaking increases by such a slope, its relative contribution would have been larger. Likewise, potential cliffs at the edge of the salt marsh would have stimulated wave damping as well (Willemsen *et al.*, 2018).

Secondly, this could be due to the difference in considering the bottom friction and vegetation. The POV-W combines the wave reducing effect of these bio-physical processes in terms of roughness, while a distinction between these two was made in this research. As a consequence, the relative contribution differs because the bio-physical processes are modelled in a non-linear way in SWAN (The SWAN Team, 2019a).

Next to this, it was found that most energy is dissipated within 150 m during a T=100-year event and within 450 m during more extreme events. Although the salt marsh was modelled while starting from the middle salt marsh zone, these findings are in line with field measurements performed during tidal flooding events at a salt marsh along the Westerschelde which suggest that this occurs within 200 m (Möller *et al.*, 1999). Moreover, the reduction in significant wave height is 50% in case of another vegetated foreland with similar characteristics in this region during a T=100 event (Vuik *et al.*, 2016), which is comparable to that of Holwerd West (45-53%). Nonetheless, for a rarer event of T=1000 years, this is 40%, while outcomes for Holwerd West showed 18-36% reduction. This could be due to the relatively high elevation varying bottom profile that was used for that study with a maximum height difference of 1.4 m. In this research, for Holwerd West, this was 0.76 m and 2.3 m for the low and high wave reducing transect.

6. Conclusions and recommendations

The goal of this study is to determine the wave reducing effect over the 'Holwerd West' salt marsh during storm event and to set up recommendations for salt marsh adaptations to increase this effect. To achieve this goal, three research questions were defined of which their answers are presented below. At last, recommendations for further research and towards stakeholders are explained.

6.1. Conclusions

Salt marsh development

The first research question is: *'How did the 'Holwerd West' salt marsh develop?'*

The development of a salt marsh can be explained by an interplay between external (i.e. wave action, human interventions and sediment availability) and internal factors (i.e. geometry, bed characteristics and vegetation). Holwerd West initiated to form after the completion of the Wadden Sea dike in 1250. Its growth has been stimulated because of the breakwater for the ferry service to Ameland since 1910 and the salt marsh works since 1950 but has stagnated up until a height of 2 m+NAP, while its width is still increasing with 20 meters per year. Nowadays, the platform is 2.8 km long (longshore direction) and 1.2 km wide (cross-shore direction) and generally exists of very fine sand and coarse silt in the top layer above which sea couch grass has established.

Quantification of the wave reducing effect

The second research question is: *'What is the wave reducing effect of the 'Holwerd West' salt marsh during storm events?'*

The wave reducing effect over the Holwerd West salt marsh was quantified using a stationary, one-dimensional SWAN wave model considering two transects.

The wave height reduction appeared highest for the wide (cross-shore) and high (elevation) varying bottom profile, respectively 53%, 36%, 35% and 31% for the storm events T=100, T=1000, T=10,000 and T=37,500 years. The relative contribution of depth-induced wave breaking to these wave height reductions was largest, especially along the first 25-50 meters. Considering the wave reducing capacity of the high wave reducing profile, the normative dike height was 23 to 41 cm lower than the original (WBI2017) value in case of a T=37,500-year event, representing the norm for an overtopping failure mechanism (GEKB).

In case of a narrow (cross-shore) and low (elevation) varying bottom profile, the wave reduction was 45%, 18%, 15% and 13% for the storm events T=100, T=1000, T=10,000 and T=37,500 years. Wave attenuation by vegetation was dominant for a T=100-year event, and wave energy dissipation by bottom friction for more extreme events.

Salt marsh adaptations

The third research question is: *'Which salt marsh adaptations can be implemented to increase its wave reducing effect?'*

In order to increase the wave reducing effect of Holwerd West, it is recommended to create a landscape with high vegetation diversity. This diversity causes a difference in salt marsh elevations as a result of the different extents in capturing sediment particles. In this way, a high (elevation) varying bottom profile can develop which reduces waves most.

This can be achieved by planting (stable and flexible) vegetation and maintaining the extensive grazing principle (by cattle, horses and sheep). At places where summer dikes are present, it is advised to preserve these because these contribute significantly to wave reduction. In general, the wave reducing effect can be increased by stimulating salt marsh growth, which can be accomplished by maintaining the salt marsh works, both the brushwood dams and ditches. Additionally, a sludge nourishment could account for a sufficient (clay-containing) sediment supply, which will decrease the erodibility of the bed as well.

6.2. Recommendations

It is possible to make several recommendations based on this thesis for future research and towards stakeholders.

Firstly, the final wave heights calculated at the WBI2017 locations for the T=100, T=1000 and T=10,000-year event can be used to base a new dike assessment for Holwerd West on (see Table 5). It is advised to use the original spectral wave values at these locations hereby. For a T=37,500-year event, the calculated wave heights and wave periods at the WBI2017 locations can be used (see Table 6). To overcome overestimation of the wave reducing effect, it is suggested to use the results for the worst-case scenarios for this. Meanwhile, it is recommended to stay up to date with findings of the POV Voorlanden, which includes the POV-W. These are namely decisive for (national) dike assessment and regulations.

Secondly, the influence of tides could be explicitly researched. In this thesis, only storm events were used to determine the wave reducing effect. A non-stationary model should be used for this while considering salt marsh development. The pioneer and lower salt marsh zones should then be included as well, because these areas are most affected by tides (see Figure 13).

Thirdly, additional functions of the Holwerd West should be considered while improving its wave reducing effectiveness. Next to coastal protection and natural values, the area has culture historical value as in traces of agricultural use and could be suitable for recreation. One natural value that has not been mentioned yet is the capability of salt marshes to store carbon(dioxide).

Moreover, recommendations are set up towards the state (Rijkswaterstaat) and to the nature conservation organization (It Fryske Gea). Rijkswaterstaat is advised to maintain the summer dikes because these play a big role in the wave reduction over a salt marsh. It Fryske Gea is suggested to maintain the extensive grazing principle. This has namely resulted in a high vegetation diversity on Holwerd West, which contributes to a high (elevation) varying landscape, because of the different extents in capturing sediment particles. The latter ensures the highest wave reducing effect over a salt marsh.

References

- AHN (2019) *AHN viewer*. Available at: <https://ahn.arcgisonline.nl/ahnviewer/> (Accessed: 3 January 2019).
- Alterra (2012a) *Een Dijk van een Kwelder: een verkenning naar de golfreducerende werking van kwelders*, *Alterra-rapport 2267*. Wageningen.
- Alterra (2012b) *Zoekkaart Kwelders en Waterveiligheid Waddengebied*. Wageningen.
- Arcadis (2018) *Slibsedimentatie in de kwelders van de Waddenzee*. Zwolle.
- Battjes, J. A. and Janssen, J. P. F. M. (1978) *ENERGY LOSS AND SET-UP DUE TO BREAKING OF RANDOM WAVES*, *Coastal Engineering*. Delft.
- Battjes, J. A. and Stive, M. J. F. (1985) 'Calibration and Verification of a Dissipation Model for Random Breaking Waves', *JOURNAL OF GEOPHYSICAL RESEARCH*, 90(C5), pp. 9159–9167.
- BE SAFE (2017) *BE SAFE: flood risk reduction using vegetated foreshores*, *YouTube*. Available at: https://www.youtube.com/watch?v=03N_gUMEcZl (Accessed: 4 January 2019).
- Best, S. N. *et al.* (2018) 'Do salt marshes survive sea level rise? Modelling wave action, morphodynamics and vegetation dynamics', *Environmental Modelling and Software*. Elsevier, 109(September 2017), pp. 152–166. doi: 10.1016/j.envsoft.2018.08.004.
- Booij, N., Ris, R. C. and Holthuijsen, L. H. (1999a) 'A third-generation wave model for coastal regions - Part I: Model description and validation', *Journal of Geophysical Research*, 104(C4), pp. 7649–7666.
- Booij, N., Ris, R. C. and Holthuijsen, L. H. (1999b) 'A third-generation wave model for coastal regions - Part II: Verification', *Journal of Geophysical Research*, 104(C4), pp. 7649–7666. doi: 10.1029/1998JC900123.
- Borsje, B. W. *et al.* (2011) 'How ecological engineering can serve in coastal protection', *Ecological Engineering*. Elsevier B.V., 37(2), pp. 113–122. doi: 10.1016/j.ecoleng.2010.11.027.
- Collins, J. I. (1972) 'Prediction of Shallow-Water Spectra', *Journal of Geophysical Research*, 77(15), p. 15. doi: 10.1029/JC077i015p02693.
- Common Wadden Sea Secretariat (2018) *Wadden Sea - World Heritage*. Available at: <https://www.waddensea-worldheritage.org/> (Accessed: 2 January 2019).
- Common Wadden Sea Secretariat (2019) *Wadden Sea World Heritage*. Available at: <https://www.waddensea-worldheritage.org/> (Accessed: 4 May 2019).
- Dalrymple, R. A., Kirby, J. T. and Hwang, P. A. (1984) 'Wave diffraction due to areas of energy dissipation', *Waterway Port Coastal and Ocean Engineering*, 1(February), pp. 67–78. doi: 10.1061/(ASCE)0733-950X(1984)110.
- Deltares (2013) *Dataset documentation Kusthoogte*, *OpenEarth*. Available at: <https://publicwiki.deltares.nl/display/OET/Dataset+documentation+Kusthoogte> (Accessed: 3 January 2019).
- Deltares (2015) *Dataset documentation Vaklodgingen*, *OpenEarth*. Available at: <https://publicwiki.deltares.nl/display/OET/Dataset+documentation+Vaklodgingen> (Accessed: 3 January 2019).

Deltares (2017a) *Achtergrondrapport Hydraulische Belastingen - Wettelijk Beoordelingsinstrumentarium 2017*. Delft.

Deltares (2017b) *Basisstochasten WTI-2017*. Delft. Available at: <http://publicaties.minienm.nl/documenten/basisstochasten-wti-2017-statistiek-en-statistische-onzekerheid>.

Dijkema, K. *et al.* (2001) *Van landwaanwinning naar kwelderwerken*. Leeuwarden: Rijkswaterstaat.

van Duin, W. E. *et al.* (2013) *Friese en Groninger kwelderwerken: monitoring en beheer 1960-2014, WOt-rapport;122*. Available at: <http://edepot.wur.nl/279715>.

van Duin, W. E. and Dijkema, K. S. (2012) *Randvoorwaarden voor kwelderontwikkeling in de Waddenzee en aanzet voor een kwelderansenkaart*. Wageningen.

Esselink, P. *et al.* (2015) *Van Polder naar kwelder: tien jaar kwelderherstel Noorderleech. Olderterp*.

Essink, K., Esselink, P. and Vroom, M. (2014) 'Geschiedenis van het Noord-Friese kustlandschap', pp. 50–56.

Gautier, C. (2010) *SWAN Calibration and Validation for HBC2011. WTI - HR Zout*. Delft. Available at: http://publications.deltares.nl/1204143_002.pdf.

Grabowski, R. C., Droppo, I. G. and Wharton, G. (2011) 'Erodibility of cohesive sediment: The importance of sediment properties', *Earth-Science Reviews*. Elsevier B.V., 105(3–4), pp. 101–120. doi: 10.1016/j.earscirev.2011.01.008.

de Groot, A. V., Wesenbeeck, B. K. and Loon-Steensma, J. M. (2013) *Stuurbaarheid van kwelders*. Leeuwarden. Available at: <http://edepot.wur.nl/220052>.

Hasselmann, K. (1973) *Measurements of wind-wave growth and swell decay during the Joint North Sea Wave Project (JONSWAP)*.

Le Hir, P. *et al.* (2000) 'Characterization of intertidal flat hydrodynamics', *Continental Shelf Research*, 20, pp. 1433–1459.

Hoekstra, H., Winkels, H. J. and Gerritsen, J. B. M. (1998) *De bodemopbouw van de buitendijkse gronden - langs de noordkust van Friesland en Groningen*. Lelystad: RIZA. Available at: <http://publicaties.minienm.nl/documenten/de-bodemopbouw-van-de-buitendijkse-gronden-langs-de-noordkust-va>.

Holthuijsen, L. H. (2007) *Waves in oceanic and coastal waters*. New York: Cambridge University Press. Available at: www.cambridge.org/9780521860284.

Klein, M. D. and Kroon, J. (2011) *Productieberekeningen Waddenzee voor WTI-2011 : rapportage fase 1*. Rotterdam.

Madsen, O. S., Poon, Y. and Graber, H. C. (1988) 'Spectral Wave Attenuation by Bottom Friction: Theory', *Coastal Engineering*, pp. 492–504.

Ministerie van Infrastructuur en Milieu (2017) *Regeling veiligheid primaire waterkeringen 2017 Bijlage III*. Den Haag. Available at: <https://www.helpdeskwater.nl/onderwerpen/waterveiligheid/primaire/beoordelen/>.

- Ministry of Transport Public Works and Water Management (2000) *A Different Approach to Water*, . The Hague.
- Möller, I. *et al.* (1999) 'Wave Transformation Over Salt Marshes : A Field and Numerical Modelling Study from North Norfolk ', *Estuarine, Coastal and Shelf Science* (1999), 49, pp. 411–426. doi: 10.1006/ecss.1999.0509.
- Nationaal Georegister (2019) *Nationaal Georegister*. Available at: www.nationaalgeoregister.nl (Accessed: 4 May 2019).
- Ng, C.-O. (2000) 'Water waves over a muddy bed: a two-layer Stokes', *Coastal Engineering*, 40(3), pp. 221–242. doi: 10.1016/S0378-3839(00)00012-0.
- Poppema, D. W. (2017) *Experiment - supported modelling of salt marsh establishment : Applying the Windows of opportunity*. University of Twente.
- POV Voorlanden (2018) *Handreiking Voorland*.
- Reise, K. (2005) 'Coast of change : habitat loss and transformations in the Wadden Sea', *Helgoland Marine Research*, pp. 9–21. doi: 10.1007/s10152-004-0202-6.
- Ribberink, J. S. (2011) *River Dynamics II : Transport Processes and Morphology*. Enschede: Universiteit Twente.
- Rijkswaterstaat (2019) *Kweldervegetatie Webviewer, Geoservices*. Available at: <https://geoservices.rijkswaterstaat.nl/ext/geoweb51/index.html?viewer=Kweldervegetatie.Webviewer> (Accessed: 3 January 2019).
- Rijkswaterstaat WVL (2018a) *Hydra-NL: Gebruikershandleiding*. Lelystad.
- Rijkswaterstaat WVL (2018b) 'Hydra-NL'. Available at: <https://www.helpdeskwater.nl/onderwerpen/applicaties-modellen/applicaties-per/omgevings/omgevings/hydra-nl-0/>.
- Salmon, J. E. *et al.* (2015) 'Scaling depth-induced wave-breaking in two-dimensional spectral wave models', *Ocean Modelling*. Elsevier Ltd, 87, pp. 30–47. doi: 10.1016/j.ocemod.2014.12.011.
- Smith, G. A. *et al.* (2011) 'Introduction of a new friction routine into the SWAN model that evaluates roughness due to bedform and sediment size changes', *Coastal Engineering*. Elsevier B.V., 58(4), pp. 317–326. doi: 10.1016/j.coastaleng.2010.11.006.
- Steetzel, H., Groeneweg, J. and Vuik, V. (2019) *Effectiviteit Voorlanden HR Verdiepend onderzoek Fase C*. Available at: <https://pov-waddenzeedijken.nl/hr-effectiviteit-voorlanden/>.
- Suzuki, T. *et al.* (2012) 'Wave dissipation by vegetation with layer schematization in SWAN', *Coastal Engineering*. Elsevier B.V., 59(1), pp. 64–71. doi: 10.1016/j.coastaleng.2011.07.006.
- Temmerman, S. *et al.* (2007) 'Vegetation causes channel erosion in a tidal landscape', *Geology*, 17(10), pp. 678–685. doi: 10.1130/G23502A.1.
- Temmerman, S. *et al.* (2013) 'Ecosystem-based coastal defence in the face of global change', *Nature*, 504(7478), pp. 79–83. doi: 10.1038/nature12859.
- The SWAN Team (2019a) *SWAN - SCIENTIFIC AND TECHNICAL DOCUMENTATION*. Delft. Available at: <http://www.swan.tudelft.nl>.

- The SWAN Team (2019b) *SWAN USER MANUAL - SWAN Cycle III version 41.20AB, Cycle*. Delft. Available at: <http://iod.ucsd.edu/~falk/modeling/swanuse.pdf>.
- TU Delft (1999) *Grondmechanica*. CTwa5300 edn. Delft: TU Delft.
- Vroom, M. (2013) *Landschapsbiografie en draagvlakanalyse voor het huidige beheer van het kwelderlandschap van Noord-Friesland Buitendijks*. Rijksuniversiteit Groningen.
- Vuik, V. et al. (2016) 'Nature-based flood protection: The efficiency of vegetated foreshores for reducing wave loads on coastal dikes', *Coastal Engineering*. Elsevier B.V., 116, pp. 42–56. doi: 10.1016/j.coastaleng.2016.06.001.
- Vuik, V., van Vuren, S., et al. (2018) 'Assessing safety of nature-based flood defenses: Dealing with extremes and uncertainties', *Coastal Engineering*. Elsevier Ltd, 139(May), pp. 47–64. doi: 10.1016/j.coastaleng.2018.05.002.
- Vuik, V., Suh Heo, H. Y., et al. (2018) 'Stem breakage of salt marsh vegetation under wave forcing: A field and model study', *Estuarine, Coastal and Shelf Science*. Elsevier Ltd, 200, pp. 41–58. doi: 10.1016/j.ecss.2017.09.028.
- Vuik, V. et al. (2019) 'Salt marshes for flood risk reduction: Quantifying long-term effectiveness and life-cycle costs', *Ocean and Coastal Management*. Elsevier, 171(February), pp. 96–110. doi: 10.1016/j.ocecoaman.2019.01.010.
- De Waal, J. P. (1999) *Achtergronden Hydraulische Belastingen Dijken IJsselmeergebied*. Lelystad.
- Wetterskip Fryslan (2018) *Project Vijfhuizen*. Available at: <https://projectvijfhuizen.nl/> (Accessed: 4 October 2019).
- Willemsen, P. W. J. M. et al. (2018) 'Quantifying Bed Level Change at the Transition of Tidal Flat and Salt Marsh: Can We Understand the Lateral Location of the Marsh Edge?', *Journal of Geophysical Research: Earth Surface*, pp. 2509–2524. doi: 10.1029/2018JF004742.
- Witteveen+Bos (2017a) *Beoordeling Waddenzeedijk Koehool-Lauwersmeer: Rapportage Veiligheidsoordeel*. Deventer.
- Witteveen+Bos (2017b) *Beoordeling waddenzeedijk Koehool-Lauwersmeer: Uitgangspuntennotitie fase 1*. Deventer.
- Witteveen+Bos (2017c) *Verkenning Waddenzeedijk Koehool-Lauwersmeer: Analyse morfologische dynamiek en stroomsnelheden voorland*. Deventer.
- Witteveen+Bos (2019) *Witteveen+Bos*. Available at: <https://www.witteveenbos.com> (Accessed: 7 May 2019).
- Zijlstra, R. et al. (2017) *Wadden Sea Quality Status Report - Coastal risk management*. Wilhelmshaven. Available at: www.qsr.waddensea-worldheritage.org/reports/.

Appendixes

Appendix A - Terminology and dictionary

| English term | Dutch term | Description |
|----------------------|--|---|
| Accretion | Aanwas/Opslibbing | Land created by leaching against the shore |
| Backshore | Droge strand | Part of the beach on which no seawater will be released during most tides |
| Bank | Bank | Shoal created by sedimentation or scraping of the environment |
| Bank | Plaat | High bank that is dry at low tide |
| Bathymetry | Bathymetrie | Measurement of the water bottom height |
| Bio-physical process | Biofysisch(e) | Process related to a combination of biology and physics |
| Breakwater | Golfbreker/Strekdam/ Veerdam | Dam in the sea to protect a coast from the force of waves (e.g. dam to the ferry to Ameland) |
| Brushwood dam | Rijzendam/ Rijshoutdam | Double pile rows with row wood (brushwood) in between |
| Cross ditch | Dwarssloot | Medium-sized water course within salt marsh works |
| Depoldering | Ontpoldering/ Verkweldering | Returning a polder to the sea so that the area again undergoes the influence of tides |
| Dike toe | Dijkteen | Location where the construction of the dike ends and turns into foreland or soil |
| Dike trajectory | Dijktraject | Section of a primary flood defense that is assessed separately |
| Dwelling mound | Terp | Man-made hill to live dry at high tide |
| Earth(fill) dam | Gronddam | Dam in a watercourse, made entirely from deposited soil |
| Foreland | Voorland/ Buitendijks land | Land located between the outside water and the dyke |
| Foreshore | Natte strand | Part of the beach that is lower than the backshore |
| Gully | Priel | Small watercourse on a mudflat that falls dry at low tide |
| High salt marsh | Hoge kwelder/ Hoog schor | Tertiary stage of the salt marsh that can flood at high spring tide |
| Hydraulic load | Hydraulische belasting | Load on the flood defense due to the local water level and associated waves and currents |
| Impoldering | Ontpolderen/ Verkweldering | Breaching the (summer) dikes of a polder so that tides influence the area |
| Laser altimetry | Laseraltimetrie | Method to determine bathymetry and coast altitudes used by Rijkswaterstaat to obtain Kusthoogte |
| Low salt marsh | Lage kwelder/ Laag schor | Secondary stage of the salt marsh that can flood at high tide |
| Lower limit | Maximaal toelaatbare overstromingskans/ Ondergrens | Maximum allowable probability of flooding |
| Lutite | Lutum | Soil particles smaller than 2 μm composed of (sabulous) clay |

| | | |
|-----------------------------------|-------------------------------------|--|
| Lutite ratio | Lutumgehalte | Clay content in the soil |
| Main ditch | Hoofduitwatering | Main water course within salt marsh works |
| Measuring section | Meetvak | Area within salt marsh works in which measurements are performed (by RWS-Noord Nederland) |
| Mud motor | Slibmotor | Same concept as 'Sand engine', but this entails a nourishment of (1,3 million m ³) mud/sludge. |
| Mudflat (also called tidal flat) | Wad(plaat) | Muddy or sandy plates with gullies |
| Normative (storm) event | Normatieve gebeurtenis | Extreme high-water event used to perform dike assessments on |
| Open field drain | Greppel | Small-sized water course within salt marsh works |
| Pioneer zone | Pionierzone | Preliminary stage of the salt marsh that can flood at high tide |
| Revetment | Bekleding | The dike cover of the core of the dike for protection against high water |
| Salt marsh | Kwelder/Schor | Overgrown foreland of sand and silt deposits that only floods during high tides |
| Salt marsh work | Kwelderwerk/ Landaanwinningswerk | Human interventions in salt marshes to stimulate land growth |
| Sedimentation field | Bezinkveld/ Slibveld | Courses along the coast of Groningen and Friesland, bordered by dams, to promote rapid sedimentation |
| Single Beam Echo Sounders | Enkele bundel echolood | Method to determine bathymetry used by Rijkswaterstaat to obtain Vaklodingen |
| Sludge/ Silt | Slib | Deposition on the bottom of particles present in (flowing) water/Mixture of silt and clay |
| Subfield | Subvak/ Kwelderpandje | Area of 100 m by 100 m within a sedimentation field |
| Succession | Successie | Ecological process in which a change in the species composition takes place within a habitat, starting at the pioneer stage and ending with a climax stage |
| Tidal amplitude/ Tidal range | Getijverschil | Difference between the high and low tide water level |
| Tidal channel/ Tidal creek | Geul | Watercourses that do not fall dry at low tide |
| Tidal flat | Slik | Bank that is under water at almost each high tide |
| Transect | Raai | Imaginary line (1D) set out for the purpose of carrying out analyses |
| Trilateral Wadden Sea Cooperation | Trilaterale Waddenzee Samenwerking | Ecological entity of Denmark, Germany and the Netherlands cooperating to protect the Wadden Sea since 1978 |
| Wave action | Golfwerking/golfslag | Movement of energy through a body of water |
| Wave attenuation/ Wave damping | Golfdemping | Decrease in wave amplitude |
| Wave breaking | Golfbreking | Collapse of a wave due to a change in water depth or an obstacle |

| | | |
|------------------|----------------|---|
| Wave overflow | (Golf)overloop | Phenomenon where water runs into the hinterland over the (crest of the) flood defense, because the outside water level is higher than the flood defense |
| Wave overtopping | (Golf)overslag | Phenomenon where water runs into the hinterland over the (crest of the) flood defense, because of wave action |
| Wave reduction | Golfreductie | Decrease in wave energy and/or wave height |

Appendix B - List with abbreviations

| Abbreviation | Description (Dutch) | Description (English) |
|---------------------|---|---|
| AHN | Actueel Hoogtebestand Nederland | Elevation map of the Netherlands |
| DP | Dijkpaal | Dike pole (location marker) |
| GEKB | Grasbekleding erosie kruin en binnentalud | Grass erosion on the inner crest and slope |
| GHW | Gemiddeld hoog water | Mean Highwater |
| HB | Hydraulische Belastingen | Hydraulic loads |
| HBN | Hydraulisch Belastingniveau/benodigde kruinhoogte | Normative dike height |
| HIGH | Raai met een potentieel hoog golfreducerende werking | High wave reducing (potential) transect |
| HR | Hydraulische Randvoorwaarden | Hydraulic boundary conditions |
| HWBP | Hoogwaterbeschermingsprogramma | N/A |
| LOW | Raai met een potentieel lag golfreducerende werking | Low wave reducing (potential) transect |
| MSL | Gemiddeld zeeniveau | Mean sea level |
| NAP | Normaal Amsterdams peil | Similar to mean sea level |
| NFB | Noord-Friesland Buitendijks | N/A |
| POV | Project Overstijgende Verkenning | N/A |
| POV-W | Project Overstijgende Verkenning aan de Waddenzeedijken | N/A |
| RC | Relatieve bijdrage | Relative contribution of each of the three bio-physical processes to wave reduction |
| RQ | Onderzoeksvraag | Research question |
| RWS | Rijkswaterstaat | Directorate-General for Public Works and Water Management |
| SBES | Single beam echolood | Single Beam Echo Sounders |
| SLR | Zeespiegelstijging | Sea Level Rise |
| SWAN | Golfsimulatie dichtbij de kust | Simulating WAVes Nearshore |
| WBI | Wettelijk beoordelingsinstrumentarium | N/A |
| WTI | Wettelijk Toetsinstrumentarium | N/A |

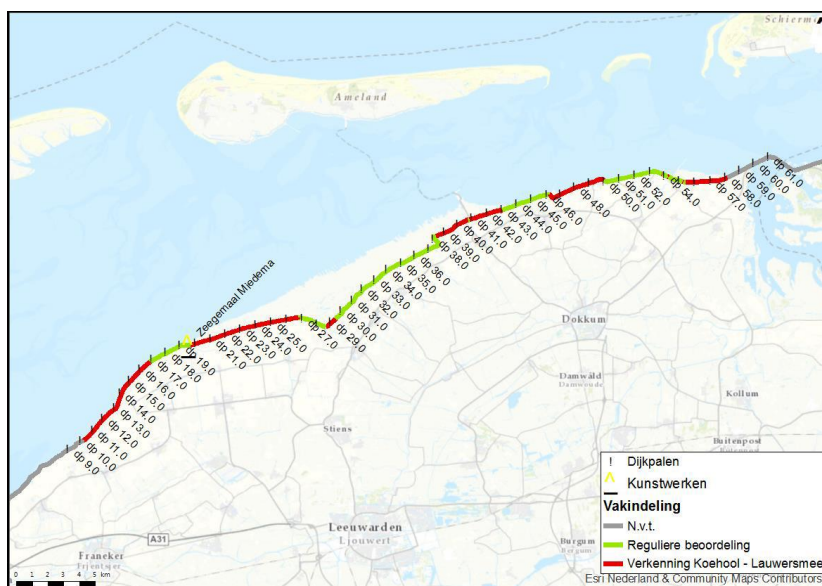
Appendix C - Wadden Sea dike assessment Koehool-Lauwersmeer

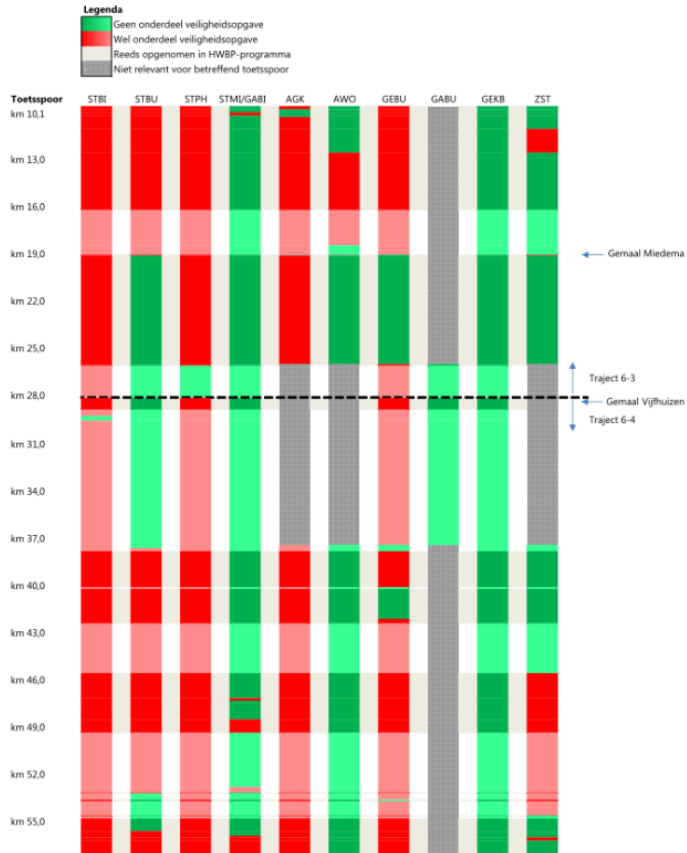
A dike safety assessment was performed by Witteveen+Bos on the Wadden Sea dike between 'Koehool' and 'Lauwersmeer' (Witteveen+Bos, 2017a). In the third safety assessment, the dike sections 'Koehool-Westholwerderpolder' and 'Westholwerderpolder-Lauwersmeerdijk' were partially rejected on coverings. In 2011, both trajectories were therefore notified to the Flood Protection Program (HWBP) and subsequently included in HWBP programming. Wetterskip Fryslân is the manager of the flood defense between 'Koehool' and 'Lauwersmeer' and from this role responsible for flood protection. The water board leads the exploration of the dike reinforcement between km 10.10 and km 58.00 and Witteveen+Bos supports the water board in a partnership during the exploration.

All trajectories marked red in the figure on the next page do not meet the dike standards. Therefore, these have been implemented into the exploration program ('Verkenningfase dijkversterking Koehool-Lauwersmeer'). For each of the trajectories, the failure mechanisms are considered for which it failed (red) or did not (green). Besides, it is addressed whether the trajectory has already been implemented in the HWBP program or not (lighter red/green).

The inclusion of existing forelands in the assessment of dikes may result in the approval of dike sections that would have been rejected in the first instance (POV Voorlanden, 2018). Since salt marshes reduce wave heights, the (hydraulic) load on the adjacent flood defense due to waves is lowered. Consequently, salt marshes can have a positive effect on failure mechanisms that are affected by the reduction of the hydraulic load. In the old dike assessment procedure, this would have resulted in a reduction in failure probability for wave overtopping/overflow (Vuik *et al.*, 2018). In the current dike assessment method, wave overtopping/overflow is incorporated into a group of failure mechanisms called 'wave impact on revetments'. An example of a failure mechanisms within this group is erosion of the revetment (e.g. asphalt or grass) on the outer slope (GEBU: 'Grasbekleding erosie buitentalud') due to the impact of breaking waves.

Furthermore, these overgrown forelands can have a positive effect on the failure mechanisms: erosion outer slope (STBU: 'Macro-instabiliteit buitenwaarts') and piping (STPH: 'Opbarsten, heave en piping') (Alterra, 2012b). The positive effect on the first can be explained by its (heavy) composition and on the second by its width in combination with its impermeable sludge layer.





| afkorting | faalmechanisme | |
|-----------|---|--|
| STBI | macro-instabiliteit binnenwaarts | bijna hele traject afgekeurd, blijft waarschijnlijk deels afgekeurd |
| STBU | macro-instabiliteit buitenwaarts | bijna hele traject afgekeurd, blijft waarschijnlijk deels afgekeurd |
| STPH | opbarsten, heave en piping | afgekeurd, wordt waarschijnlijk goedgekeurd |
| STMI/GABI | micro-instabiliteit en grasbekleding afschuiven binnentalud | op een aantal locaties afgekeurd |
| AGK | asfaltbekleding golfklappen | afgekeurd (vanwege freatische lijn onder asfalt), wordt waarschijnlijk deels goedgekeurd |
| AWO | asfaltbekleding wateroverdrukken | gepenetreerde klinkers afgekeurd |
| GEBU | grasbekleding erosie buitentalud | afgekeurd: groene dijk en te lage overgang op gras |
| GABU | grasbekleding afschuiven buitentalud | goedgekeurd |
| GEKB | grasbekleding erosie kruin en binnentalud | goedgekeurd |
| ZST | stabiliteit bekleding steenzetting | strekking koperslakblokken afgekeurd |

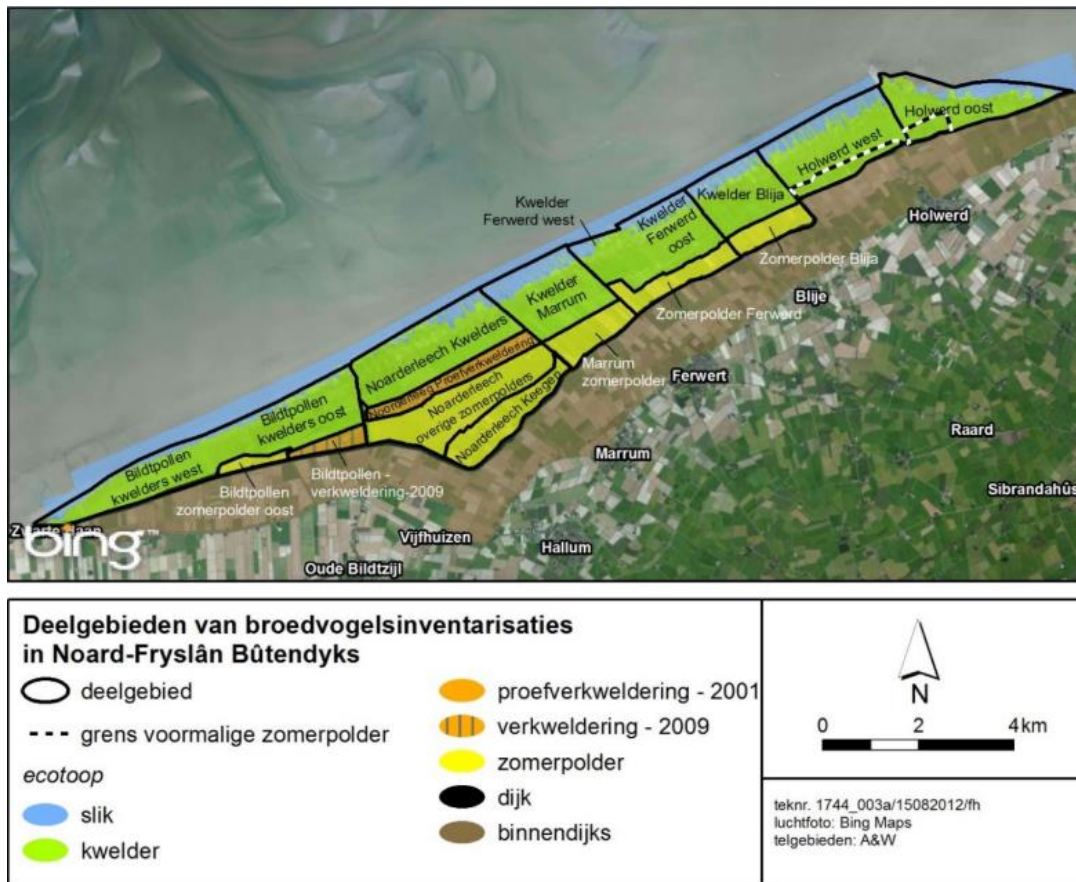
Appendix D - Considered locations of the POV-W

Considered locations in Friesland for the wave reducing effect determination of the 'HR Effectiviteit Voorlanden' investigation, calculated from a WTI 2011 location (red) until a WBI 2017 location (blue) (Steetzel *et al.*, 2019).



Appendix E - Sublocations of NFB

An overview of the sublocations within the salt marsh 'Noard-Fryslân Bûtendyks' is presented in the figure below (Esselink *et al.*, 2015). This is in accordance with the management areas of the nature conservation organization 'It Fryske Gea'.



Appendix F - Geometry of Holwerd West

The salt marsh geometry of Holwerd West is presented in the figures below, representing the years 1949, 1958, 1989, 2004, 2007, 2008 and 2011 (Deltares, 2013, 2015).



Appendix G - Transformation of the soil map of 2014

Nowadays, soil types are distinguished in many different classes (see figure below) (Nationaal Georegister, 2019). Soil types that can be found in NFB are 'Initiale vaaggronden', which contains the subcategories:

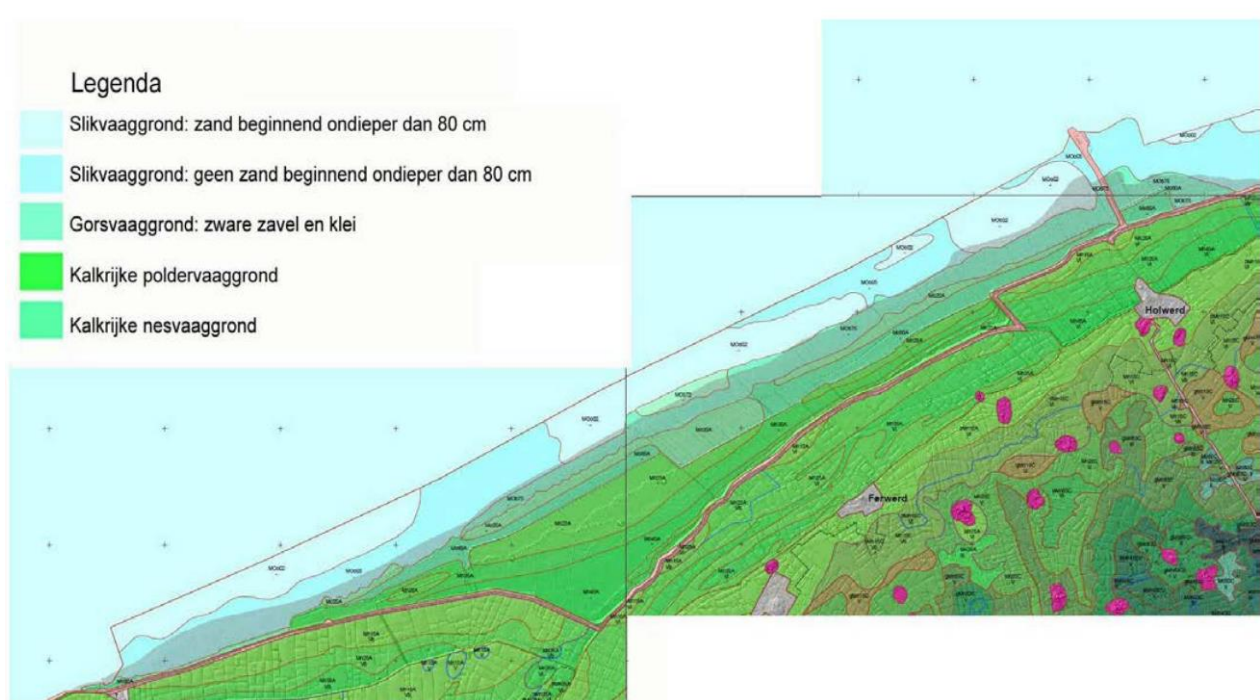
- (1) 'Slikvaaggrond (MOo02): zand beginnend ondieper dan 80 cm'
- (2) 'Slikvaaggrond (MOo05): geen zand beginnend ondieper dan 80 cm'
- (3) 'Gorsvaaggrond (MOB75): zware zavel en klei; geen zand beginnend ondieper dan 80 cm'

The difference between the first two is that within 80 cm underneath the first mentioned, sand can be found, and in the second this cannot. The first is therefore addressed to be very fine sand ('sterk lutumhoudend zand'), while the second is referred to as coarse/medium silt ('lichte zavel'). The third subcategory is combined to this layer, because it contains similar materials.

Another soil category is called 'Hydro(klei)vaaggronden', in which 'Kalkrijke nesvaaggronden' and 'Kalkrijke poldervaaggronden' exist. The latter is not present in the study area, so was left out of consideration. The first can be subdivided:

- (4) Kalkrijke nesvaaggronden (Mo20A): zware zavel
- (5) Kalkrijke nesvaaggronden (Mo80A): klei

Consequently, the fourth subcategory was translated to (very) fine silt ('zware zavel') and the fifth to all sorts of clay ('klei').



Appendix H - Physical processes in SWAN (version 41.20)

Physical processes that affect the wave energy (density) in the SWAN wave model (version 41.20) are described below. The last three are the bio-physical processes that cause wave reduction due to salt marsh characteristics.

Wind input and growth S_{in}

This process is active by default in the third SWAN generation and represents wave growth as a result of wind stress exerted on the water surface. The higher the wind speed and its duration i.c.w. the fetch length, the higher the waves get. Both linear and exponential wind growth are included following principles of Cavaleri and Malanotte-Rizzoli (1981), and Snyder et al. (1981) or Janssen (1991). As input, the wind velocity and direction at 10 m elevation are needed. By the command WIND, constant wind is generated.

Wave-wave interactions S_{nl3} and S_{nl4}

In very shallow water, triad (3-)wave-wave interactions transfer energy from lower frequencies to higher frequencies often resulting in higher harmonics (Holthuijsen, 2007). This process is modeled according to Hasselmann et al. (1985). In deep water, quadruplet (4-)wave-wave interactions dominate the evolution of the spectrum. They transfer wave energy from the spectral peak to lower frequencies (thus moving the peak frequency to lower values) and to higher frequencies (where the energy is dissipated by whitecapping), following the principles of Eldeberky (1996).

Whitecapping $S_{ds,w}$

Whitecapping indicates steepness-induced wave crest breaking into white foam so that wave decay. Two principles can be followed: a pulse-based model according to Komen et al. (1984) or an expression that covers nonlinear hydrodynamics within wave groups (The SWAN Team, 2019b).

Depth-induced wave breaking/Surf breaking $S_{ds,di}$

Depth-induced wave breaking represents a collapsing wave due to a change in water depth as a result of a varying bottom level. This process of surf breaking can be modelled in two ways: considering a constant breaker index according to Battjes and Janssen (1978) or applying a breaker index that scales with both the bottom slope and the (dimensionless) water depth consistent with Salmon et al. (2015).

The Battjes and Janssen (1978) model was originally developed to predict the wave energy dissipation of random waves breaking on a beach (Battjes and Janssen, 1978). Its parameterization is based on measurements showing similarity in wave breaking in a 1D bore. This implied that the wave height decayed in constant proportion to the mean depth, according to $H(x) = \gamma \cdot h(x)$. Consequently, the constant breaker index (γ) could be calculated by $\gamma = H_{max}/h$ and appeared to be 0.8. This was later improved by Battjes and Stive (1985) who averaged the values for γ over a more extensive data set and came to a value of 0.73, which is the default in SWAN (Battjes and Stive, 1985). Besides, α is the proportionality coefficient of the rate of dissipation, which is of order one.

The Salmon et al. (2015) model was set up after the conclusion that significant wave heights over horizontal bathymetries (smaller than 1:700) were typically under-predicted in locally generated

wave conditions (Salmon *et al.*, 2015). Therefore, laboratory observations entailed using a varying breaker index that is dependent on both the bottom slope (β) and the normalized wave number (kd). Considering this, waves can be better predicted, especially in 2D spectral wave models due to the acknowledgement of wave directionality.

Bottom friction $S_{ds,bf}$

The bottom friction (roughness) of a vegetated foreland is formed by its bed characteristics consisting of sediment (ripples) that counteract the water flow so that wave energy gets dissipated more offshore (Alterra, 2012a). Considering the large variations in bottom conditions in coastal areas (bottom material, bottom roughness length, ripple height, etc.), there is no field data evidence to give preference to a particular friction model (The SWAN Team, 2019b). Available bottom friction considerations are JONSWAP, Collins, Smith and Madsen. Furthermore, bed characteristics can be considered as a mud layer following Ng (2000).

Based on the JONSWAP results, energy dissipation by bottom friction can be assumed to be constant over the bed (Hasselmann, 1973). This constant is used for typical sandy bottom and semi-empirically derived from wave spectra measurements along the North Sea. This value appeared to be $0.067 \text{ m}^2\text{s}^{-3}$ for wind seas (e.g. North Sea) but after calibration was calibrated to $0.038 \text{ m}^2\text{s}^{-3}$ for swell waves on the ocean driven by surface gravity.

Collins *et al.* (1972) proposed a simplified drag law model. based on a nonlinear formulation stated by Hasselmann and Collins (1968), to approximate the bottom friction effect (Collins, 1972). This includes turbulent bottom friction on the one hand and percolation on the other. The first phenomena can be described as the work done against turbulent shear stresses induced at the bed by the water particle motions. The second can be explained as the work done against viscous forces induced by a permeable bottom that allows water particle motions between grains.

The soil types were classified according to their lutite ratio, grain diameter and wet density value (Table 1). The latter two determine the extent of bottom friction according to Smith *et al.* 2011 as a result of the presence of bottom ripples (Smith *et al.*, 2011). Sediment grains, especially in ripples, namely counteract the water flow, so that wave energy gets dissipated more offshore. Validation was performed using measurements at two fields in Australia where a sand and silt bed were considered and showed an overall improvement of the model prediction for wave conditions when compared to default friction routines in SWAN.

An eddy-viscosity model was set up by Madsen *et al.* (1988) in which a bottom boundary layer represents bottom friction (Madsen, Poon and Graber, 1988). Within this layer, of thickness a few cm, flow is sheared, generally turbulent, and therefore causes dissipation of wave energy.

Since the top layer of Holwerd West mainly consists of clay and silt (see 2.2.2 Bed characteristics), which is classified as mud, the mud layer routine in SWAN could represent its bed characteristics. This thin layer of viscous mud forms a boundary layer which dissipates wave energy (Ng, 2000).

Vegetation $S_{ds,veg}$

Wave damping by vegetation can be explained by vegetation stems, branches and leaved that exert (drag) force on incoming water. The wave reducing properties of vegetation can be modelled in two ways: considering extra roughness (Nikuradse roughness) following Madsen *et al.* (1988) or using the vegetation module according to Dalrymple (1984). The wave attenuation capacity of

vegetation is considered at times when vegetation is fully grown (between July and September), so seasonal variations are not taken into account.

The expression of Madsen et al. (1988) for the bottom friction can be applied for wave attenuation by vegetation as well (Madsen, Poon and Graber, 1988). This can be done by assuming that the bottom is smooth and has therefore a small roughness. Since some vegetation types behave more as roughness than as cylinder shaped objects, these can be given values for the Nikuradse roughness length scale.

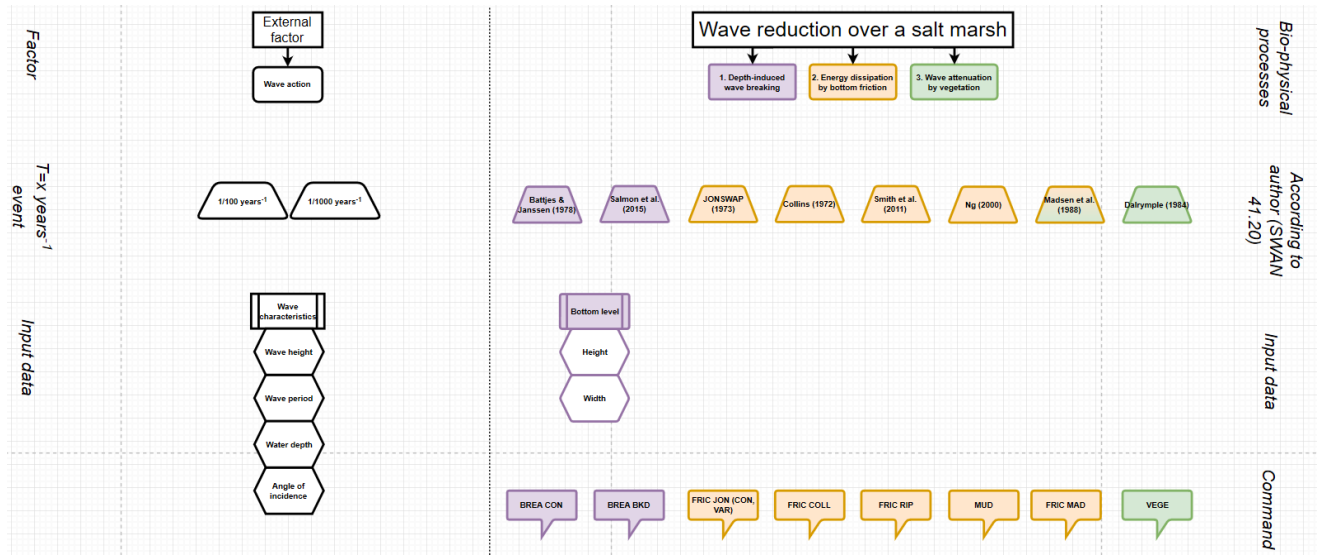
The second option is the use of a vegetation module in which vegetation properties as stem height, diameter, the density of patches and drag coefficient are considered (Dalrymple *et al.*, 1984). The SWAN version 41.20 is the first in which this vegetation module was implemented for vegetation fields such as mangroves or salt marsh vegetation (The SWAN Team, 2019a). Energy is dissipated due to the work done by the waves on the vegetation, schematized as cylinders at variable depths. In cases that vegetation breaks (for T=1000 years or rarer storm events), stem breakage was considered (Vuik *et al.*, 2018). In such cases, the stem height decreased to 20% of the original (up to 10 cm high), because the lower part of the stem is thickest (Vuik *et al.*, 2019).

An overview of the available (bio-)physical processes (sink/source terms) available in SWAN is presented in the table below.

| Physical process | Command | Description | Authors |
|-------------------------------|---|---|---|
| <u>Sink/Source Terms (S)</u> | | | |
| Linear wind growth/input | GEN1,GEN2, GEN3* (1 st , 2 nd or 3 rd generation) | Wind stress on surface results in wave growth due to pressure differences at either side of the crest | Cavaleri and Malanotte-Rizzoli (1981) |
| Exponential wind growth/input | GEN1,GEN2, GEN3* | N/A | Snyder et al. (1981) Janssen (1989, 1991) Yan (1987) (modified) |
| Wind drag | WIND DRAG | Wind stress | Wu (1982) |
| Whitecapping | GEN1,GEN2, GEN3*/WCAP | Steepness-induced wave crest breaking into white foam | Komen et al. (1984) Janssen (1991) Alves and Banner (2003) |
| Quadruplets | GEN3*/QUAD | In <u>deep water</u> , quadruplet (4-)wave-wave interactions dominate the evolution of the spectrum. They transfer wave energy from the spectral peak to lower frequencies (thus moving the peak frequency to lower values) and to higher frequencies (where the energy is dissipated by whitecapping). | Hasselmann et al. (1985) |

| | | | |
|------------------------|------------|--|-----------------------------------|
| Triads | TRIAD | In <u>very shallow water</u> , triad (3-)wave-wave interactions transfer energy from lower frequencies to higher frequencies often resulting in higher harmonics | Eldeberky (1996) |
| Depth-induced breaking | BREAKING* | When waves propagate towards shore, shoaling leads to an increase in wave height. When the ratio of wave height over water depth (steepness) exceeds a certain limit, waves start to break, thereby dissipating energy rapidly | Battjes and Janssen (1978) |
| | | | Salmon et al. (2015) |
| Bottom friction | FRICTION | For typical sandy bottoms | JONSWAP (1973) |
| | | N/A | Collins (1972) |
| | | Varying (Nikuradse) roughness field | Madsen et al. (1988) |
| | | N/A | Smith et al. (1988) |
| <u>Other terms</u> | | | |
| Obstacle transmission | OBSTACLE | Characteristics of sub-grid obstacles | Seelig (1979), d'Angremond (1996) |
| Wave-induced set up | SETUP | Increase in mean water level due to the presence of breaking waves | |
| Vegetation dissipation | VEGETATION | Vegetation stems exert (drag) force on the incoming water | Dalrymple (1984) |
| Mud dissipation | MUD | Mud functions as bottom friction | Ng (2000) |
| Turbulence dissipation | TURBULENCE | N/A | |
| Diffraction | DIFFRAC | N/A | |
| | | | |
| * = active by default | | | |

As explained before, the bio-physical processes can be modelled in different ways following the approach of a different author in SWAN. An overview of the alternatives is shown in the figure on the next page.

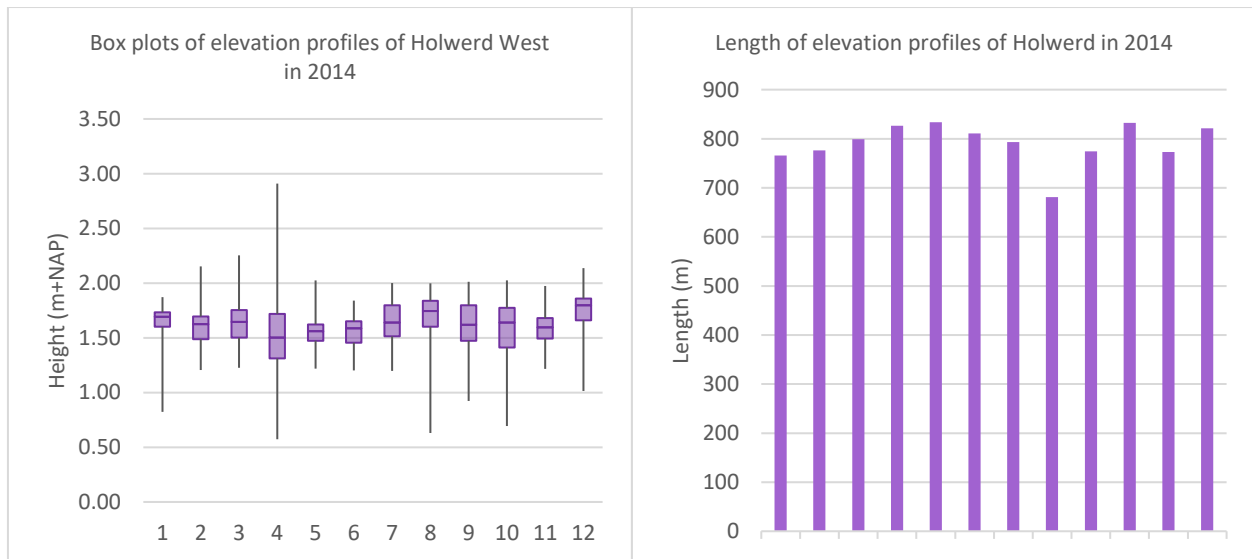


Appendix I - Choice from transects of Holwerd West

Transects were taken from a WTI2011 location to a WBI2017 location. These were as much as possible drawn in the lateral ditch direction, which is mostly perpendicular to the dike and corresponds to the dominant wind direction of 330 degrees North. Twelve transects were created this way and are numbered from West to East in ascending order, depicted in the figure below.



For 2014, the elevation profiles that correspond to these transects were extracted using AHN3 with a resolution of 0.5 meters (AHN, 2019). Since it was expected that the extent of depth-induced wave breaking is highest for wide (cross-shore) and irregular (varying) elevation profiles, the transects were assessed on these criteria in terms of salt marsh height variance, and length. The first is depicted using a boxplot per profile that indicates the variation around its median height, presented in the left figure below. The length (cross-shore) of the transects from a WTI2011 location to a WBI2017 location is presented on the right-side.



From the left figure above can be concluded that profiles 5/11/6 have the lowest and profiles 4/10/8 have the highest variation in salt marsh height. The transect length, which approximates the salt marsh width, is lowest for 8/1/11 and highest for 5/10/4. Consequently, profile 11 represents the lowest wave reducing potential and profile 4 the highest wave reducing potential of Holwerd West.

Appendix J - SWAN model parameters

In the tables below, the terms GRID, WLEV, WIND, BC/IC, and PHYSICS correspond to the SWAN script. The parameters values are presented per profile and T=x event. These are described and their database is clarified. Values for other physical processes (e.g. wind growth, whitecapping, triads) are not described below; SWAN default values were used for these.

| Symbol | Value | | | | | | | | Unit |
|--------------------|--|--------|--------|--------|--------|--------|--------|--------|----------------------|
| <i>Transect</i> | Low | | | | High | | | | |
| T=x | 100 | 1000 | 10,000 | 37,500 | 100 | 1000 | 10,000 | 37,500 | years |
| GRID | | | | | | | | | |
| xlenc | 773 | 773 | 773 | 773 | 827 | 827 | 827 | 827 | m |
| dx | 0.5 | 0.5 | 0.5 | 0.5 | 0.5 | 0.5 | 0.5 | 0.5 | m |
| N | 1547 | 1547 | 1547 | 1547 | 1655 | 1655 | 1655 | 1655 | (-) |
| flow | 0.03 | 0.03 | 0.03 | 0.03 | 0.03 | 0.03 | 0.03 | 0.03 | Hz |
| fhigh | 2 | 2 | 2 | 2 | 2 | 2 | 2 | 2 | Hz |
| WLEV | | | | | | | | | |
| h | 3.98 | 4.52 | 5.02 | 5.31 | 3.97 | 4.51 | 4.97 | 5.23 | m+NAP |
| WIND | | | | | | | | | |
| U ₁₀ | 28.3 | 32.1 | 36.2 | 38.7 | 28.3 | 32.2 | 35.9 | 38.4 | m/s |
| dir | 300 | 330 | 330 | 330 | 300 | 330 | 330 | 330 | °N |
| BC/IC | | | | | | | | | |
| H _{s_WTI} | 1.356 | 1.676 | 2.000 | 2.182 | 1.448 | 1.770 | 2.095 | 2.276 | m |
| T _{p_WTI} | 5.202 | 5.656 | 6.139 | 6.277 | 5.161 | 5.604 | 6.033 | 6.238 | s |
| Θ | 300 | 330 | 330 | 330 | 300 | 330 | 330 | 330 | ° |
| dd | 30 | 30 | 30 | 30 | 30 | 30 | 30 | 30 | ° |
| PHYSICS | | | | | | | | | |
| BREA | | | | | | | | | |
| alpha* | 1.0 | 1.0 | 1.0 | 1.0 | 1.0 | 1.0 | 1.0 | 1.0 | (-) |
| gamma0 | 0.54 | 0.54 | 0.54 | 0.54 | 0.54 | 0.54 | 0.54 | 0.54 | (-) |
| a1 | 7.59 | 7.59 | 7.59 | 7.59 | 7.59 | 7.59 | 7.59 | 7.59 | (-) |
| a2 | -8.06 | -8.06 | -8.06 | -8.06 | -8.06 | -8.06 | -8.06 | -8.06 | (-) |
| a3 | 8.09 | 8.09 | 8.09 | 8.09 | 8.09 | 8.09 | 8.09 | 8.09 | (-) |
| FRIC | | | | | | | | | |
| S | 1.37 | 1.37 | 1.37 | 1.37 | 1.37 | 1.37 | 1.37 | 1.37 | (-) |
| D* | 62 | 62 | 62 | 62 | 62 | 62 | 62 | 62 | µm |
| VEGE | | | | | | | | | |
| height* | 0.50 | 0.10 | 0.10 | 0.10 | 0.50 | 0.10 | 0.10 | 0.10 | m |
| diamtr | 0.0013 | 0.0013 | 0.0013 | 0.0013 | 0.0013 | 0.0013 | 0.0013 | 0.0013 | m |
| nstems | 1000 | 1000 | 1000 | 1000 | 1000 | 1000 | 1000 | 1000 | stems/m ² |
| drag | 0.3 | 0.3 | 0.3 | 0.3 | 0.3 | 0.3 | 0.3 | 0.3 | (-) |
| * | <i>Sensitivity analysis is executed on these variables</i> | | | | | | | | |

| Symbol | Description | Database |
|--|--|---|
| GRID | | |
| xlenc | Transect length from WTI2011 to WBI2017 location | AHN3 (2014) |
| dx | Step size in x-direction | AHN3 (2014) |
| N | Number of grid points | AHN3 (2014) |
| flow | Lowest discrete (wind wave) frequency | POV-W, productieberekeningen fase 1 |
| fhigh | Highest discrete (wind wave) frequency | POV-W |
| WLEV | | |
| h | Water level along the transect | Hydra-NL |
| WIND | | |
| u ₁₀ | Wind speed at 10 m elevation | Hydra-NL |
| dir | Dominant wind direction | Hydra-NL |
| BC/IC | | |
| H _{s_WTI} | Significant wave height at the WTI2011 location | Hydra-NL |
| T _{p_WTI} | Peak wave period at the WTI2011 location | Hydra-NL |
| Θ | Direction of wave propagation, which is assumed equal to the wave direction | Hydra-NL |
| dd | Directional spreading, which accounts for the difference in wave direction (300°-330°) | Hydra-NL |
| PHYSICS | | |
| <u>BREA</u> alpha* gamma a1 a2 a3 | <u>Depth-induced wave breaking</u> Coefficient of dissipation rate Reference breaker index First tunable coefficient Second tunable coefficient Third tunable coefficient | SWAN 41.20AB default based on Salmon et al. (2015) |
| <u>FRIC</u> S D* | <u>Bottom friction</u> Specific gravity of sediment Grain diameter | Sediment values according to Table 1 applied to principles of Smith et al. (2011) |
| <u>VEGE</u> height* diamtr nstems drag | <u>Vegetation</u> Stem height Stem diameter Stem density Drag coefficient | Vegetation properties (Table 3) correspond to sea couch grass which is dominant along both transects (see Figure 14). |

On the next page, a part of the SWAN script is presented in which the physical processes are set up. This script represented the T=100-year event for the low wave reducing transect (in which vegetation stems were assumed not to break).

```

$*****MODEL INPUT*****
SET NAUT                                !The direction of the vector from geographic North measured clockwise
MODE STAT ONED                          !STATIONary and ONEDimensional

|$*****GRID*****
CGRID REGULAR xpc=0. ypc=0. alpc=0. xlenc=773. ylenc=0. mxc=1546 myc=0 CIRCLE mdc=36 flow=0.03 fhigh=2.

INPGRID BOTTOM xpinp=0. ypinp=0. alpinp=0. mxinp=1546 myinp=0 dxinp=0.5 dyinp=0
INPGRID WLEV xpinp=0. ypinp=0. alpinp=0. mxinp=1 myinp=0 dxinp=1547 dyinp=0

READINP BOTTOM -1 'low_bottom_level.dep' 1 0          !Bottom level profile input file, multiplied with -1
READINP WLEV 1 'low_100_watlev.lev' 1 0             !Water level input file

$*****WIND INPUT*****
WIND 28.3 300 DRAG WU                        !Wind velocity/Direction and Wind drag

$*****BOUNDARY CONDITIONS*****
BOU SHAP Jon PEAK DSPR DEGR                !BOUnd/SHAPespec/JONSWAP spectrum/Peak period/Directional spreading/Degrees
BOU W CON PAR hs= 1.356 per= 5.202 dir=300. dd=30. !BOUndspec/West/Constant/Parameters(Hs,Tp,theta,dd)

$*****INITIAL CONDITIONS*****
INIT PAR 1.356 5.202 300. 30.              !Parameters(Hs,Tp,theta,dd)

$*****PHYSICS*****
GEN3 KOMEN                                !Wind growth
WCAPPING KOMEN                             !Whitecapping
QUAD iquad=2 lambda=0.25 Cnl4=3.0e+07      !Quadruplets
LIMITER ursell=10.0 qb=1.0                !Limits quadruplets when >ursell
TRIAD itriad=1 trfac=0.8 cutfr=2.5        !Triads
BREA BKD alpha=1.0 gamma0=0.54 a1=7.59 a2=-8.06 a3=8.09 !Depth-induced wave breaking
FRIC Ripples 1.37 0.000062                !Bottom friction
VEGETation 0.50 0.0013 1000 0.3          !Vegetation dissipation

$*****NUMERICS*****
NUM STOPC 0.00 0.01 0.001 99. &          !Numeric properties in a stationary computation
STAT 80 0.002

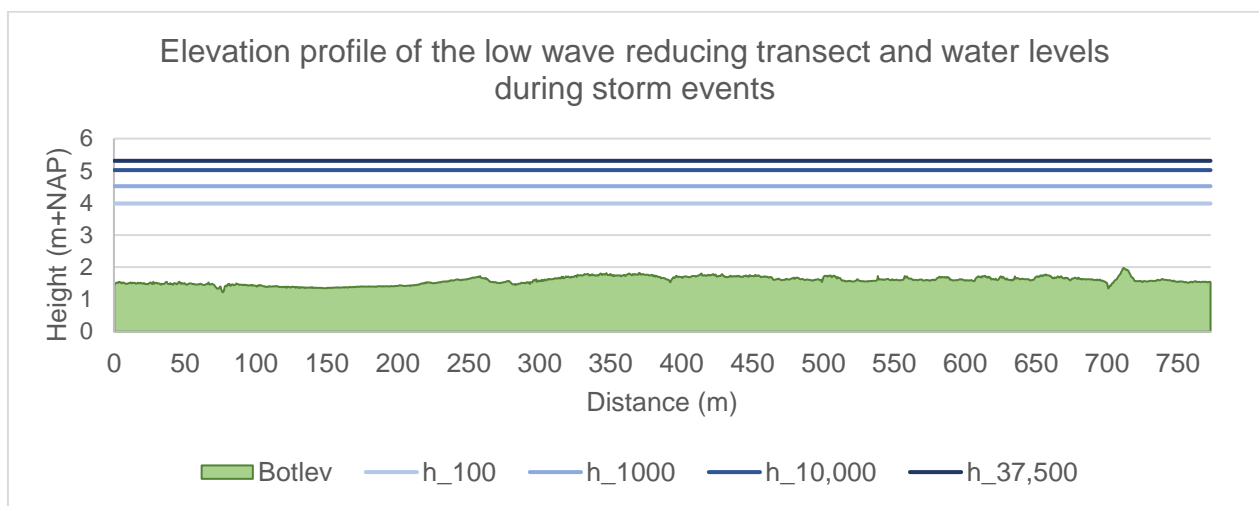
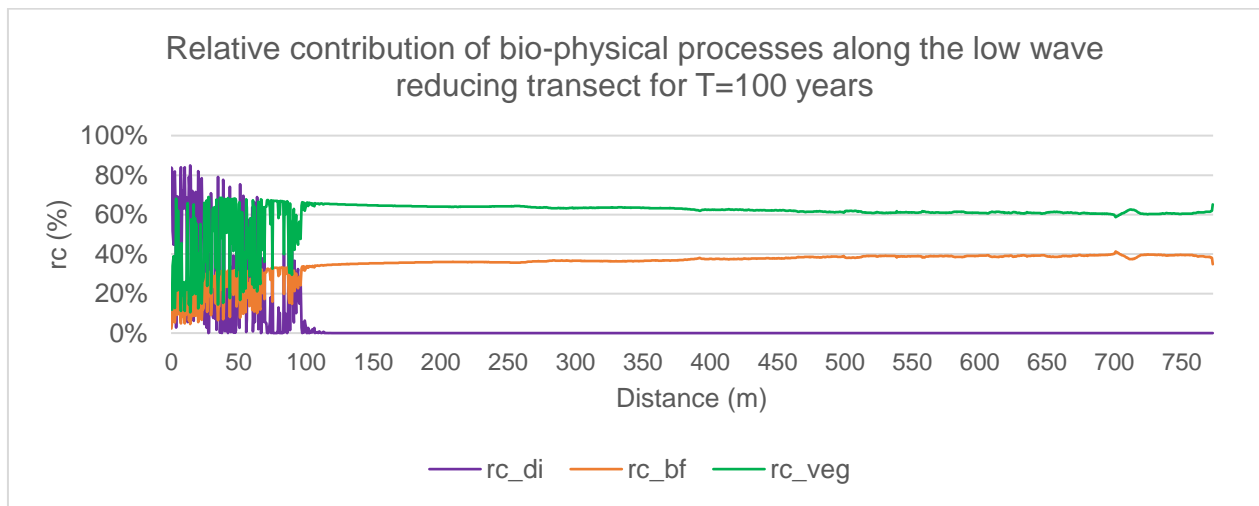
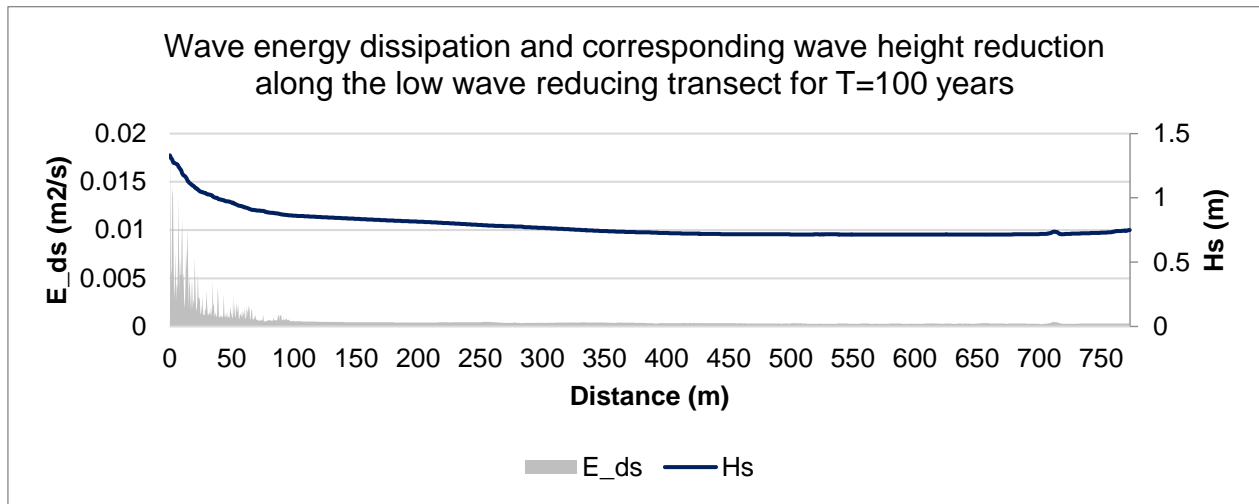
```

Appendix K - Wave energy change along both transects

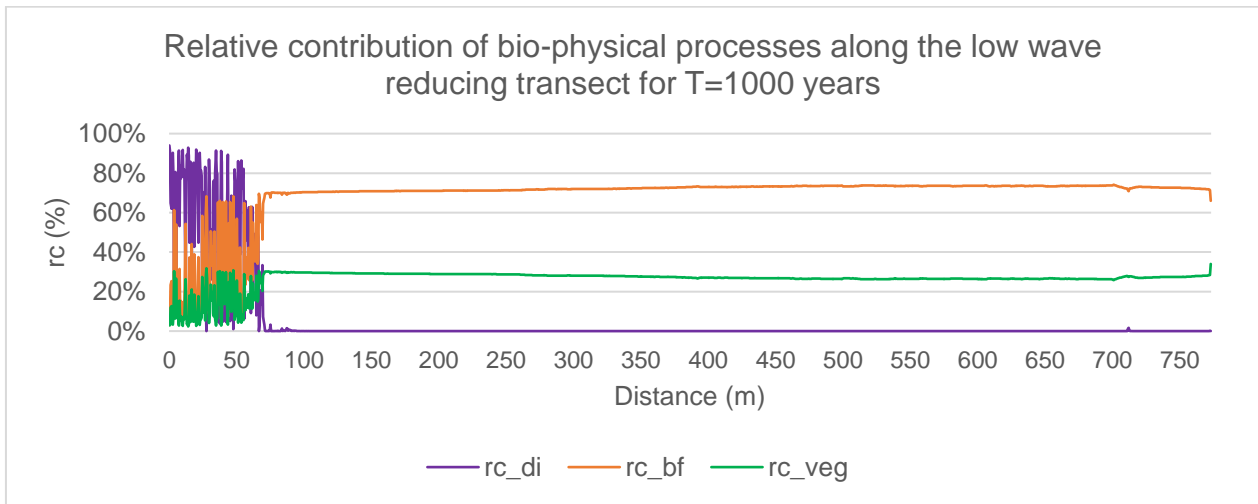
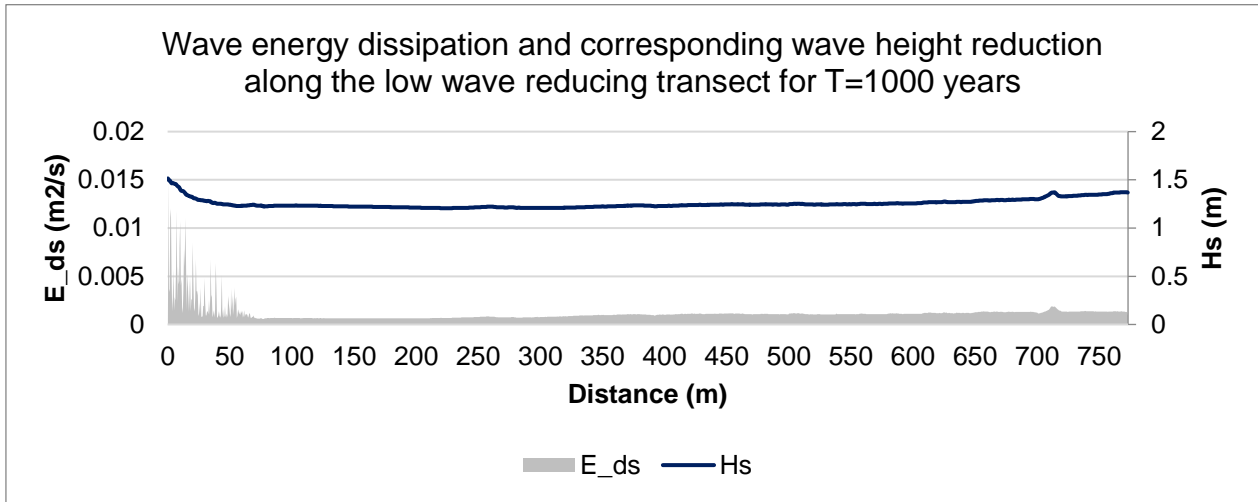
In order to investigate the behavior of the bio-physical processes along the transect, the wave energy change was investigated. On the next pages, the results for the wave energy dissipation and corresponding wave height change and relative contribution of each of the bio-physical processes are presented along the transect. In these figures, is E_{ds} the wave energy dissipation (m^2/s) per space step (0.5m) as a consequence of physical processes, H_s the significant wave height (m), and rc the relative contribution (%) while neglecting whitecapping (accounts on average for 36% of the total wave energy dissipation). The transects were taken from a WTI2011 location to a WBI2017 location; this length is represented by the distance (m). It should be noted that the *absolute* wave energy dissipation due to bottom friction and vegetation is more or less constant along the profile. This can be perceived from the relative contribution figures below where these approximately appear as horizontal lines when waves do not break. The observations on the several storm events are summarized in the table below.

| Transect | T=x (years) | ΔH_s (m) | Observations |
|----------|-------------|------------------|---|
| Low | 100 | E_{ds} | most dissipated within 100 m |
| | | H_s | decreases most within 100 m then still decreases up until a distance of 600 m |
| | | rc | di is dominant at the first 55 m, then veg is dominant |
| | 1000 | E_{ds} | most dissipated within 400 m |
| | | H_s | decreases most within 50 m then still decreases up until a distance of 200 m |
| | | rc | di is dominant at the first 65 m, then bottom friction is dominant |
| | 10000 | E_{ds} | most dissipated within 420 m |
| | | H_s | decreases at the first 70 m, then increases |
| | | rc | di is dominant at the first 70 m, then bottom friction is dominant |
| | 37500 | E_{ds} | most dissipated within 450 m |
| | | H_s | decreases at the first 60 m, then increases |
| | | rc | di is dominant at the first 70 m, then bottom friction is dominant |
| High | 100 | E_{ds} | most dissipated within 150 m |
| | | H_s | decreases most within 50 m, then still decreases which is strengthened by the summer dike, after which it increases |
| | | rc | di is dominant up until 50 m, then veg is dominant except for at the summer dike where di is dominant and above the adjacent ditch where bf is dominant |
| | 1000 | E_{ds} | most dissipated within 400 m |
| | | H_s | decreases most within 30 m, then stagnates up, then decreases by the summer dike, after which it increases |
| | | rc | di is dominant up until 50 m, then bf is dominant except for at the summer dike where di is dominant |
| | 10000 | E_{ds} | most dissipated within 400 m |
| | | H_s | decreases most within 30 m, then stagnates up, then decreases by the summer dike, after which it increases |
| | | rc | di is dominant up until 65 m, then bf is dominant except for at the summer dike where di is dominant |
| | 37500 | E_{ds} | most dissipated within 400 m |
| | | H_s | decreases most within 25 m, then stagnates up, then decreases by the summer dike, after which it increases |
| | | rc | di is dominant up until 65 m, then bf is dominant except for at the summer dike where di is dominant |

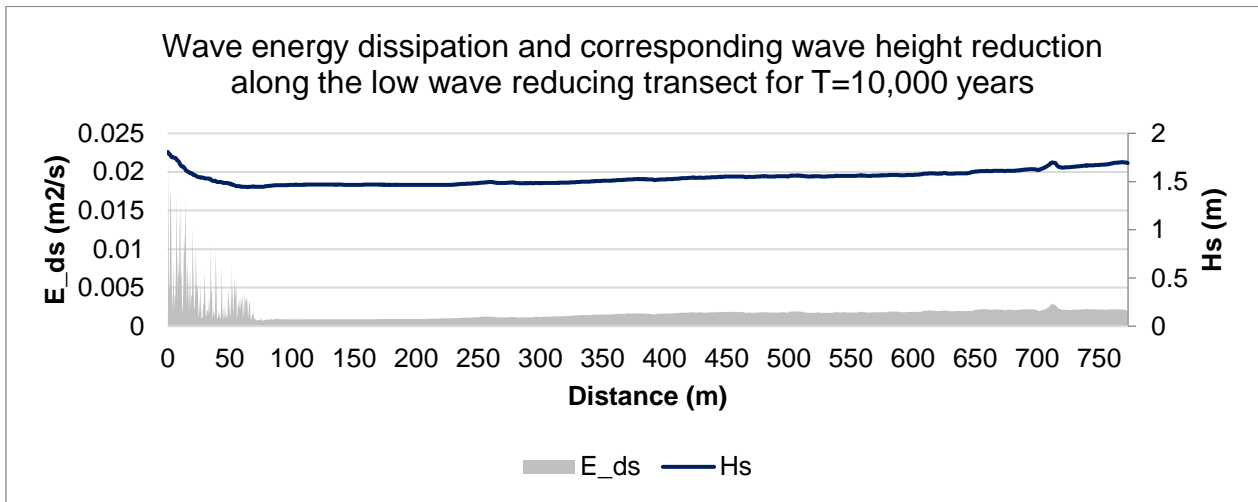
Low wave reducing transect – T=100 years

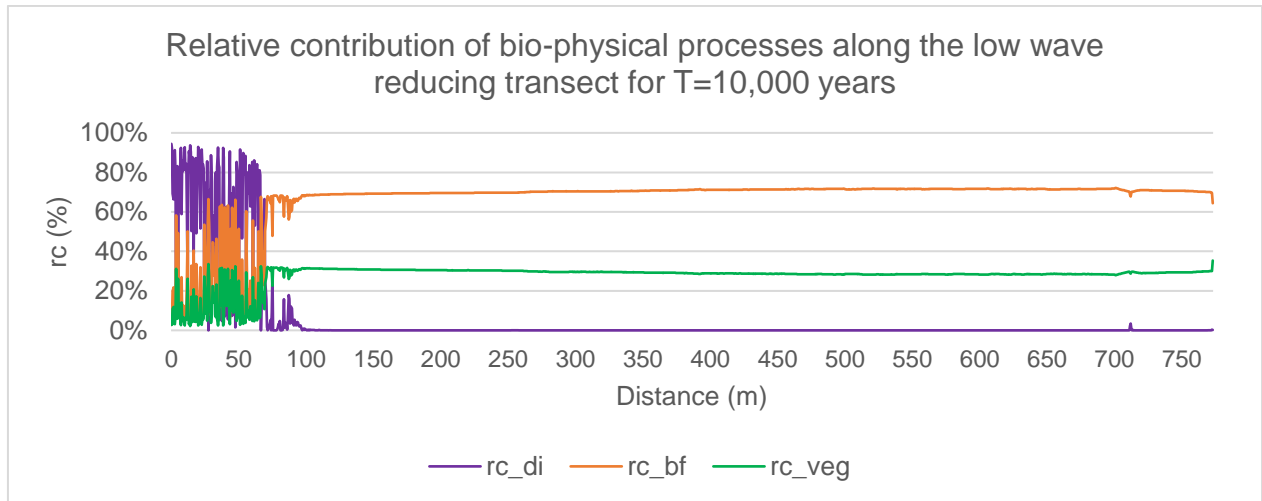


Low wave reducing transect – T=1000 years

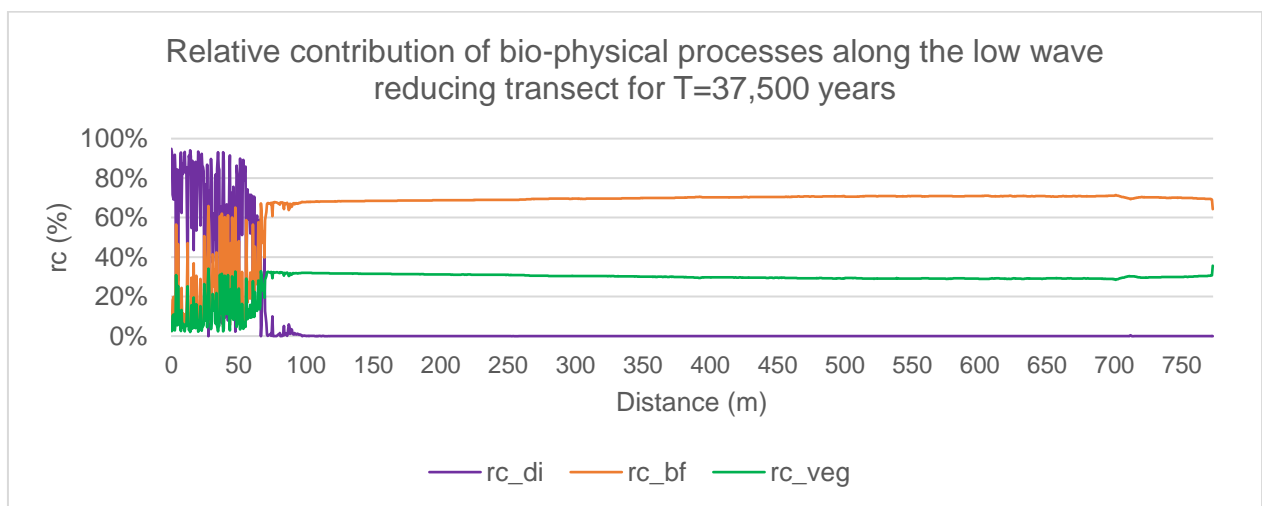
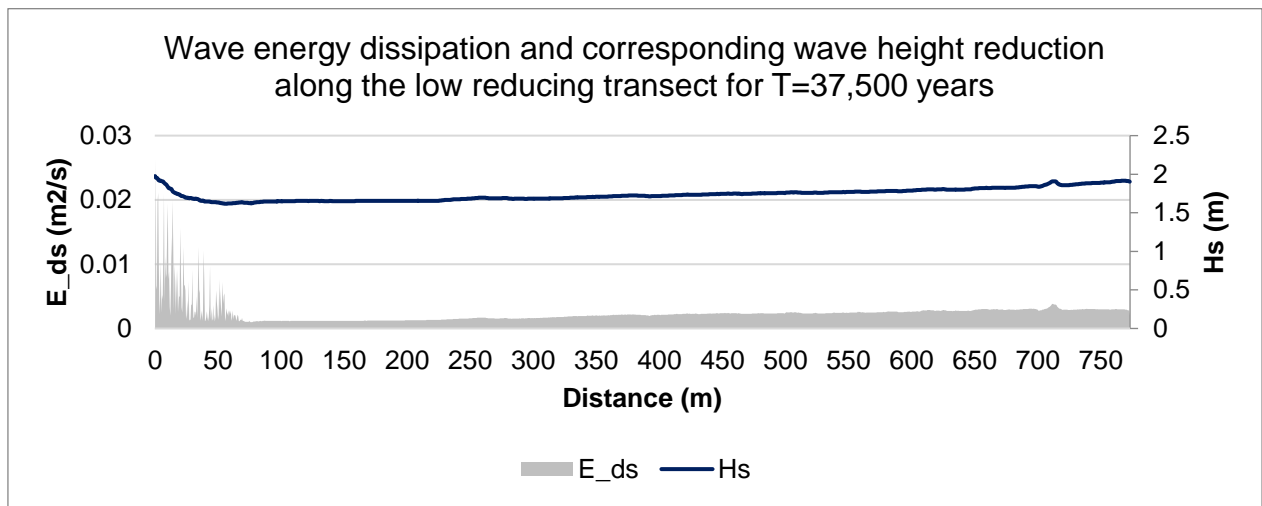


Low wave reducing transect – T=10,000 years

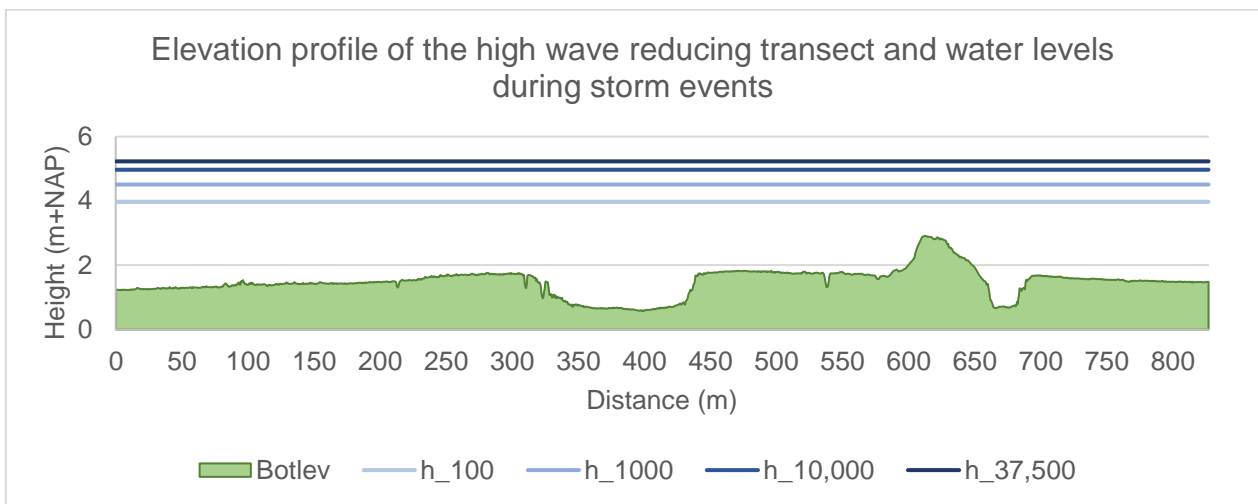
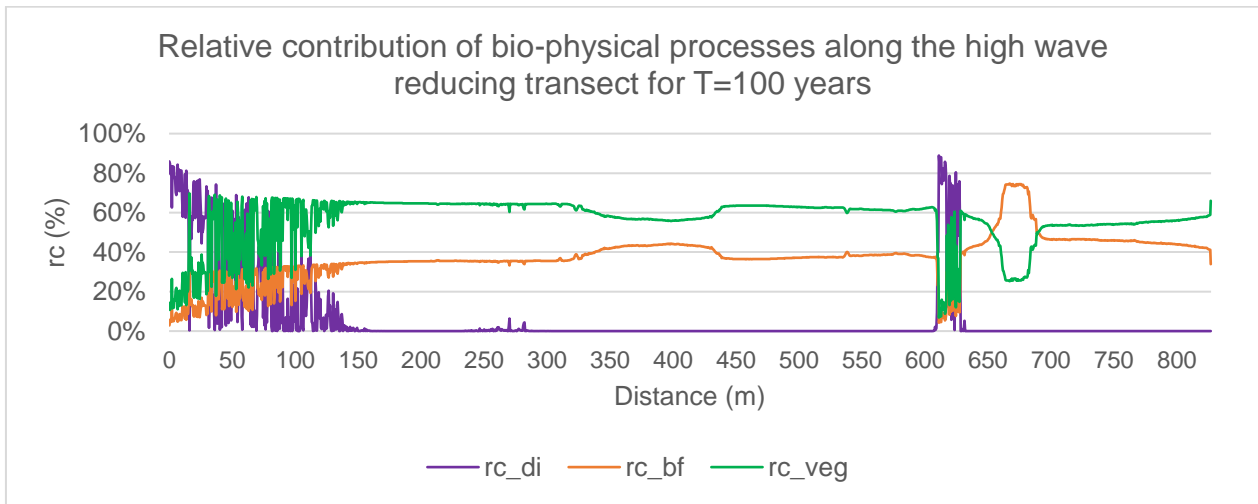
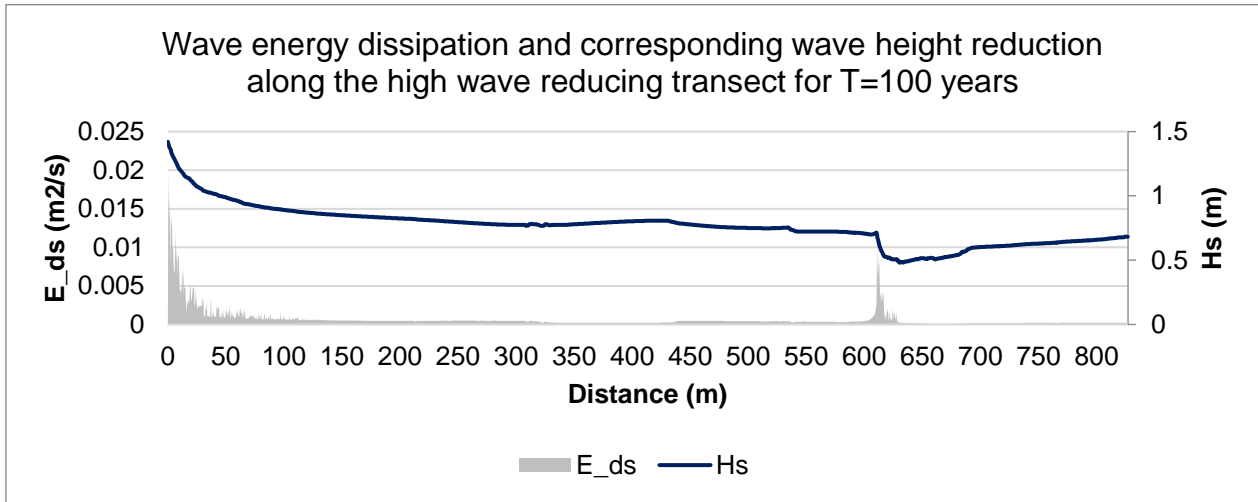




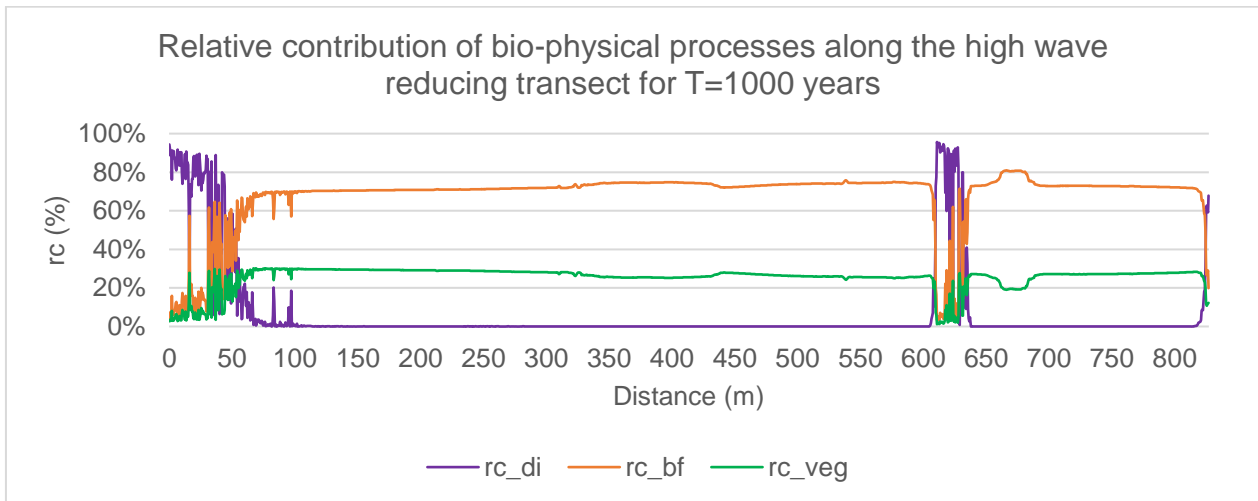
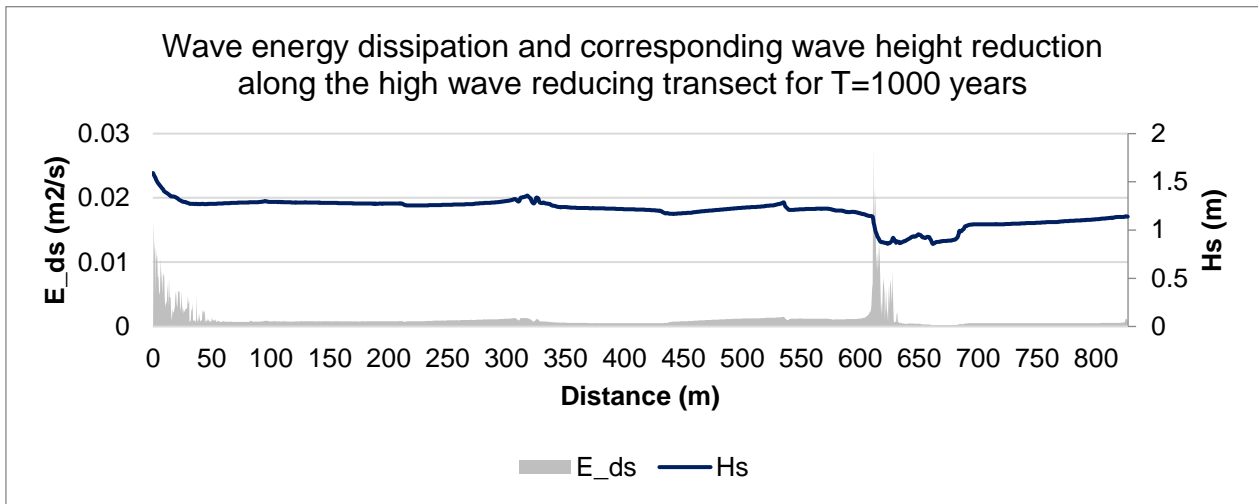
Low wave reducing transect – T=37,500 years



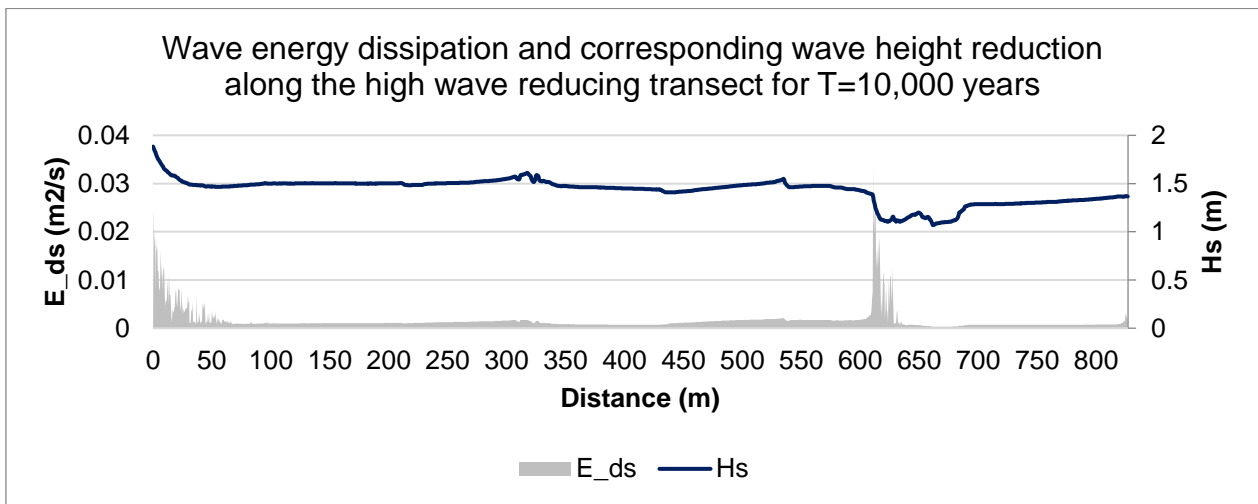
High wave reducing transect – T=100 years

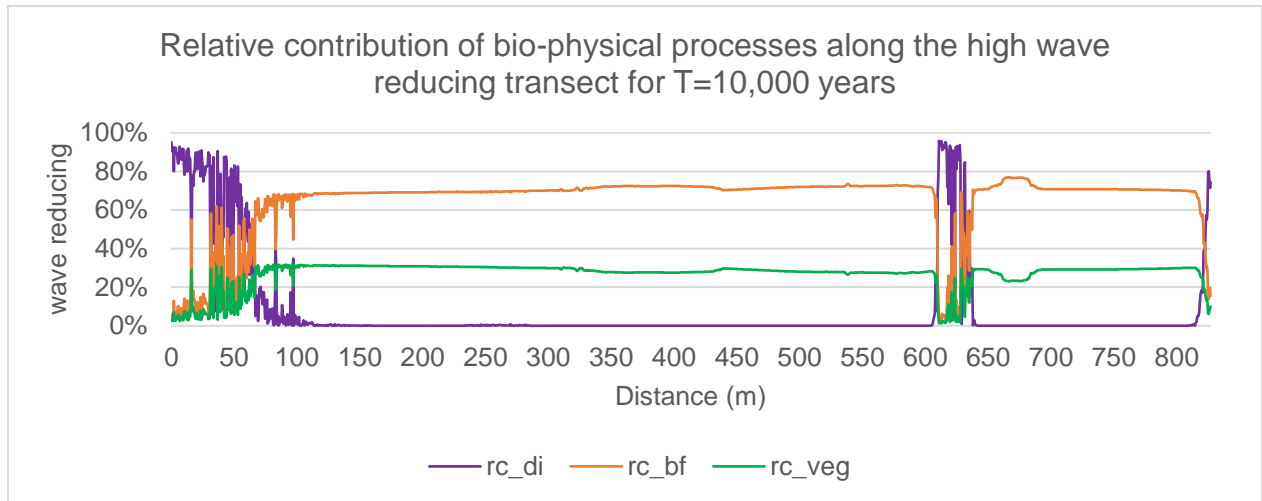


High wave reducing transect – T=1000 years

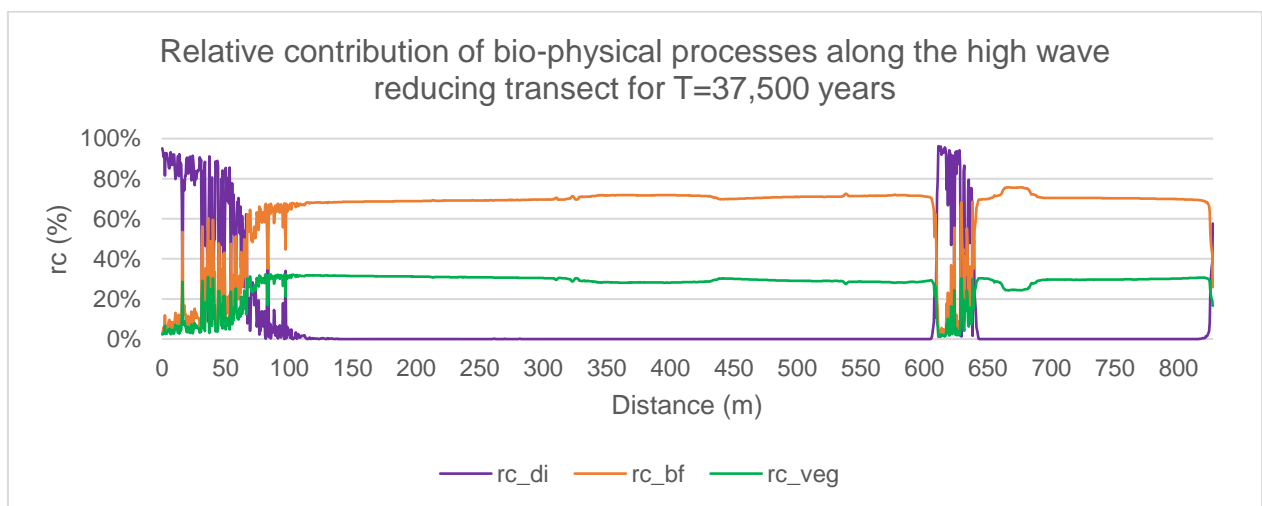
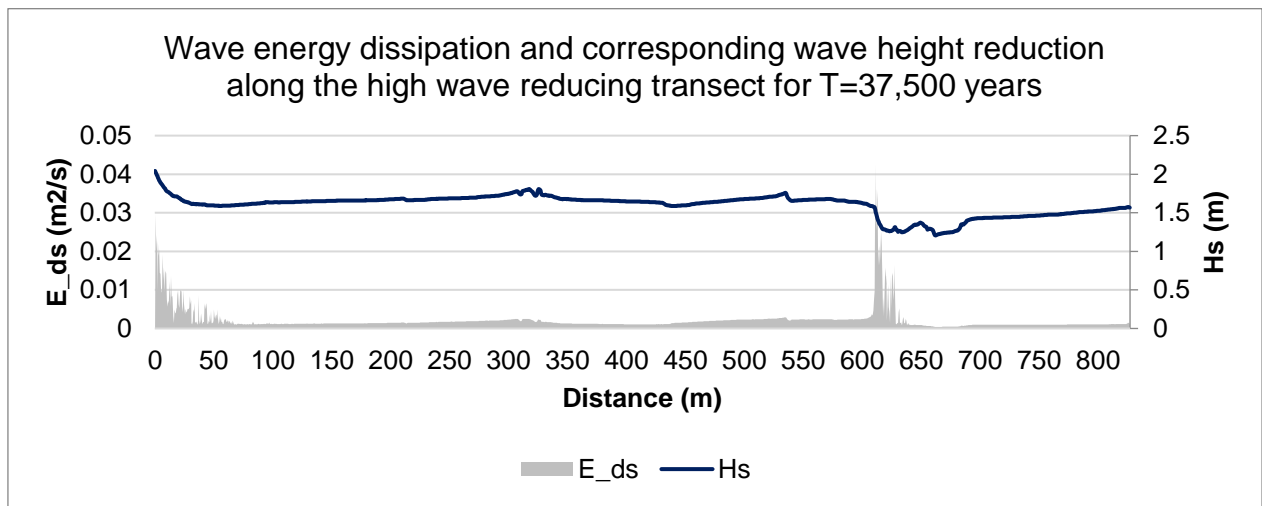


High wave reducing transect – T=10,000 years





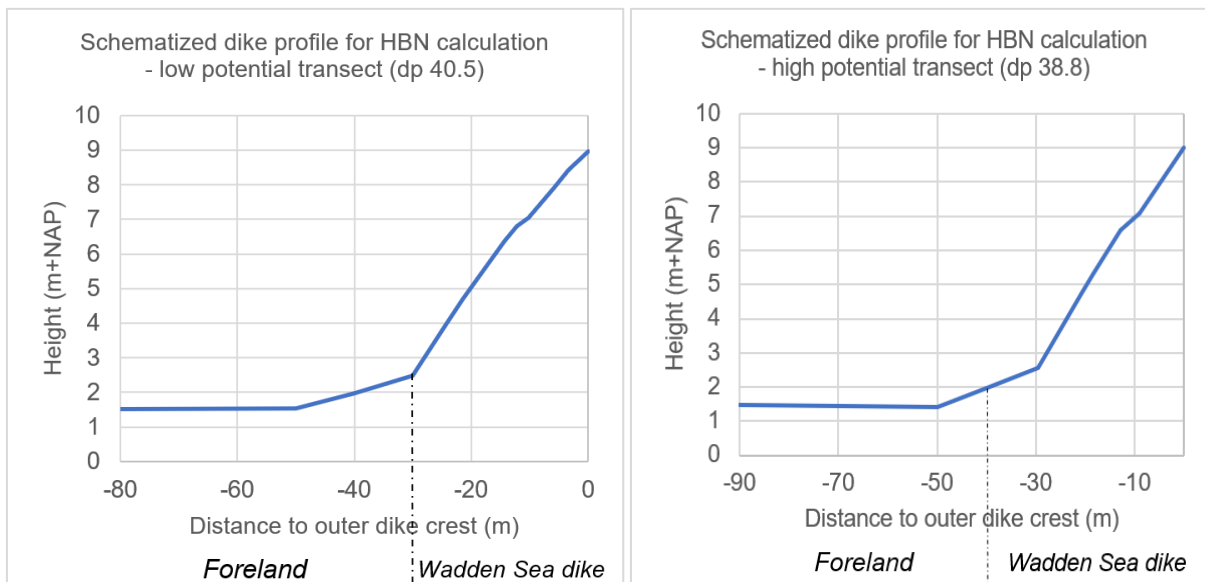
High wave reducing transect – T=37,500 years



Appendix L - Method for HBN calculations

The normative dike height ('Hydraulisch belastingniveau' of 'benodigde kruinhoogte') was determined with Hydra-NL software, which is also used to base dike assessments on (Rijkswaterstaat WVL, 2018b). For the low and high wave reducing transect, wave conditions were calculated 50 m from the dike toe (e.g. significant wave height and spectral wave period) and the corresponding water level and angle of incidence were derived from Hydra-NL. These together with the (additional) bottom level profile from this location towards the dike crest, formed the input for the HBN calculation for the T=37,500-year storm event. These elevation profiles, consisting of foreland and dike, were schematized before application in Hydra-NL. The roughness of the foreland from the WBI2017 location towards the outer dike crest has a value of 1, indicating a grass surface with a very low roughness. In this way, the wave conditions at 50 m from the dike toe represented the conditions in front of the Wadden Sea dike at the outer dike toe. With the tool 'Narekenen illustratiepunt' in Hydra-NL, these wave characteristics were used to calculate the HBN for the assessment year of 2017 (Rijkswaterstaat WVL, 2018a).

The high and low wave reducing transects end at the WBI2017 locations 'WZ_1_6-4_dk_0046' and 'WZ_1_6-4_dk_0053', but were extended towards the dike poles 38.8 km and 40.5 km (see Figure 20). Their (schematized) bottom level profiles are shown in the figures below. From the figures can be seen that the shape of the profiles, and the crest height (about 9 m+NAP) are comparable.



Appendix M - Latest flood protection projects along Koehool-Lauwersmeer

Since Witteveen+Bos supports Wetterskip Fryslân during the exploration phase for several HWBP projects at the Wadden Sea dike between 'Koehool' and 'Lauwersmeer', and I have been working at this firm, the latest flood protection projects along this part of the coast are presented in the table and figure below. Besides, in this overview map can be acknowledged which parts of the Wadden Sea dike do not fulfill the current dike standards.

| Project # | Location | Project | Description | Stakeholders |
|-----------|---|--|--|---|
| 1 | Koehool - Lauwersmeer | HWBP - Koehool-Lauwersmeerdijk (2016-2023) | Part of dike ring 6: trajectory is 48 km of which 23 km was rejected | Wetterskip Fryslân and partners (e.g. W+B) |
| 2 | Zwarte Haan - Wierum | HWBP - Steenbekleding Waddenzeedijk (2010-2021) | Application of 'Elastocoast' and pouring stone to aggravate and fix existing stone coverage | Wetterskip Fryslân and partners (e.g. W+B) |
| 3 | Koehool - Westhoek | 'Kwelderontwikkeling Koehoal-Westhoek' (since 2016) | A 'mud motor' increases sediment supply so that salt marsh growth is stimulated | It Fryske Gea, Gemeente Harlingen, EcoShape (&partners), Waddenfonds |
| 4 | Noard-Fryslân Bûtendyks (Oude Bildtzijl) | 'Verkweldering Bildtpôlen' (since 2009) | Depoldering of summer polder to a salt marsh | It Fryske Gea, Waddenfonds, Rijkswaterstaat |
| 5 | Noard-Fryslân Bûtendyks (Noarderleech at Nieuwebildtzijl) | 'Van Polder naar Kwelder: 10 jaar ontwikkeling' (2001-2011) | Depoldering of summer polder to a salt marsh | It Fryske Gea, Provincie Fryslân, Waddenfonds, Rijkswaterstaat |
| 6 | Noard-Fryslân Bûtendyks (Noarderleech) | Project Vijfhuizen 'fan swiet nei sâlt' (2017-2018) | A gradual transition from sweet inner-dike land to the salty Wadden Sea to stimulate nature development | Wetterskip Fryslân, Provincie Fryslân, Gemeente Ferwerderadiel, It Fryske Gea |
| 7 | Peazemerlannen (Paesens - Moddergat) | a. Preparation of salt marsh project b. Salt Marsh monitoring (2007-2017) | a. Depoldering of summer polder to a salt marsh b. At Moddergat is a gas field of the NAM located which is subject to soil subsidence, so its elevation is being measured | a. It Fryske Gea b. NAM, Artemisia, Rijkswaterstaat |
| 8 | Lauwersmeer | HWBP - Lauwersmeerdijk (28H) (2016-2018) | Dike improvement along 3.7 km | Wetterskip Fryslân and partners (e.g. W+B) |



POV PROJECT OVERSTIJGENDE VERKENNING HAVBP

waddenzeedijken
liefde op de dijk

- Onderzoeken POV-Waddenzeedijken
- Voldoet aan norm
- Voldoet niet aan norm voor de lange termijn
- Dijkkring
- Grens waterschap
- Provinciegrens
- Te beschermen laaggelegen gebieden (indicatief)